

Structure-Based Optimization of 3-Phenyl-*N*-(2-(3-phenylureido)ethyl)thiophene-2-sulfonamide Derivatives as Selective Mcl-1 Inhibitors

Yan Li,[†] Wenjie Fan,[†] Qineng Gong,[†] Jie Tian, Mi Zhou, Qing Li, Laura B. Uwituze, Zhichao Zhang,* Ran Hong,* and Renxiao Wang*



Cite This: *J. Med. Chem.* 2021, 64, 10260–10285



Read Online

ACCESS |



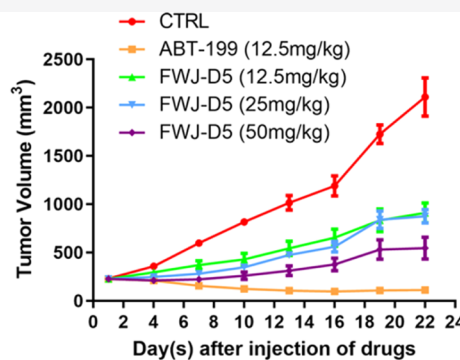
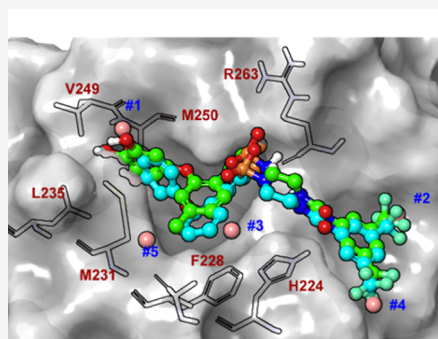
Metrics & More



Article Recommendations



Supporting Information



ABSTRACT: Selective Mcl-1 inhibitors may overcome the drug resistance caused by current anti-apoptotic Bcl-2 protein inhibitors in tumors with Mcl-1 overexpression. Based on previously discovered compounds with a 3-phenylthiophene-2-sulfonamide core moiety, in this work, we have obtained new compounds with improved binding affinity and/or selectivity under the guidance of structure-based design. The most potent compounds achieved sub-micromolar binding affinities to Mcl-1 ($K_i \sim 0.4 \mu\text{M}$) and good cytotoxicity ($\text{IC}_{50} < 10 \mu\text{M}$) on several tumor cells. ^{15}N -heteronuclear single-quantum coherence NMR spectra suggested that these compounds bound to the BH3-binding groove on Mcl-1. Several cellular assays revealed that FWJ-D4 as well as its precursor FWJ-D5 effectively induced caspase-dependent apoptosis, and their target engagement at Mcl-1 was confirmed by co-immunoprecipitation experiments. Treatment with FWJ-D5 at 50 mg/kg every 2 days on an RS4;11 xenograft mouse model for 22 days led to 75% reduction in tumor volume without body weight loss.

INTRODUCTION

Apoptosis, also known as programmed cell death, is an essential process for eliminating aging or abnormal cells in the living system. Dysregulation of apoptosis is critical for various malignant tumor diseases and drug resistance in anti-tumor therapies.^{1–4} Bcl-2 family proteins are key regulators of the mitochondrial apoptotic pathway, which includes anti-apoptotic members containing BH1–BH4 domains (such as Bcl-x_L, Bcl-2, Mcl-1, Bcl-w, and A1), pro-apoptotic members with BH1–BH3 domains (such as Bax and Bak), and BH3-only proteins (such as Bim and Bad).⁵ At the molecular level, the BH3 domain on the pro-apoptotic proteins binds to a groove on the surface of the anti-apoptotic proteins.⁶ Various studies have shown that overexpression of the anti-apoptotic proteins is resistant to chemotherapies in a variety of tumor cells.^{7–9} Blocking the protein–protein interactions (PPIs) formed by the anti-apoptotic proteins by small-molecule inhibitors can release the apoptotic signal and recover the apoptosis process. Thus, discovery of small-molecule inhibitors targeting the PPIs

between Bcl-2 family proteins has become an appealing approach to the development of new anti-cancer drugs since the beginning of this century.^{10,11}

Although PPIs are generally challenging as drug targets, a range of small-molecule inhibitors of anti-apoptotic Bcl-2 proteins have been reported in the literature.¹² A batch of such small-molecule inhibitors have entered clinical trials.^{13–20} Among them, the ABT series of compounds developed by Abbott, such as ABT-263,¹⁵ and ABT-737,¹⁶ is widely known. In fact, ABT-199 (i.e., Venetoclax)¹³ has been approved for treating chronic lymphocytic leukemia or small lymphocytic lymphoma. Most of these inhibitors,⁷ such as the ABT

Received: April 15, 2021

Published: July 6, 2021



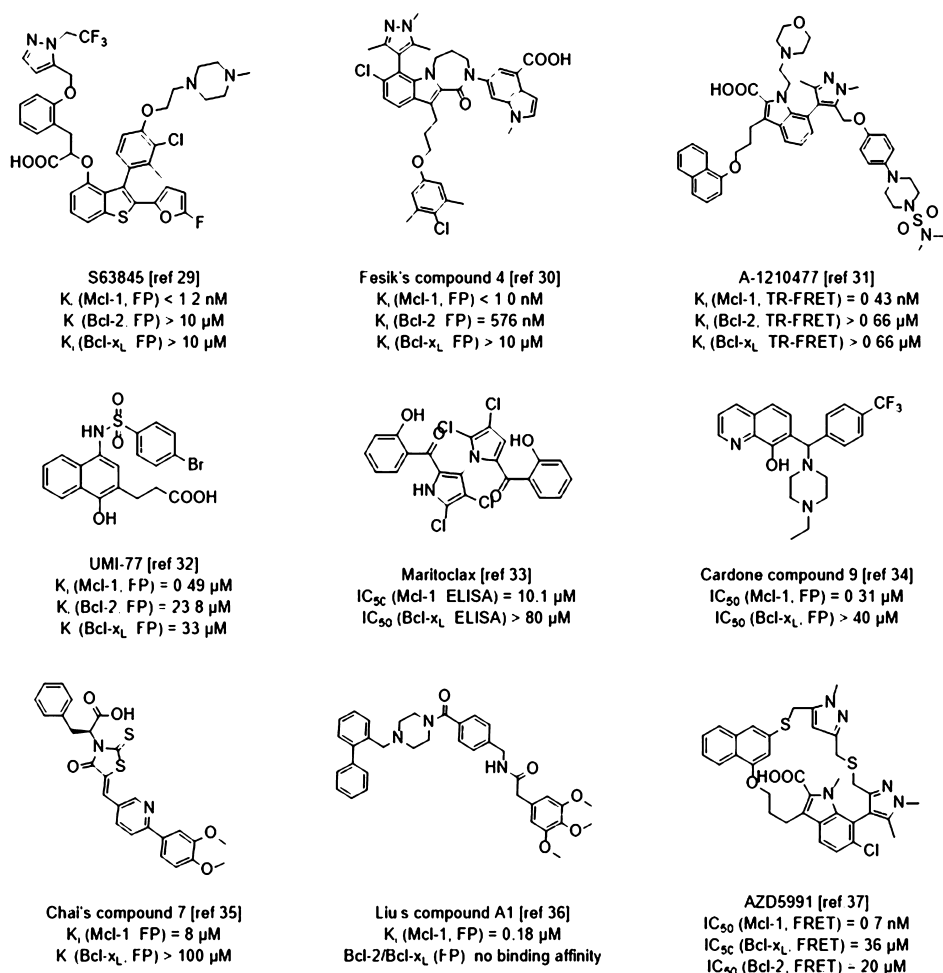


Figure 1. Structures and binding affinity data of some small-molecule Mcl-1 inhibitors reported in the literature.

compounds, are known to target Bcl-2 or Bcl-x_L. However, it has been discovered that selective Bcl-2 or Bcl-x_L inhibitors potentially face drug resistance problems in tumor cells overexpressing Mcl-1 or other less-noted anti-apoptotic proteins.^{21,22} For example, ABT-737 inhibits Bcl-x_L, Bcl-2, and Bcl-w, but it lacks efficacy on some types of tumor cells with Mcl-1 overexpression.²² Therefore, developing selective inhibitors targeting other anti-apoptotic Bcl-2 proteins (such as Mcl-1 and Bcl-w) can be a useful supplement to the current efforts on targeting the Bcl-2 family proteins.²³

The Mcl-1 protein has quite different biological functions as compared to other anti-apoptotic Bcl-2 proteins (such as Bcl-2 and Bcl-x_L).^{24,25} In fact, the crystal structure of Mcl-1 reveals that it has a smaller and less flexible binding pocket as compared to Bcl-2 or Bcl-x_L.²⁶ All these prompt that Mcl-1 has its independent characteristics from other anti-apoptotic Bcl-2 proteins. A number of selective small-molecule Mcl-1 inhibitors have been reported in the past 10 years or so.^{27,28} Some of them are summarized as representatives in Figure 1.^{29–38} Nevertheless, many of the Mcl-1 inhibitors reported in the literature are tested only in the *in vitro* binding assay and cytotoxicity assay. Only one of them, that is, AMG176, is in the first-phase clinical trial for relapsed or refractory multiple myeloma.²⁰ Therefore, development of new classes of Mcl-1 inhibitors is still a compelling demand.

In our previous work, we obtained a hit compound containing a phenyltetrazole and a hydrazinecarbothioamide moiety

through virtual screening of over 56,000 commercial compounds. Later, we optimized it into a class of compounds with a 3-phenylthiophene-2-sulfonamide core moiety.³⁸ Our binding assay results indicated that among the three major anti-apoptotic Bcl-2 proteins, this class of compounds showed selectivity toward Mcl-1 and Bcl-2 but not Bcl-x_L. Cytotoxicity assay results indicated that such compounds inhibited the proliferation of several types of tumor cells, such as A549 (human nonsmall cell lung cancer cell), H1299 (human lung adenocarcinoma cells), HL-7702 (human liver cells), BEL-7404 (human liver cancer cells), and Hep3B (human liver cancer cells). Several most active compounds, for example, YCW-E5, YCW-E10, and YCW-E11, were observed to induce mitochondrial-pathway apoptosis at the micromolar level.

In this work, we further optimized this class of compounds under the guidance of structural analysis and molecular modeling. Among the newly synthesized compounds, we obtained some compounds with improved binding affinity as well as selectivity toward Mcl-1. We also obtained some compounds with improved binding affinity as pan inhibitors of anti-apoptotic Bcl-2 proteins. ¹⁵N-heteronuclear single-quantum coherence (HSQC) NMR spectra of two selected compounds suggested that they bound to the BH3-domain binding pocket on Mcl-1. Cellular mechanism-of-action studies indicated that these compounds induced caspase-independent apoptosis via disruption of the PPIs involving Mcl-1 (such as Bim/Mcl-1 interactions). Moreover, the most potent com-

pounds exhibited a significant dose-dependent tumor-inhibition effect on an RS4;11 xenograft mouse model without obvious weight loss. Overall, these new compounds are more promising than the lead compound as potential candidates for developing new anti-cancer drugs.

RESULTS AND DISCUSSION

Structural Optimization and Structure–Activity Relationship. In this study, three most active compounds developed in our previous work,³⁸ that is, YCW-E5, YCW-E10, and YCW-E11, were chosen as the starting point for structural optimization. In fact, these three lead compounds share the same structural scaffold with minor difference in substituent groups (Figure 2a). In this work, we have synthesized five sets of

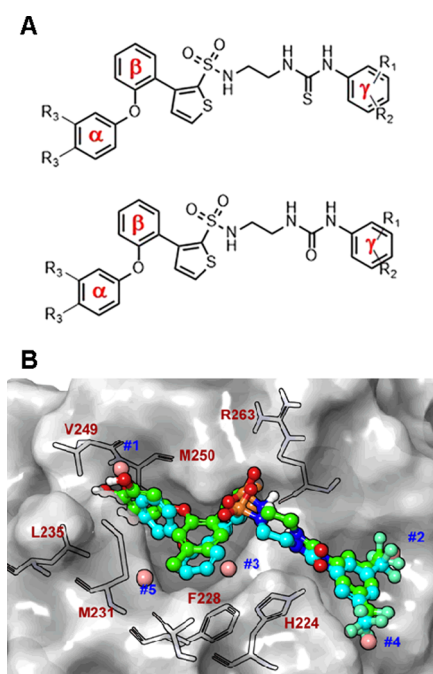


Figure 2. (A) Chemical structures of the lead compounds YCW-E5 [$X = S$, $R_1 = 3\text{-CF}_3$, $R_2 = 5\text{-CF}_3$, $R_3 = \text{OH}$, $K_i(\text{Bcl-2}) = 5.6 \pm 1.6 \mu\text{M}$; $K_i(\text{Mcl-1}) = 0.84 \pm 0.32 \mu\text{M}$; no binding to Bcl- x_L], YCW-E10 [$X = \text{O}$, $R_1 = 3\text{-CF}_3$, $R_2 = 5\text{-CF}_3$, $R_3 = \text{OH}$, $K_i(\text{Bcl-2}) = 17 \pm 0.6 \mu\text{M}$; $K_i(\text{Mcl-1}) = 2.1 \pm 0.58 \mu\text{M}$; no binding to Bcl- x_L], and YCW-E11 [$X = \text{O}$, $R_1 = 3\text{-Cl}$, $R_2 = 5\text{-Cl}$, $R_3 = \text{OH}$, $K_i(\text{Bcl-2}) = 4.6 \pm 1.4 \mu\text{M}$; $K_i(\text{Mcl-1}) = 1.4 \pm 0.54 \mu\text{M}$; no binding to Bcl- x_L]. (B) Illustration of the binding modes of YCW-E10 (colored in cyan) and FWJ-D4 (colored in green) to Mcl-1, which were predicted by molecular dynamics (MD) simulation. The binding pocket is displayed with a translucent surface, with the ligand and key residue colored in cyan and gray, respectively. Several critical hydration sites predicted by WATsite are displayed as spheres in pink. The desolvation energies (in kcal/mol) associated with these hydrations sites are 3.94 (#1), 3.68 (#2), 2.66 (#3), 2.06 (#4), and 0.96 (#5). The Mcl-1 protein structure used in MD simulation was from the Mcl-1/BRD inhibitor complex (PDB code: 4WWMR).

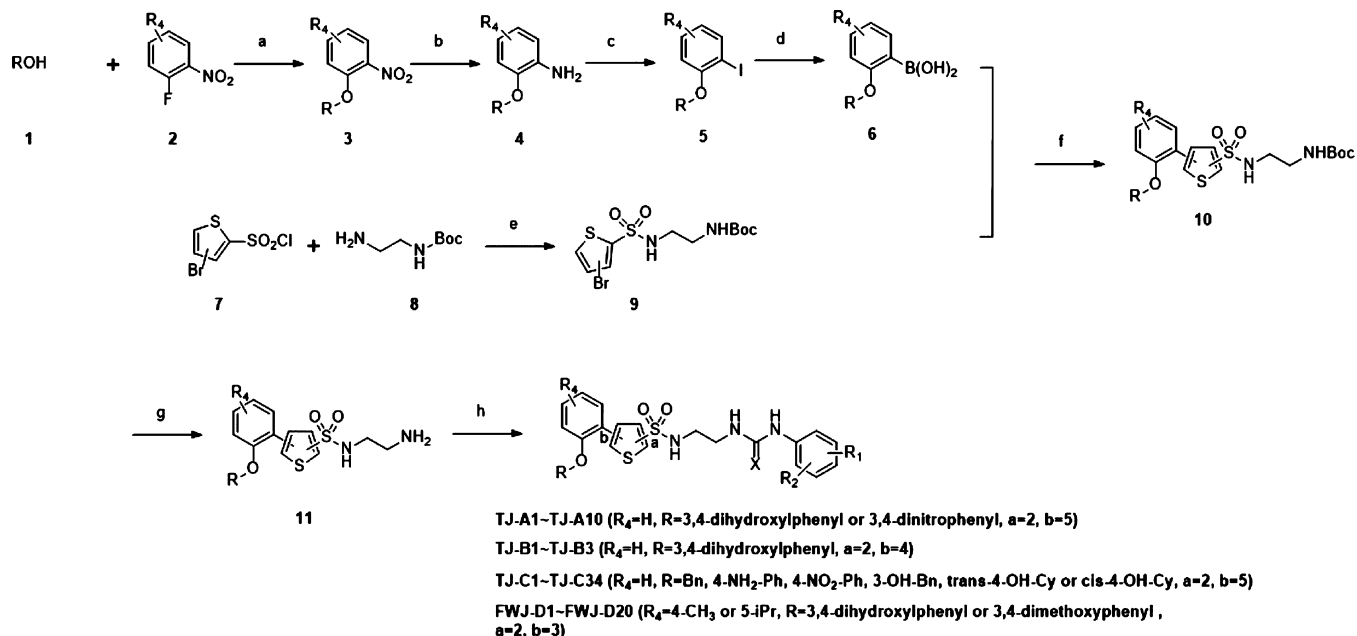
derivative compounds based on these lead compounds. Below, we will describe these new compounds and discuss their activities in a stepwise manner, so the readers can understand the basic logic in our molecular design.

Our first attempt of structural optimization was to alter the relative position of the sulfonamide and the phenyl group on the thiophene moiety while keeping the other parts unchanged. As a result, compounds TJ-A1–TJ-A10 and TJ-B1–TJ-B3 were synthesized with the methods outlined in Scheme 1. Here, *tert*-

butyl (2-((4-bromothiophene)-2-sulfonamido)ethyl)carbamate and *tert*-butyl (2-((5-bromothiophene)-2-sulfonamido)ethyl)carbamate were key reagents for deciding the positions of sulfonamide and phenyl groups on the thiophene ring. TJ-A1–TJ-A10 and TJ-B1–TJ-B3 were tested in a FP-based binding assay (Table 1), which was applied successfully in our previous works.^{39,40} Binding assay results indicate that both the compounds containing the 5-phenyl-*N*-(2-(3-phenylureido)ethyl)thiophene-2-sulfonamide moiety (i.e., TJ-A1–TJ-A3) and the compounds containing the 4-phenyl-*N*-(2-(3-phenylureido)ethyl)thiophene-2-sulfonamide moiety (i.e., TJ-B1–TJ-B3) bind to Mcl-1 with inhibition constants ranging between 0.3 and 1.0 μM . In terms of binding affinity to Mcl-1, these new compounds are comparable to or slightly better than the chosen lead compounds (e.g., YCW-E5, $K_i = 0.84 \mu\text{M}$). Note that the lead compounds exhibit selectivity to Mcl-1 and Bcl-2 without obvious binding to Bcl- x_L , but these new compounds bind to all three major anti-apoptotic Bcl-2 proteins (i.e., Bcl-2, Bcl- x_L , and Mcl-1) with inhibition constants around the micromolar level. Therefore, these new compounds may serve better as pan inhibitors of anti-apoptotic Bcl-2 proteins. When R_3 is replaced with a nitro group, the resulting compounds (i.e., TJ-A4–TJ-A10) generally lose their binding affinities to all three anti-apoptotic Bcl-2 proteins. It is thus clear that keeping the two hydroxyl groups as R_3 is essential for maintaining the desired binding affinity for this class of compounds. In addition, CCK8 cell viability assay results indicate that compounds TJ-A1–TJ-A3 exhibit obvious cytotoxicity ($\text{IC}_{50} < 20 \mu\text{M}$) on the two leukemia cell lines (i.e., HL-60 and RS4;11) compared to HeLa (Table 1). However, they exhibit obvious cytotoxicity on HEK293T cells as well. In contrast, compounds TJ-B1 and TJ-B2 also exhibit obvious cytotoxicity on HL-60 and RS4;11 cells ($\text{IC}_{50} < 10 \mu\text{M}$) but far less cytotoxicity on HEK293T ($\text{IC}_{50} > 20 \mu\text{M}$). In particular, TJ-B2 has the IC_{50} value of 1.3 and 3.9 μM on HL-60 and RS4;11 cells, respectively, without obvious toxicity on HEK293T at the maximal applied concentration of 50 μM .

In order to recover the selectivity toward Mcl-1, we then kept the 3-phenyl-*N*-(2-(3-phenylureido)ethyl)thiophene-2-sulfonamide core moiety on the lead compound and tried to replace the dihydroxyphenyl moiety (i.e., α -ring in Figure 2a) with other aromatic groups. Such derivative compounds were obtained with the methods outlined in Scheme 1, producing compounds TJ-C1–TJ-C34 (Table 2). Binding assay results indicate that when this dihydroxyphenyl moiety is changed to a benzyl, 4-aminophenyl, or 4-nitrophenyl moiety, most of the compounds totally lose their binding affinity to the three anti-apoptotic Bcl-2 proteins. Only a few compounds (such as TJ-C5, TJ-C6, TJ-C8, TJ-C9, TJ-C14, TJ-C16, and TJ-C18) maintain the binding affinity to Mcl-1 with K_i values between 1.0 and 13 μM , but the structure–activity relationship is not clear. Moreover, these several compounds do not have the desired cytotoxicity profile on HL-60, RS4;11, and HEK293T cells. Therefore, our efforts of changing the dihydroxyphenyl moiety on the lead compounds did not lead to improved bioactivities.

To explain the structure–activity relationship of the newly synthesized compounds, we applied an MD simulation of 100 ns long to obtain the binding mode of the lead compound YCW-E10 to Mcl-1 (Figure 2b). Based on this complex structural model, several critical hydration sites inside the binding pocket before ligand binding were predicted with the WATsite method.⁴¹ As shown in Figure 2b, site #1 can form a hydrogen bond with the backbone amide group on residue V249. The high

Scheme 1. Synthesis of Compounds TJ-A1–TJ-A10, TJ-B1–TJ-B3, TJ-C1–TJ-C34, and FWJ-D1–FWJ-D20^a

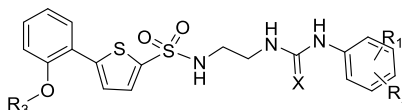
^aReagents and conditions: (a) NaH, THF, reflux; (b) Pd/C, N₂H₄·H₂O, EtOH, N₂; (c) (1) H₂SO₄, NaNO₂, 0 °C; (2) KI; (d) (1) *n*BuLi, THF; (2) B(OMe)₃, −78 °C; (3). HCl, CH₂Cl₂; (e) DCM, triethylamine (TEA); (f) Pd(OAc)₂, PPh₃, K₃PO₄, THF, reflux; (g) CF₃COOH, CH₂Cl₂, RT; (h) aryl isothiocyanate, THF, RT.

Table 1. Chemical Structures, Binding Data, and Cytotoxicity of Compounds TJ-A1–TJ-A10 and TJ-B1–TJ-B3

compound	X	R ₁	R ₂	R ₃	binding data (K_i , μM) ^a			cytotoxicity (IC_{50} , μM) ^b			
					Bcl-x _L	Bcl-2	Mcl-1	HeLa	HL-60	RS4;11	HEK293T
TJ-A1	S	3-CF ₃	5-CF ₃	OH	0.93 ± 0.27	2.6 ± 0.60	0.37 ± 0.17	>20	18.3 ± 0.06	10.3 ± 0.84	12.3 ± 1.96
TJ-A2	O	3-CF ₃	5-CF ₃	OH	1.5 ± 0.49	3.9 ± 0.85	0.42 ± 0.10	>20	10.5 ± 0.28	4.9 ± 0.10	17.1 ± 0.95
TJ-A3	O	3-Cl	5-Cl	OH	1.7 ± 0.17	3.6 ± 0.80	0.94 ± 0.37	>20	10.4 ± 0.72	4.5 ± 0.25	12.4 ± 0.25
TJ-A4	O	4-Cl	H	NO ₂	N.A.	N.A.	5.9 ± 2.3	>20	8.1 ± 1.07	6.7 ± 1.10	>20
TJ-A5	O	3-OMe	H	NO ₂	N.A.	N.A.	N.A.	>20	6.7 ± 0.66	1.3 ± 0.09	17.8 ± 1.90
TJ-A6	O	3-Cl	5-Cl	NO ₂	N.A.	N.A.	N.A.	>20	2.3 ± 0.57	2.1 ± 0.79	>20
TJ-A7	O	3-Me	5-Me	NO ₂	weak	N.A.	N.A.	12.0 ± 0.19	9.1 ± 0.61	3.6 ± 0.76	>50
TJ-A8	O	4-NO ₂	H	NO ₂	N.A.	N.A.	N.A.	>20	0.34 ± 0.10	3.0 ± 0.59	16.6 ± 0.86
TJ-A9	O	4-OMe	H	NO ₂	N.A.	N.A.	N.A.	>20	5.4 ± 0.21	1.4 ± 0.13	18.5 ± 0.87
TJ-A10	O	3-CF ₃	5-CF ₃	NO ₂	N.A.	N.A.	N.A.	>50	1.9 ± 0.26	2.4 ± 0.11	>50
TJ-B1	S	3-CF ₃	5-CF ₃	OH	1.0 ± 0.39	4.6 ± 2.1	0.32 ± 0.12	>20	0.6 ± 0.23	4.5 ± 0.77	>20
TJ-B2	O	3-CF ₃	5-CF ₃	OH	1.7 ± 0.12	5.2 ± 0.2	0.51 ± 0.08	>20	1.3 ± 0.57	3.9 ± 0.81	>50
TJ-B3	O	3-Cl	5-Cl	OH	1.7 ± 0.50	8.4 ± 4.9	0.77 ± 0.10	>50	>20	>50	>20
YCW-E5	S	3-CF ₃	5-CF ₃	OH	N.A.	5.6 ± 1.6	0.84 ± 0.32	>50	4.3 ± 0.51	4.8 ± 0.05	7.5 ± 0.41
YCW-E10	O	3-CF ₃	5-CF ₃	OH	N.A.	17.0 ± 0.6	2.1 ± 0.58	>50	5.7 ± 0.18	4.9 ± 0.17	8.9 ± 1.06
YCW-E11	O	3-Cl	5-Cl	OH	N.A.	4.6 ± 1.4	1.4 ± 0.54	>50	6.9 ± 1.24	6.2 ± 0.32	10.7 ± 1.58
YCW-E16	S	3-CF ₃	5-CF ₃	OMe	N.A.	N.A.	N.A.	6.4 ± 0.74	2.8 ± 0.13	3.3 ± 0.22	6.8 ± 0.08
ABT-199					<0.001	<0.001	N.A.	>20	0.077 ± 0.0057	0.0043 ± 0.00019	>20
A1210477					N.A.	N.A.	<0.001	>20	2.46 ± 0.21	7.31 ± 0.83	>50

^aThe mean values and standard deviations of the K_i values were derived based on the outcomes of three parallel measurements. N.A.: no obvious sign of binding was observed; weak: dose-dependent FP signals were observed, but the change in the FP signals (up to a 100 μM concentration) was not significant enough to determine the K_i value accurately. ^bThe mean values and standard deviations of the IC_{50} values were derived based on the outcomes of three parallel measurements.

Table 2. Chemical Structures, Binding Data, and Cytotoxicity of Compounds TJ-C1–TJ-C34



compound	X	R ₁	R ₂	R ₃	K _i (μM) ^a			cytotoxicity (IC ₅₀ , μM) ^b			
					Bcl-x _L	Bcl-2	Mcl-1	Hela	HL-60	RS4;11	HEK293T
TJ-C1	S	3-CF ₃	5-CF ₃	Bn	N.A.	N.A.	N.A.	4.7 ± 0.06	2.1 ± 0.14	>50	8.5 ± 0.76
TJ-C2	O	3-CF ₃	5-CF ₃	Bn	N.A.	N.A.	N.A.	13.5 ± 0.34	11.4 ± 0.32	>50	>20
TJ-C3	S	3-Cl	H	Bn	N.A.	N.A.	N.A.	8.4 ± 0.25	>50	>50	10.2 ± 0.58
TJ-C4	O	3-Me	5-Me	Bn	N.A.	N.A.	N.A.	>50	2.2 ± 0.18	>50	>20
TJ-C5	O	3-OMe	H	Bn	N.A.	N.A.	11 ± 3.9	>50	1.7 ± 0.39	>20	>20
TJ-C6	S	4-Cl	H	Bn	N.A.	N.A.	4.3 ± 0.76	7.0 ± 0.17	>50	>50	12.1 ± 1.15
TJ-C7	O	3-NO ₂	H	Bn	N.A.	N.A.	N.A.	>20	2.8 ± 0.22	>20	13.3 ± 0.86
TJ-C8	S	4-NO ₂	H	Bn	N.A.	N.A.	9.0 ± 1.7	7.1 ± 0.86	>50	11.3 ± 0.78	8.9 ± 1.17
TJ-C9	S	3-NO ₂	H	Bn	N.A.	N.A.	10.0 ± 3.4	12.8 ± 0.24	>50	11.6 ± 1.34	18.3 ± 0.53
TJ-C10	O	3-Cl	5-Cl	Bn	N.A.	N.A.	N.A.	>20	11.7 ± 0.81	>20	41% @ 20 μM
TJ-C11	O	4-OMe	H	Bn	N.A.	N.A.	weak	>50	>50	20.0 ± 0.12	>50
TJ-C12	O	4-Cl	H	4-NH ₂ -Ph	N.A.	N.A.	N.A.	>20	>50	13.6 ± 0.16	>20
TJ-C13	O	3-CF ₃	5-CF ₃	4-NH ₂ -Ph	N.A.	N.A.	N.A.	>20	>50	11.9 ± 1.53	>20
TJ-C14	O	3-Me	5-Me	4-NH ₂ -Ph	N.A.	N.A.	1.6 ± 0.66	>20	>50	>20	>20
TJ-C15	S	3-CF ₃	5-CF ₃	4-NO ₂ -Ph	N.A.	N.A.	N.A.	9.9 ± 0.49	7.2 ± 1.50	6.3 ± 0.90	6.0 ± 0.59
TJ-C16	S	3-OMe	H	4-NO ₂ -Ph	N.A.	N.A.	13.0 ± 6.5	>50	>50	>50	>20
TJ-C17	S	3-Cl	H	4-NO ₂ -Ph	N.A.	N.A.	N.A.	4.6 ± 0.04	>50	>50	4.99 ± 0.05
TJ-C18	O	4-OMe	H	4-NO ₂ -Ph	N.A.	N.A.	4.6 ± 0.36	>20	>50	>50	>20
TJ-C19	S	4-NO ₂	H	3-OH-Bn	N.A.	N.A.	N.A.	28% @ 20 μM	10.8 ± 0.83	10.1 ± 1.42	>20
TJ-C20	S	3-NO ₂	H	3-OH-Bn	N.A.	N.A.	N.A.	11.1 ± 0.99	11.4 ± 0.64	9.8 ± 0.54	13.8 ± 0.81
TJ-C21	O	3-CF ₃	5-CF ₃	3-OH-Bn	N.A.	N.A.	N.A.	17.3 ± 0.42	4.0 ± 0.83	3.0 ± 0.33	>20
TJ-C22	O	3-Cl	5-Cl	3-OH-Bn	N.A.	N.A.	N.A.	>50	2.8 ± 0.45	>50	>20
TJ-C23	O	4-OMe	H	3-OH-Bn	N.A.	N.A.	N.A.	>20	>20	9.4 ± 0.13	>20
TJ-C24	O	3-Me	5-Me	3-OH-Bn	N.A.	N.A.	N.A.	>20	>20	5.8 ± 0.22	>20
TJ-C25	S	3-CF ₃	5-CF ₃	3-OH-Bn	N.A.	N.A.	N.A.	14.9 ± 1.04	>50	12.0 ± 0.58	>20
TJ-C26	S	3-Cl	H	3-OH-Bn	N.A.	N.A.	N.A.	10.7 ± 0.59	1.8 ± 0.36	5.8 ± 0.22	17.4 ± 0.53
TJ-C27	O	3-CF ₃	5-CF ₃	<i>trans</i> -4-OH-Cy	N.A.	N.A.	N.A.	>20	7.1 ± 0.89	10.1 ± 1.06	50% @ 20 μM
TJ-C28	O	3-Cl	5-Cl	<i>trans</i> -4-OH-Cy	N.A.	N.A.	N.A.	>20	>20	14.1 ± 0.61	>50
TJ-C29	S	4-NO ₂	H	<i>trans</i> -4-OH-Cy	N.A.	N.A.	N.A.	5.4 ± 0.55	11.6 ± 1.19	1.5 ± 0.75	10.5 ± 1.01
TJ-C30	O	4-NO ₂	H	<i>trans</i> -4-OH-Cy	N.A.	N.A.	N.A.	10.5 ± 1.38	8.9 ± 0.22	4.1 ± 0.07	9.0 ± 0.56
TJ-C31	S	3-CF ₃	5-CF ₃	<i>cis</i> -4-OH-Cy	N.A.	N.A.	N.A.	10.9 ± 0.50	2.6 ± 1.08	6.3 ± 0.34	>20
TJ-C32	O	3-CF ₃	5-CF ₃	<i>cis</i> -4-OH-Cy	N.A.	N.A.	N.A.	14.1 ± 1.37	3.1 ± 0.44	9.3 ± 0.66	14.1 ± 0.57
TJ-C33	S	4-NO ₂	H	<i>cis</i> -4-OH-Cy	N.A.	N.A.	N.A.	>20	>50	9.4 ± 0.84	20.0 ± 1.23
TJ-C34	O	4-NO ₂	H	<i>cis</i> -4-OH-Cy	N.A.	N.A.	N.A.	>20	>20	12.4 ± 0.01	8.6 ± 0.18

^aThe mean values and standard deviations of the K_i values were derived based on the outcomes of three parallel measurements. N.A.: no obvious sign of binding was observed; weak: dose-dependent FP signals were observed, but the change in the FP signals (up to a 100 μM concentration) was not significant enough to determine the K_i value accurately. ^bThe mean values and standard deviations of the IC₅₀ values were derived based on the outcomes of three parallel measurements. Cell viability percentage at 20 μM was provided for the case that could not be normally fitted.

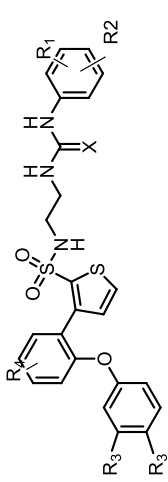
positive energy of 3.94 kcal/mol associated with this site indicates its poor stability inside the binding pocket. According to our predicted binding mode, the terminal hydroxyl group on YCW-E10 forms a hydrogen bond with V249 after displacing the unstable water molecule at this site. This may explain why the newly synthesized compounds with hydrogen bond donors at this location can maintain good binding affinity to Mcl-1. In addition, there are two high-energy sites at the right part of the binding pocket, that is, site #2 and site #4. Interestingly, locations of these two sites overlap with the 3- and 5-substituent positions on the γ-phenyl ring on YCW-E10 (Figure 2a). In fact, the compounds with 3,5-dichloro or 3,5-ditri-fluoromethyl substituents on this phenyl ring generally show high binding affinity to Mcl-1. Besides, this binding mode also reveals that the α-phenyl ring on YCW-E10 fills up a relatively narrow cavity

formed by residues M231, V249, and M250. It thus explains why the attempt of replacing the α-phenyl ring essentially failed.

It appears that this predicted binding mode is able to interpret the basic structure–activity relationship observed among the newly obtained compounds summarized in Tables 1 and 2. Encouraged by the outcome of this analysis, we turned our attention to the other two hydration sites with positive energies near the β-phenyl ring on the lead compound, that is, site #3 (2.66 kcal/mol) and site #5 (0.96 kcal/mol). These two sites are surrounded mainly by hydrophobic residues, such as A227, F228, and M231. Therefore, introduction of small-size, hydrophobic groups onto the β-phenyl ring may further improve binding affinity to Mcl-1 protein.

Accordingly, a total of 20 compounds with 4-methyl or 5-isopropyl substitutions on the β-phenyl ring (i.e., FWJ-D1–D20) were synthesized with the methods outlined in Scheme 1

Table 3. Chemical Structures, Binding Data, and Cytotoxicity of Compounds FWJ-D1–FWJ-D20



compound	X	K_i (μM) ^a										cytotoxicity (IC ₅₀ , μM) ^b				
		R ₁	R ₂	R ₃	R ₄	Bcl-x _L	Bcl-2	Mcl-1	HeLa	HL-60	RS4;11	HEK293T				
YCW-E5	S	3-CF ₃	5-CF ₃	OH	H	N.A.	N.A.	0.84 ± 0.32	>50	4.3 ± 0.51	4.8 ± 0.05	7.5 ± 0.41				
FWJ-D1	S	3-CF ₃	5-CF ₃	OH	4-Me	N.A.	N.A.	0.73 ± 0.09	8.0 ± 0.52	3.2 ± 0.07	4.8 ± 0.41	8.0 ± 0.33				
FWJ-D2	S	3-CF ₃	5-CF ₃	OH	5- <i>i</i> Pr	4.9 ± 2.5	4.9 ± 2.5	2.1 ± 0.51	>20	8.2 ± 0.77	3.7 ± 0.29	18.1 ± 0.74				
FWJ-D3	S	3-CF ₃	5-CF ₃	OMe	5- <i>i</i> Pr	N.A.	N.A.	12 ± 1.2	8.3 ± 0.53	6.9 ± 0.89	5.5 ± 0.04	10.2 ± 0.25				
YCW-E10	O	3-CF ₃	5-CF ₃	OH	H	N.A.	N.A.	17.0 ± 0.6	>50	5.7 ± 0.18	4.9 ± 0.17	8.9 ± 1.06				
FWJ-D4	O	3-CF ₃	5-CF ₃	OH	4-Me	N.A.	N.A.	0.49 ± 0.10	9.7 ± 0.78	3.7 ± 0.74	5.6 ± 0.14	>20				
FWJ-D5	O	3-CF ₃	5-CF ₃	OMe	4-Me	N.A.	N.A.	4.9 ± 0.79	10.2 ± 0.16	5.3 ± 0.06	5.6 ± 0.39	9.0 ± 1.06				
FWJ-D6	O	3-CF ₃	5-CF ₃	OH	5- <i>i</i> Pr	N.A.	N.A.	0.36 ± 0.06	>50	23% @ 20 μM	6.8 ± 0.82	>20				
FWJ-D7	O	3-CF ₃	5-CF ₃	OMe	5- <i>i</i> Pr	N.A.	N.A.	N.A.	11.6 ± 0.72	7.4 ± 0.63	11.7 ± 0.11	12.1 ± 0.36				
YCW-E11	O	3-Cl	5-Cl	OH	H	N.A.	N.A.	1.4 ± 0.54	>50	6.9 ± 1.24	6.2 ± 0.32	10.7 ± 1.58				
FWJ-D8	O	3-Cl	5-Cl	OH	4-Me	N.A.	N.A.	0.59 ± 0.10	6.5 ± 0.36	3.5 ± 0.08	5.1 ± 0.26	6.7 ± 1.00				
FWJ-D9	O	3-Cl	5-Cl	OH	5- <i>i</i> Pr	N.A.	N.A.	0.36 ± 0.04	>50	6.5 ± 1.13	6.4 ± 0.38	>20				
FWJ-D10	O	3-Cl	5-Cl	OMe	5- <i>i</i> Pr	N.A.	N.A.	weak	11.6 ± 0.19	6.5 ± 0.35	9.0 ± 1.03	11.9 ± 0.84				
FWJ-D11	S	3-NO ₂	H	OH	4-Me	N.A.	N.A.	7.5 ± 2.0	40% @ 20 μM	3.4 ± 0.35	6.1 ± 0.63	7.9 ± 0.26				
FWJ-D12	O	3-NO ₂	H	OH	4-Me	N.A.	N.A.	13.0 ± 7.2	>20	6.0 ± 1.01	9.1 ± 0.49	6.8 ± 0.67				
FWJ-D13	S	4-NO ₂	H	OH	4-Me	N.A.	N.A.	1.5 ± 0.67	6.8 ± 0.90	2.9 ± 0.54	5.1 ± 0.93	8.2 ± 0.50				
FWJ-D14	S	4-NO ₂	H	OH	5- <i>i</i> Pr	N.A.	N.A.	N.A.	>20	8.8 ± 0.93	5.1 ± 0.10	16.3 ± 1.74				
FWJ-D15	S	4-NO ₂	H	OMe	5- <i>i</i> Pr	N.A.	N.A.	N.A.	11.9 ± 0.95	11.2 ± 0.33	5.8 ± 0.52	11.4 ± 0.51				
FWJ-D16	O	4-NO ₂	H	OH	4-Me	N.A.	N.A.	13.0 ± 1.2	>20	3.9 ± 0.47	7.7 ± 0.42	48% @ 20 μM				
FWJ-D17	S	3-OMe	H	OH	4-Me	N.A.	N.A.	6.0 ± 0.76	>50	>50	>20	>50				
FWJ-D18	O	3-OMe	H	OH	4-Me	N.A.	N.A.	weak	>20	3.6 ± 0.23	7.5 ± 0.05	>20				
FWJ-D19	S	4-OMe	H	OH	4-Me	N.A.	N.A.	N.A.	>20	4.1 ± 0.78	8.3 ± 1.28	>20				
FWJ-D20	O	4-OMe	H	OH	4-Me	N.A.	N.A.	weak	>20	6.1 ± 0.67	8.2 ± 0.12	>20				

^aThe mean values and standard deviations of the K_i values were derived based on the outcomes of three parallel measurements. N.A.: no obvious sign of binding was observed; weak: dose-dependent FP signals were observed, but the change in the FP signals (up to a 100 μM concentration) was not significant enough to determine the K_i value accurately. ^bThe mean values and standard deviations of the IC₅₀ values were derived based on the outcomes of three parallel measurements. Cell viability percentage at 20 μM was provided for the case that could not be normally fitted.

(Table 3). Note that this set of compounds shares exactly the same structural scaffold as the lead compounds. Binding assay results indicate that most of these new compounds reserve the selectivity toward Mcl-1 as the lead compounds. Here, some derivative compounds with the 4-Me or 5-*i*-Pr group on the β -phenyl ring achieve improved binding affinity to Mcl-1. For example, the Mcl-1 binding affinity of FWJ-D4 or FWJ-D6 is improved by 4–6 times as compared to YCW-E10. Considering that the methyl or isopropyl group is rather small in size, this amount of improvement is promising. The predicted binding mode of FWJ-D4 to Mcl-1 protein is shown in Figure 2b. One can see here that the additional methyl group introduced on the β -phenyl ring displaces the high-energy water site #3, which provides an explanation for the improvement in binding affinity. In addition, FWJ-D4 and FWJ-D6 now bind to Mcl-1 specifically, while YCW-E10 is still a dual inhibitor of Mcl-1 and Bcl-2. Here, another observation is that if the two hydroxyl groups on the α -phenyl ring are protected as methoxy groups, Mcl-1 binding affinity of the resulting compounds (i.e., FWJ-D3, FWJ-D5, FWJ-D7, FWJ-D10, and FWJ-D15) will decrease significantly or even lose completely. This again verifies the critical role of the two hydroxyl groups. In terms of cytotoxicity on cell lines, most of this set of compounds shows good cytotoxicity ($IC_{50} < 10 \mu M$) on two leukemia cell lines (i.e., HL-60 and RS4;11) and obvious cytotoxicity (typically $IC_{50} < 12 \mu M$) on HEK293T cells as well. Nevertheless, FWJ-D4 and FWJ-D9 show much less toxicity ($IC_{50} > 20 \mu M$) on HEK293T while maintaining IC_{50} values of 3–7 μM on the leukemia cell lines. Selective cytotoxicity toward leukemia cells is another notable improvement achieved in our optimization.

Two-dimensional HSQC spectroscopy was employed in our work to characterize the binding of these active compounds to ^{15}N -labeled Mcl-1 protein. Three of our compounds, including YCW-E10, FWJ-D2, and FWJ-D4, were selected for this test. In addition, a known selective Mcl-1 inhibitor, A-1210477,³¹ was also considered as the positive control. The HSQC spectrum of the free Mcl-1, which is publicly available from the Biological Magnetic Resonance Data Bank (<http://www.bmrb.wisc.edu/>, access number 19654), was used as the reference for assignment of chemical shifts. After superimposing the ^{15}N -HSQC spectra of the free Mcl-1 protein and the Mcl-1 complex, the chemical shift of each residue was calculated. By comparing the ^{15}N -HSQC spectra of the Mcl-1 protein in complex with A-1210477 and those with our thiophene-2-sulfonamide compounds, a number of residues with similar chemical shifts can be found (Figure 3a–d). Here, the residues with significant chemical shifts after adding the compounds include H224, F228, M231, L235, M250, and R263. These residues generally locate around the BH3 binding groove on Mcl-1. Although HSQC spectroscopy does not provide structural information at the atomic level, the results shown in Figure 3 are still strong proofs of our hypothesis, that is, the thiophene-2-sulfonamide derivative compounds bind at the BH3 binding groove on Mcl-1 as expected. It also supports the predicted binding mode shown in Figure 2b.

Despite the encouraging results obtained in bioassays, we have observed that many compounds obtained in our work encounter water solubility problem in sample preparation. We suspect that it is one of the reasons that prevent this class of compounds that achieves an even higher level of potency. Among the newly synthesized compounds, we managed to obtain the crystal structure of FWJ-D7 (Figure 4), which was deposited into the CSD database on May 20, 2019 (access

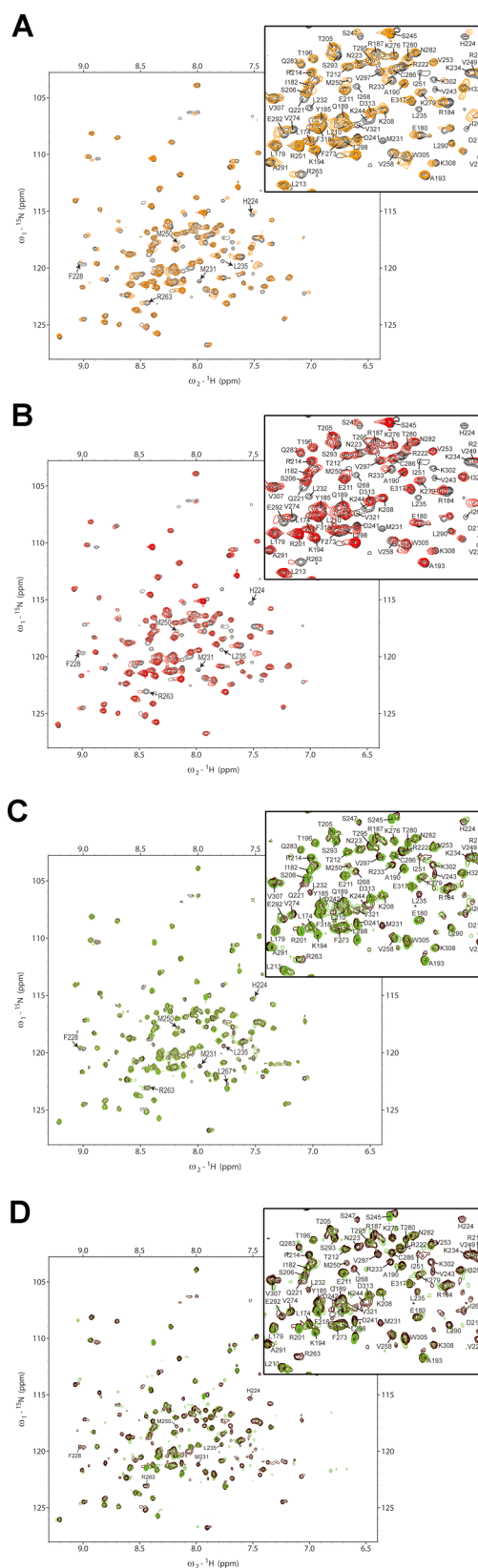


Figure 3. Superimposed ^{15}N -HSQC spectra of the free Mcl-1 (in black) and Mcl-1 in complex with compounds (A) YCW-E10, (B) FWJ-D2, (C) FWJ-D4, and (D) A1210477. The six residues with obvious chemical shifts near the BH3 peptide binding pocket are labeled explicitly. The enlarged view of the focused residues is provided in the upper right corner of each figure.

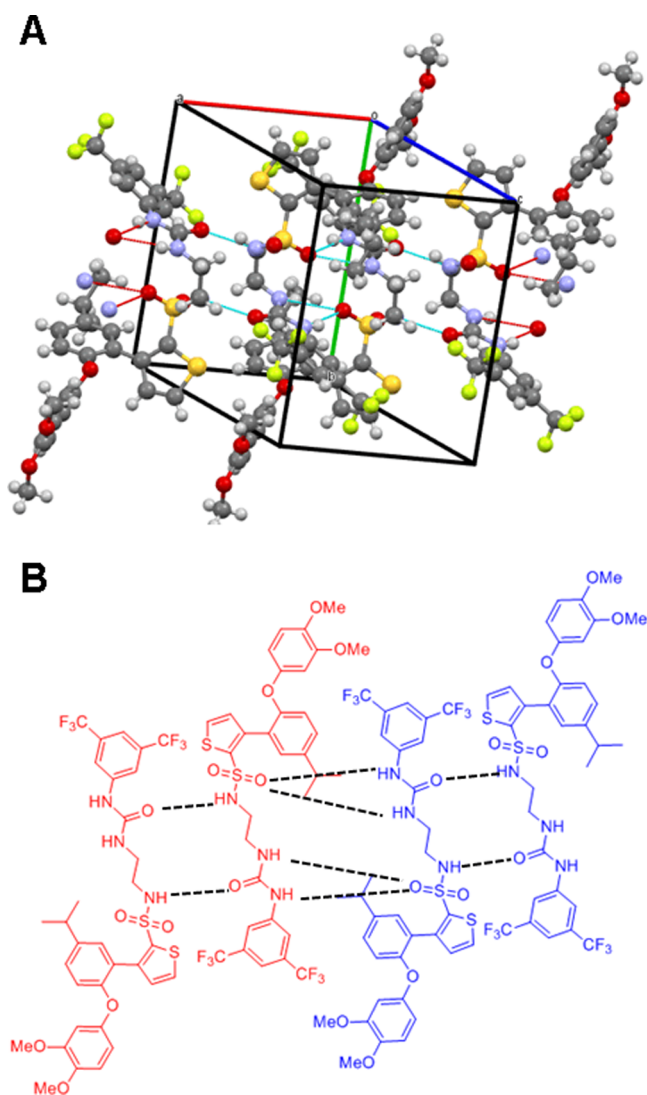


Figure 4. (A) Crystal packing of FWJ-D7 (CSD number: 1917331); (B) two-dimensional illustration of the hydrogen bonding network observed in this crystal structure.

number: 1917331). This structure indicates that there is a complex hydrogen bond network formed between FWJ-D7 molecules due to crystal packing (Figure 4). Such a hydrogen bond network certainly enhances the crystal lattice energy, which in turn results in the poor water solubility.

In an attempt to reduce this effect, we designed another set of compounds by replacing the ethylenediamine moiety with a piperazine ring (Table 4). The aim was to remove the intermolecular hydrogen bonds existing in the crystal structure. The piperazine ring was chosen mainly due to the convenience of synthesis. As a result, compounds FWJ-E1–FWJ-E18 were synthesized with the methods outlined in Scheme 2. Although water solubility of this set of compounds was somewhat improved according to our qualitative judgement, basically, all of them do not have the desired affinity to Mcl-1 (i.e., inhibition ratio >50% in the FP binding assay at a dose of 100 μ M). Interestingly, all such weak Mcl-1 inhibitors have two naked hydroxyl groups on the α -phenyl ring, which is consistent with the structure–activity relationship observed in other sets of

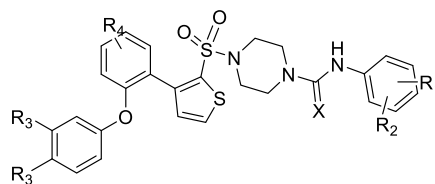
compounds in our work. Moreover, all such weak Mcl-1 inhibitors still have obvious cytotoxicity (typically $IC_{50} < 10 \mu$ M) on the two leukemia cell lines (i.e., HL-60 and RS4;11) and a reasonable selectivity toward HEK293T cells ($IC_{50} > 20 \mu$ M). In contrast, the corresponding compounds with the two critical hydroxyl groups protected in the methoxy form do not exhibit any obvious cytotoxicity on all four cell lines considered in our work. We therefore conclude that this set of compounds still has potential if their structures are properly optimized. This hypothesis, however, was not testified in this work because we had obtained other more promising candidates for further investigation.

Characterization of the Pro-Apoptotic Effects of the Thiophene-2-Sulfonamide Compounds. Three compounds obtained in our work, that is, FWJ-D4, FWJ-D5, and YCW-E16, were selected and examined in several types of assays to characterize their apoptosis-inducing effects on the RS4;11 cells. Here, FWJ-D4 was the most potent one in the binding assay and cell viability assay. FWJ-D5 is the precursor of FWJ-D4 with the hydroxyl groups protected by methoxy groups. The binding affinity of FWJ-D5 to Mcl-1 is about 10-fold weaker than that of FWJ-D4. However, it has similar toxicities to FWJ-D4 on HL-60 and RS4;11 cell lines. The lead compound YCW-E16 was chosen for making a comparison. ABT-199 was used as the positive reference in all assays.

Several commonly used indicators for characterizing apoptosis include changes in mitochondrial membrane potential (MOMP), transfer of phosphatidyl-serine (PS), and changes of plasma membrane permeability. These indicators could be quantified by using the corresponding dyeing methods. In our study, flow cytometry analysis with MitoDamage staining was employed to detect the three indicators of apoptosis mentioned above. After treatment by the selected compounds at five doses, that is, 2.5, 5, 10, 20, and 40 μ M for 24 h, RS4;11 cells were stained with 7-AAD, annexin V, and MitoSense Red and then analyzed by flow cytometry. Annexin V and 7-AAD were used to detect the state of PS and the plasma membrane permeability of the cells, respectively. The combination of 7-AAD and annexin V was used to differentiate cells in early apoptosis [annexin V (+) and 7-AAD (–)] and late apoptosis [annexin V (+) and 7-AAD (+)], corresponding to the bottom and upper right regions in Figure 5. As for the cells treated with dimethyl sulfoxide (DMSO), less than 5% of them were observed to be in the early or late stage of apoptosis. After the tested compounds were added, the ratio of apoptotic cells increased in an obvious dose-dependent manner (as shown in Figure S1 in the Supporting Information, Part II). For example, when the cells were treated by the given compound at 20 μ M, the ratio of apoptotic cells reached 97, 88, and 98% for YCW-E16, FWJ-D4, and FWJ-D5, respectively (Figure 5). MitoSense Red was used to detect the changes in MOMP, where cells with intact MOMP exhibited high Red2 fluorescence and cells with impaired MOMP exhibited low Red2 fluorescence. As shown in Figure 6, Red2 fluorescence gradually shifted to the left as the concentration of the given compound increased, which was consistent with the results obtained from 7-AAD + annexin V staining. These results indicate that these tested compounds are able to induce cell apoptosis.

To further verify the pro-apoptotic mechanism of these compounds, they were tested in a western blot assay for detecting caspase activation. Here, poly-ADP-ribose polymerase protein (PARP) is a major substrate of activated caspases. Cleavage of PARP is one of the indicators of caspase-dependent

Table 4. Chemical Structures, Binding Data, and Cytotoxicity of Compounds FWJ-E1–FWJ-E18



compound	X	R ₁	R ₂	R ₃	R ₄	inhibition at 100 μM			cytotoxicity (IC ₅₀ , μM) ^a			
						Bcl-x _L (%)	Bcl-2 (%)	Mcl-1 (%)	HeLa	HL-60	RS4;11	HEK293T
FWJ-E1	S	4-NO ₂	H	OH	H	28	31	81	49% @ 20 μM	5.3 ± 0.25	9.0 ± 0.89	>20
FWJ-E2	S	4-NO ₂	H	OMe	H	18	16	33	>50	>50	>50	>20
FWJ-E3	S	4-NO ₂	H	OMe	5-NO ₂	27	16	26	>50	>50	>50	>50
FWJ-E4	O	4-NO ₂	H	OH	H	29	33	63	>20	4.9 ± 0.33	14.3 ± 1.17	>20
FWJ-E5	O	4-NO ₂	H	OMe	H	20	17	22	>50	>50	>50	>20
FWJ-E6	O	4-NO ₂	H	OMe	5-NO ₂	44	19	37	>50	>50	>50	>20
FWJ-E7	O	3-NO ₂	H	OH	H	34	30	74	>20	4.5 ± 0.27	9.8 ± 1.00	>20
FWJ-E8	O	3-NO ₂	H	OMe	H	19	18	31	>50	>50	>50	>20
FWJ-E9	S	3-CF ₃	5-CF ₃	OH	H	12	20	72	>20	2.2 ± 0.22	7.3 ± 0.28	>20
FWJ-E10	S	3-CF ₃	5-CF ₃	OH	5-NO ₂	14	12	52	>20	8.4 ± 0.42	9.5 ± 0.30	>20
FWJ-E11	S	3-CF ₃	5-CF ₃	OMe	H	29	25	66	>50	38% @ 20 μM	>50	42% @ 20 μM
FWJ-E12	O	3-CF ₃	5-CF ₃	OH	H	-8	7	47	20% @ 20 μM	15% @ 20 μM	10% @ 20 μM	29% @ 20 μM
FWJ-E13	O	3-CF ₃	5-CF ₃	OMe	H	24	23	44	>50	>20	>50	>20
FWJ-E14	S	4-Cl	H	OH	H	3	2	20	>50	5.5 ± 0.39	7.5 ± 0.48	>50
FWJ-E15	S	4-Cl	H	OMe	H	33	18	43	>50	>50	>50	>20
FWJ-E16	S	4-Cl	H	OMe	5-NO ₂	37	18	41	>50	>50	>50	>50
FWJ-E17	O	4-F	H	OH	H	32	33	95	14.8 ± 2.08	8.1 ± 1.56	6.8 ± 0.28	15.5 ± 1.29
FWJ-E18	O	4-F	H	OMe	H	33	15	28	>20	>20	14.9 ± 3.10	>50

^aThe mean values and standard deviations of the IC₅₀ values were derived based on the outcomes of three parallel measurements. Cell viability percentage at 20 μM was provided for the case that could not be normally fitted.

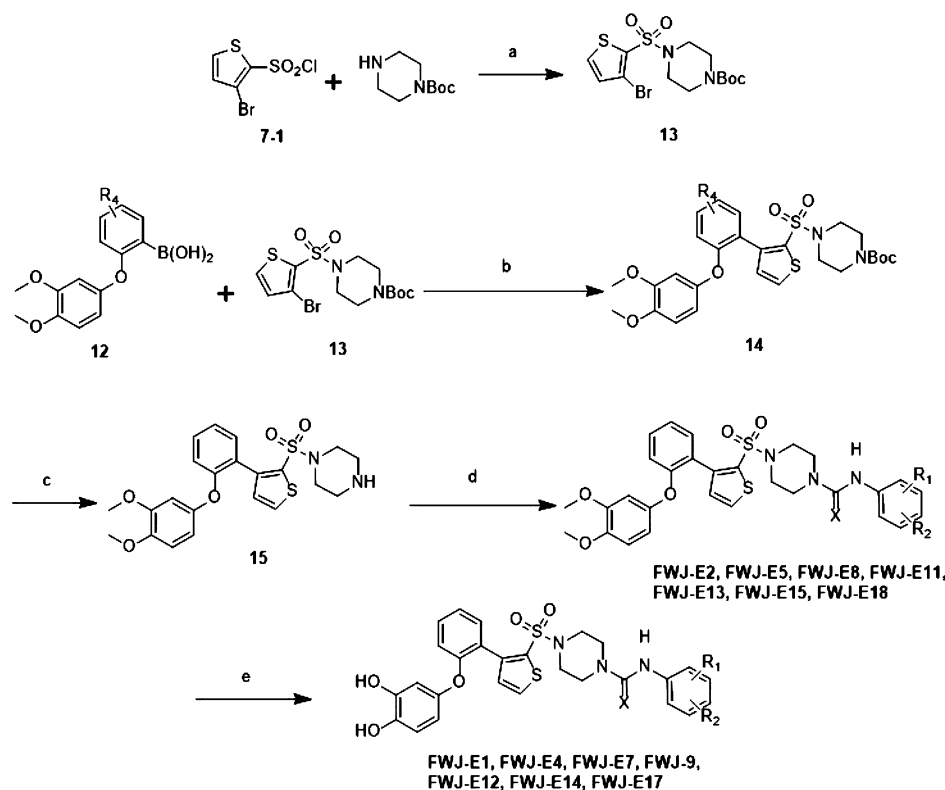
apoptosis. In our work, YCW-E16 and FWJ-D5 exhibited significant pro-apoptotic signals in flow cytometry analysis, and thus, they were tested in the caspase activation assay. Again, DMSO and ABT-199 were used as the negative and positive controls, respectively. Our results showed that the full-length PARP (116 kDa) degraded and the cleaved PARP (89 kDa) increased after treatment with these two compounds (Figure 7). After the compound concentration was increased from 2.5 to 40 μM, the cleaved PARP, cleaved caspase-3, and cleaved caspase-9 were increased generally in a dose-dependent manner. This observation again confirms the results of our flow cytometry analysis that these compounds are able to induce the caspase-dependent apoptosis.

To verify target engagement at the cellular level, we performed the co-immunoprecipitation (co-IP) assay on MCF-7 cells that expressed high levels of both Bcl-2 and Mcl-1. ABT-199 (a selective Bcl-2 inhibitor) and A-1210477 (a selective Mcl-1 inhibitor) were used as controls in this assay. As can be seen in Figure 8, both compounds produced the biological effects as expected. Here, FWJ-D4 and FWJ-D5 treatment at 10 μM led to the disruption of Mcl-1/Bim interactions by 70 and 30%, respectively, where they had no obvious effect on the Bcl-2/Bim complex. Notably, YCW-E16 treatment at 10 μM disrupted both Mcl-1/Bim and Bcl-2/Bim interactions by 30 and 20%, respectively. All these observations were in full agreement with the results obtained in our binding assay, that is, FWJ-D4 and FWJ-D5 are selective Mcl-1 inhibitors, while YCW-E16 is a dual inhibitor of Bcl-2 and Mcl-1.

In Vivo Efficacy of FWJ-D5 on the Xenograft Mouse Model. Compound FWJ-D5 was chosen to be tested on a

xenograft mouse model of human acute lymphoblastic leukemia cells (RS4;11) because it was among the most potent compounds identified in our binding assay and cellular assays. At the same time, it was expected to have a low toxicity due to protection of the dihydroxyl groups. When the tumor on the xenograft mice grew to a volume of 250 mm³, the mice were grouped and treated intraperitoneally with FWJ-D5 in 12.5, 25, and 50 mg/kg every 2 days for 22 days. Tumor volumes were measured every 3 days. Among the high-dose group (i.e., 50 mg/kg), tumor volume was reduced by up to 75% (Figure 9a). Treatment of FWJ-D5 at 12.5 and 25 mg/kg also suppressed the tumor growth significantly, with an inhibition rate over 60%. Notably, FWJ-D5 was well tolerated by the mice without obvious body weight loss as compared to the blank group (Figure 9b).

FWJ-D5 was also evaluated in terms of the tumor mitotic index (Ki-67) using histological and immunohistochemical techniques. When the RS4;11 xenograft mice were treated by FWJ-D5 for 19 days, tumor samples were collected and analyzed. Tumor tissues from the blank group (i.e., DMSO only) were stained strongly with Ki-67, indicating a large fraction of highly proliferative cells (Figure 10a). In comparison, positive cells under Ki-67 staining decreased in a dose-dependent manner under the treatment of FWJ-D5 (Figure 10c–e). When the xenograft mice were treated by FWJ-D5 in 50 mg/kg, positive cells under Ki-67 staining generally disappeared, achieving an effect comparable to that of ABT-199 (Figure 10b). The results of this assay proved that FWJ-D5 was able to attenuate the proliferation of RS4;11 tumor cells.

Scheme 2. Synthesis of Compounds FWJ-E1, FWJ-E2, FWJ-E4, FWJ-E5, FWJ-E7–FWJ-E9, FWJ-E11–FWJ-E15, FWJ-E17, and FWJ-E18^a

^aReagents and conditions: (a) TEA, DCM, 0 °C; (b) Pd(OAc)₂, K₃PO₄, Ph₂Pcy, THF; (c) TFA, DCM; (d) aryl isothiocyanate, DCM; (e) BBr₃, DCM.

CONCLUSIONS

In this work, we have selected the compounds obtained in our previous work, which contain a 3-phenylthiophene-2-sulfonamide core moiety, for structural optimization with the aim of improving their binding affinity and selectivity toward Mcl-1. ¹⁵N-HSQC spectra of a chosen lead compound (i.e., YCW-E10) suggested that it bound to the BH3-binding groove on Mcl-1. Its binding mode to Mcl-1 was predicted by MD simulation and then used to guide structure-based optimization. A total of 85 new compounds were synthesized and all tested in a FP-based binding assay and cytotoxicity assays. As compared to the lead compound, some new compounds, such as FWJ-D4, FWJ-D6, and FWJ-D9, achieved 4–6-fold higher affinity and excellent selectivity toward Mcl-1 in the binding assay. Moreover, such compounds exhibited a micromolar level of cytotoxicity on HL-60 and RS4;11 cells and much less cytotoxicity on HEK293T cells. Interestingly, we also obtained some compounds, such as TJ-A1–TJ-A3 and TJ-B1–TJ-B3, with a microlevel of binding affinity to all three targets (i.e., Mcl-1, Bcl-2, and Bcl-x_L). Their potential as pan inhibitors of anti-apoptotic Bcl-2 family proteins provides other possibilities for further investigation. In this work, we selected FWJ-D4 and its precursor FWJ-D5 for in-depth study. Several apoptotic assays indicated that they effectively induced caspase-dependent apoptosis. An additional co-immunoprecipitation assay proved target engagement at Mcl-1 at the cellular level for both compounds. FWJ-D5 was further tested on an RS4;11 xenograft mouse model, where it exhibited a tumor inhibition effect in a clear dose-dependent manner. Treatment of xenograft mice with FWJ-D5 at the dose of 12.5–50 mg/kg led to 60–75% reduction in tumor volume without

body weight loss. In conclusion, this class of compounds can serve as promising candidates for developing new anti-cancer drugs by targeting the anti-apoptotic Bcl-2 family proteins.

EXPERIMENTAL SECTION

Synthesis. The overall synthetic route of all new compounds essentially followed the protocol reported in our previous work.³⁸ All reagents and starting materials used in our synthesis were purchased from Lancaster, Acros, and Shanghai Chemical Reagent Corp. They were used without further purification unless specified.

The general procedure for the synthesis of compounds TJ-A1–TJ-A10, TJ-B1–TJ-B3, TJ-C1–TJ-C34, and FWJ-D1–FWJ-D20 (see Scheme 1) is described as follows:

Phenol 1 (25.9 mmol) and 2-nitrofluorobenzene 2 (23.5 mmol) were added into a 100 mL flask with 60% NaH (39.9 mmol) and tetrahydrofuran (THF) (38 mL). The mixture was heated at reflux for 2 h with stirring to give 3. 3 (23.3 mmol) was reduced to its amino product 4 by reacting with 10% Pd/C (640 mg), EtOH (80 mL), and hydrazine (13 mL) under nitrogen protection. The reaction of 4 (22.8 mmol) with H₂SO₄ (68.4 mmol), NaNO₂ (45.6 mmol), and KI (45.6 mmol) in an ice-water bath gave iodine product 5. Under argon protection, 5 (19.1 mmol) was reacted with *n*-butyllithium (38.2 mmol) and trimethyl borate (47.8 mmol) to obtain product 6.

Intermediate 9 was obtained via the reaction of bromo-substituted 2-sulfonamidothiophene 7 (7.64 mmol) with single Boc-protected ethylenediamine 8 (11.46 mmol).

Compound 6 (2.56 mmol), 9 (2.13 mmol), palladium acetate (0.213 mmol), triphenylphosphine (0.425 mmol), and potassium phosphate (6.38 mmol) were added into a 100 mL flask. After full deoxygenation, THF (25 mL) and water (5 mL) were added to dissolve the reactants. The solution was then heated under reflux for 4 h. The residue was concentrated and extracted by water (15 mL) and ethyl acetate (30 mL) three times. It was purified by chromatography (EtOAc/

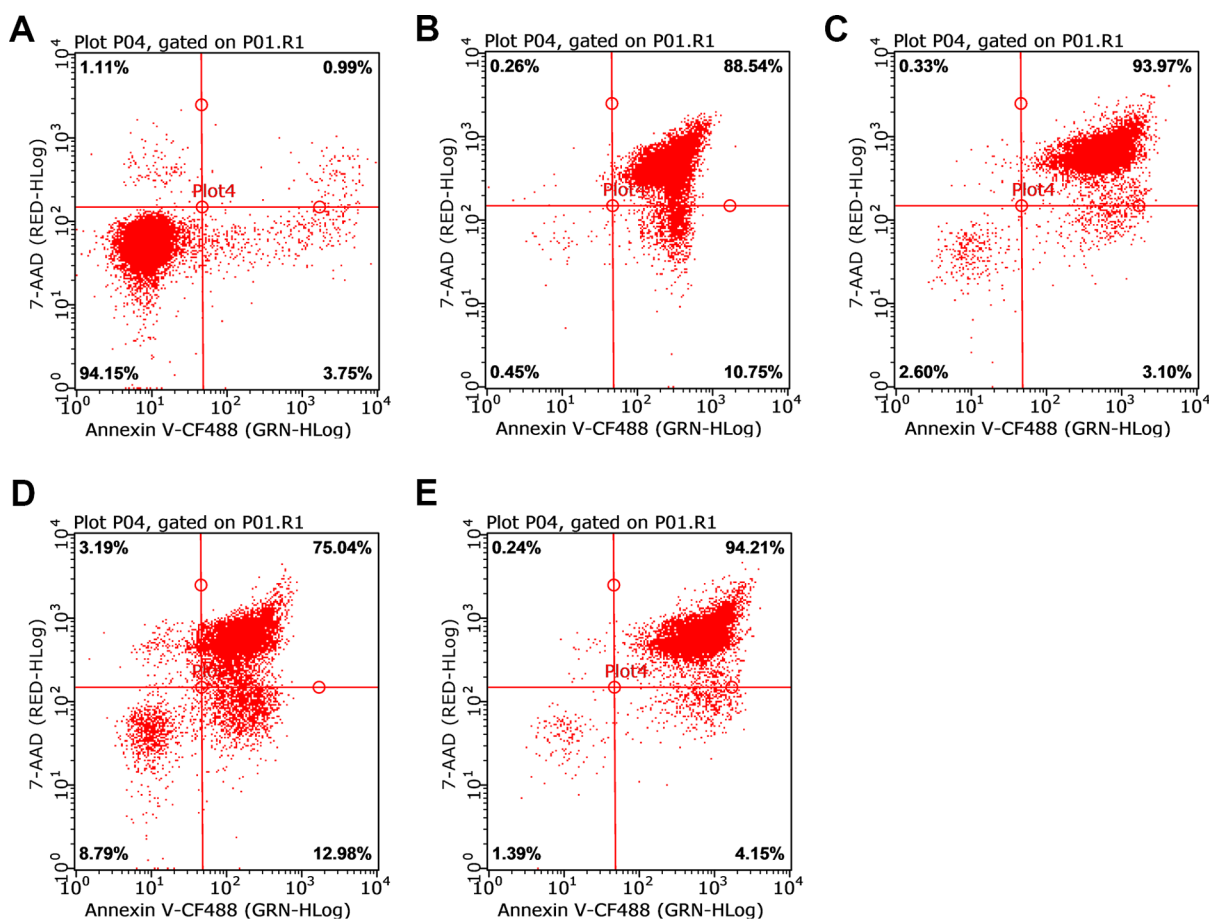


Figure 5. Results of flow cytometric analysis on Annexin V- and 7-AAD-stained RS4;11 cells for DMSO [(A), 1%], ABT-199 [(B), 1 μ M], and three selected compounds, that is, YCW-E16 [(C), 20 μ M], FWJ-D4 [(D), 20 μ M], and FWJ-D5 [(E), 20 μ M]. Cells were treated by compounds for 24 h. Here, DMSO and ABT-199 were used as the negative control and the positive control, respectively.

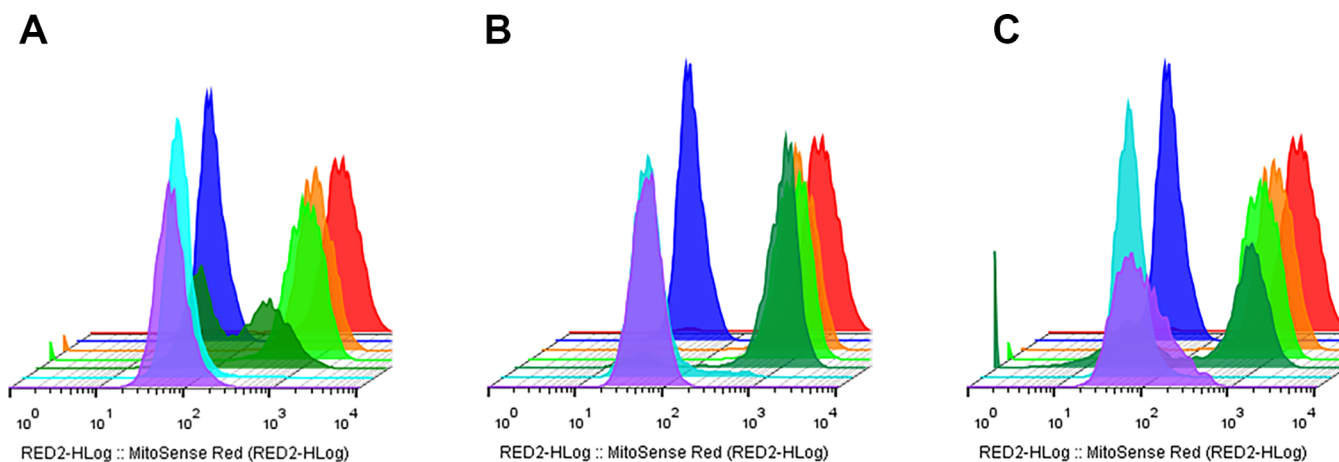


Figure 6. Results of flow cytometric analysis with MitoSense Red-stained RS4;11 cells for three selected compounds: (A) YCW-E16; (B) FWJ-D4; (C) FWJ-D5. Cells were treated by compounds at doses of 2.5 μ M (orange), 5 μ M (green), 10 μ M (dark green), 20 μ M (cyan), and 40 μ M (purple) for 24 h. Here, DMSO (red) and ABT-199 (1 μ M, blue) were used as the negative control and the positive control, respectively.

petroleum ether 1:10–1:5) to obtain **10**, which was further reacted with DCM and TFA to give **11** by removing the Boc-protecting group.

Compound **11** (~50 mg), CH_2Cl_2 (3 mL), and 1.2 equiv of isocyanate or isothiocyanate were added into a 25 mL flask. The mixture was stirred at room temperature until the reaction was complete. The residue was purified by chromatography (EtOAc/petroleum ether 1:3) to obtain the final compounds described in this

work, including TJ-A1–TJ-A10, TJ-B1–TJ-B3, TJ-C1–TJ-C34, and FWJ-D1–FWJ-D20.

N-(2-(3-(3,5-Bis(trifluoromethyl)phenyl)thioureido)ethyl)-5-(2-(3,4-dihydroxyphenoxy)phenyl)thiophene-2-sulfonamide (TJ-A1). Overall yield: 9.4%, purity: 96.6%. ^1H NMR (400 MHz, CDCl_3): δ 8.32 (s, 1H), 7.81 (s, 2H), 7.62 (d, J = 8.0 Hz, 1H), 7.55 (s, 1H), 7.50 (d, J = 4.0 Hz, 1H), 7.35 (d, J = 4.0 Hz, 1H), 7.24 (t, J = 8.4 Hz, 1H), 7.10 (t, J = 7.6 Hz, 1H), 7.01–6.99 (m, 1H), 6.91 (d, J = 8.4 Hz, 1H),

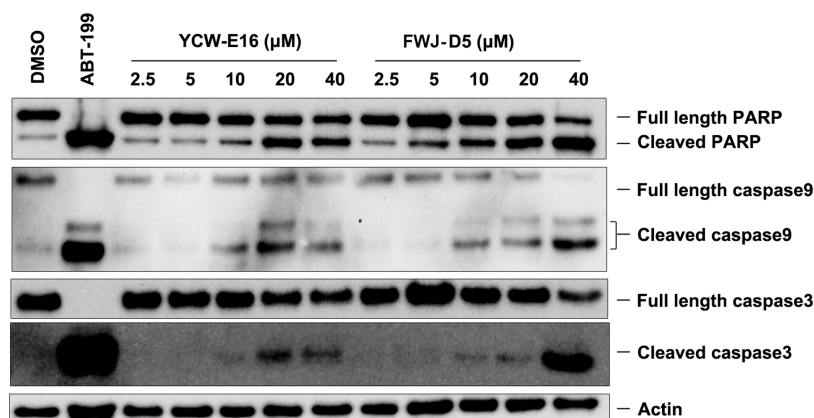


Figure 7. Activation of caspase-3, caspase-9, and PARP by YCW-E16 and FWJ-D5. RS4;11 cells were treated by the given compounds at multiple doses for 48 h. Expression levels of caspase-3, caspase-9, and PARP were detected by western blot.

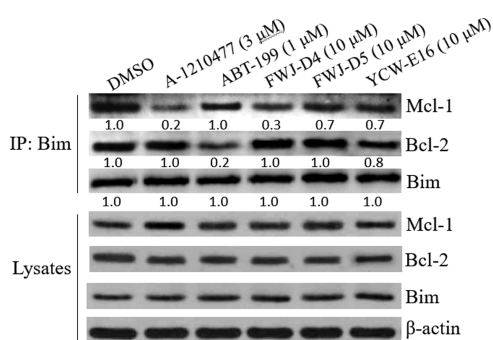


Figure 8. MCF-7 cells were treated with ABT-199 (1 μ M), A-1210477 (3 μ M), FWJ-D4 (10 μ M), FWJ-D5 (10 μ M), and YCW-E16 (10 μ M). Bcl-2 and Mcl-1 immunoprecipitation assays were performed, and the immunoprecipitated fractions were analyzed by immunoblotting for the indicated proteins. The numbers underneath the blots were scanned and semi-quantified by densitometry, which were normalized to loading control (β -actin).

6.73 (d, J = 8.4 Hz, 1H), 6.59 (d, J = 2.8 Hz, 1H), 6.34 (dd, J = 8.4, 2.8 Hz, 1H), 6.03 (s, 1H), 5.74–5.72 (m, 1H), 3.72–3.71 (m, 2H), 3.20–3.19 (m, 2H); 13 C NMR (100 MHz, acetone- d_6): δ 182.5, 155.1, 149.1, 146.8, 145.4, 142.7, 142.4, 141.2, 132.3, 132.2, 132.0, 131.7, 131.5, 130.7, 128.8, 125.7, 125.3, 124.0, 123.8, 123.5, 123.1, 118.9, 117.6, 116.5, 111.3, 108.2, 44.6, 42.9; ESI-MS: m/z 677.9 [M + H] $^+$, 699.8 [M + Na] $^+$; MALDI-HRMS $C_{27}H_{22}N_3O_5F_6S_3$ [M + H] $^+$ calcd, 678.0620; obs., 678.0623.

N-(2-(3-(3,5-Bis(trifluoromethyl)phenyl)ureido)ethyl)-5-(2-(3,4-dihydroxyphenoxy)phenyl)thiophene-2-sulfonamide (TJ-A2). Overall yield: 13.3%, purity: 96.7%. 1 H NMR (400 MHz, acetone- d_6): δ 8.57 (s, 1H), 7.98 (s, 2H), 7.73 (dd, J = 8.0, 1.2 Hz, 1H), 7.51 (d, J = 4.0 Hz, 1H), 7.45 (d, J = 4.0 Hz, 1H), 7.37 (s, 1H), 7.19 (dt, J = 7.8, 1.2 Hz, 1H), 7.02 (dt, J = 7.6, 0.8 Hz, 1H), 6.80 (d, J = 8.4 Hz, 1H), 6.73–6.70 (m, 2H), 6.47 (d, J = 2.8 Hz, 1H), 6.30 (dd, J = 8.4, 2.8 Hz, 1H), 6.10 (m, 1H), 3.29–3.25 (m, 2H), 3.06–3.02 (m, 2H); 13 C NMR (100 MHz, acetone- d_6): δ 156.0, 155.3, 149.6, 147.1, 145.4, 143.5, 143.0, 141.8, 132.9, 132.6, 132.2, 132.1, 131.9, 130.8, 129.1, 128.6, 125.9, 124.2, 123.1, 119.2, 118.5, 118.5, 116.6, 114.9, 111.3, 108.3, 44.4, 40.4; ESI-MS: m/z 661.9 [M + H] $^+$, 683.9 [M + Na] $^+$; MALDI-HRMS $C_{27}H_{22}N_3O_6F_6S_2$ [M + H] $^+$ calcd, 662.0849; obs., 662.0850.

N-(2-(3-(3,5-Dichlorophenyl)ureido)ethyl)-5-(2-(3,4-dihydroxyphenoxy)phenyl)thiophene-2-sulfonamide (TJ-A3). Overall yield: 14.3%, purity: 95.3%. 1 H NMR (400 MHz, acetone- d_6): δ 8.39 (s, 1H), 8.21 (s, 1H), 7.95 (s, 1H), 7.87 (dd, J = 8.0, 1.6 Hz, 1H), 7.65 (d, J = 4.0 Hz, 1H), 7.59 (d, J = 4.0 Hz, 1H), 7.51 (d, J = 1.6 Hz, 1H), 7.33 (td, J = 7.6, 1.6 Hz, 1H), 7.17 (td, J = 7.6, 1.2 Hz, 1H), 6.97 (t, J = 1.6 Hz, 1H), 6.94 (dd, J = 8.4, 0.8 Hz, 1H), 6.87–6.83 (m, 2H), 6.61 (d, J = 2.8 Hz, 1H), 6.44 (dd, J = 8.4, 2.8 Hz, 1H), 6.14–6.13 (m, 1H),

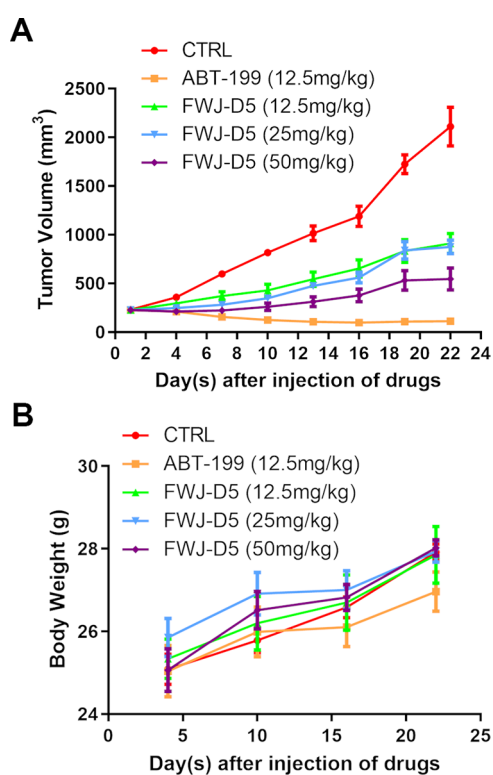


Figure 9. Inhibition of tumor growth of FWJ-D5 on an RS4;11 xenograft mouse model. (A) Changes in tumor volume. (B) Changes in the body weight of the xenograft mouse. Here, xenograft mice were administrated with the vehicle control (red line) or ABT-199 in 12.5 mg/kg (orange line) and FWJ-D5 in 12.5 mg/kg (green line), 25 mg/kg (blue line), and 50 mg/kg (purple line) every 2 days for 22 days.

3.40–3.36 (m, 2H), 3.19–3.15 (m, 2H); 13 C NMR (100 MHz, acetone- d_6): δ 155.9, 155.2, 149.4, 147.0, 145.2, 143.8, 142.9, 141.6, 135.4, 132.0, 130.8, 129.0, 125.8, 124.1, 124.0, 121.5, 119.0, 116.9, 116.6, 111.3, 108.3, 44.4, 40.3; ESI-MS: m/z 593.9 [M + H] $^+$; MALDI-HRMS $C_{25}H_{21}N_3O_6Cl_2S_2Na$ [M + Na] $^+$ calcd, 616.0141; obs., 616.0143.

N-(2-(3-(4-Chlorophenyl)ureido)ethyl)-5-(2-(3,4-dinitrophenoxy)phenyl)thiophene-2-sulfonamide (TJ-A4). Overall yield: 11.4%, purity: 98.8%. 1 H NMR (400 MHz, acetone- d_6): δ 8.24 (d, J = 9.2 Hz, 1H), 8.15 (s, 1H), 7.93 (dd, J = 8.0, 1.6 Hz, 1H), 7.70 (d, J = 2.4 Hz, 1H), 7.58–7.55 (m, 3H), 7.48–7.43 (m, 4H), 7.39 (dd, J = 8.0, 0.8 Hz, 1H), 7.22–7.20 (m, 2H), 6.93–6.90 (m, 1H), 6.01–5.98 (m, 1H), 3.34–3.30 (m, 2H), 3.14–3.10 (m, 2H); 13 C NMR (100 MHz,

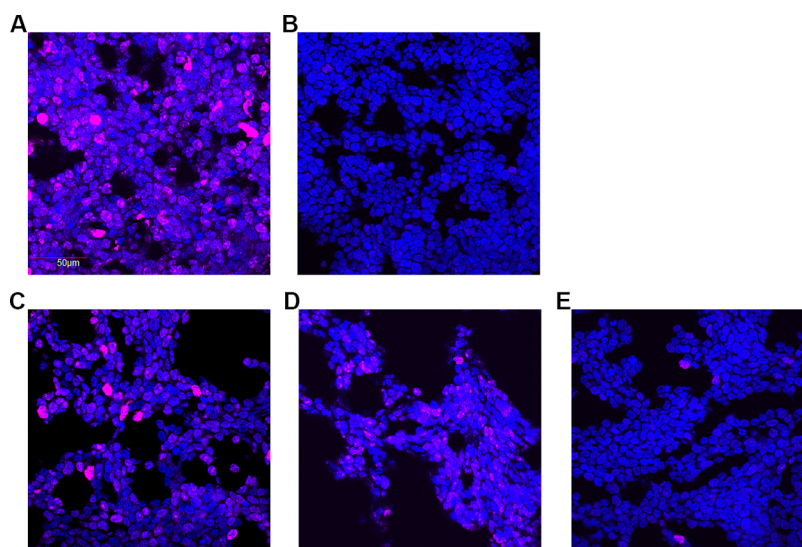


Figure 10. FWJ-D5 inhibited the proliferation of RS4;11 cells in xenograft mice in a dose-dependent manner. Results of Ki-67 staining in tumor tissues treated with (A) DMSO, (B) ABT-199 in 12.5 mg/kg, (C) FWJ-D5 in 12.5 mg/kg, (D) FWJ-D5 in 25 mg/kg, and (E) FWJ-D5 in 50 mg/kg.

acetone- d_6): δ 162.0, 156.3, 151.0, 146.1, 143.5, 142.8, 140.3, 137.3, 132.4, 131.8, 130.7, 129.3, 129.1, 127.9, 127.5, 126.5, 126.4, 122.9, 121.2, 120.3, 114.2, 44.8, 40.2; ESI-MS: m/z 617.9 [M + H]⁺; DART-HRMS C₂₅H₁₉ClN₃O₈S₂ [M - H]⁻ calcd, 616.0369; obs., 616.0350.

N-(2-(3-(3-Methoxyphenyl)ureido)ethyl)-5-(2-(3,4-dinitrophenoxy)phenyl)thiophene-2-sulfonamide (TJ-A5). Overall yield: 11.4%, purity: 98.1%. ¹H NMR (400 MHz, acetone- d_6): δ 8.23 (d, J = 8.8 Hz, 1H), 8.00 (s, 1H), 7.93 (dd, J = 8.0, 1.6 Hz, 1H), 7.70 (d, J = 2.0 Hz, 1H), 7.58–7.55 (m, 3H), 7.48–7.41 (m, 3H), 7.23 (t, J = 2.0 Hz, 1H), 7.10 (t, J = 8.0 Hz, 1H), 6.96–6.89 (m, 2H), 6.50 (dd, J = 8.0, 1.6 Hz, 1H), 5.96–5.93 (m, 1H), 3.73 (s, 3H), 3.34–3.30 (m, 2H), 3.14–3.10 (m, 2H); ¹³C NMR (100 MHz, acetone- d_6): δ 162.1, 161.1, 156.5, 151.0, 143.6, 142.9, 142.6, 132.4, 131.8, 130.8, 130.2, 129.1, 127.9, 127.5, 126.5, 122.9, 121.3, 114.2, 111.3, 107.8, 104.9, 55.3, 45.0, 40.2; ESI-MS: m/z 612.0 [M - H]⁻; DART-HRMS C₂₆H₂₂N₅O₉S₂ [M - H]⁻ calcd, 612.0864; obs., 612.0845.

N-(2-(3-(3,5-Dichlorophenyl)ureido)ethyl)-5-(2-(3,4-dinitrophenoxy)phenyl)thiophene-2-sulfonamide (TJ-A6). Overall yield: 10.1%, purity: 97.2%. ¹H NMR (400 MHz, acetone- d_6): δ 8.35 (s, 1H), 8.25 (d, J = 8.8 Hz, 1H), 7.94 (d, J = 7.6 Hz, 1H), 7.71 (d, J = 2.0 Hz, 1H), 7.59–7.45 (m, 7H), 7.40 (d, J = 8.0 Hz, 1H), 6.97 (t, J = 2.0 Hz, 1H), 6.87–6.84 (m, 1H), 6.10–6.08 (m, 1H), 3.35–3.30 (m, 2H), 3.15–3.11 (m, 2H); ¹³C NMR (100 MHz, acetone- d_6): δ 162.1, 155.8, 151.1, 143.9, 143.7, 143.0, 137.5, 135.5, 132.5, 131.9, 130.8, 129.1, 128.0, 127.6, 126.6, 122.9, 121.6, 121.3, 117.0, 116.9, 114.3, 44.6, 40.3; ESI-MS: m/z 651.9 [M + H]⁺; ESI-HRMS C₂₅H₁₈Cl₂N₅O₈S₂ [M - H]⁻ calcd, 649.9979; obs., 649.9952.

N-(2-(3-(3,5-Dimethylphenyl)ureido)ethyl)-5-(2-(3,4-dinitrophenoxy)phenyl)thiophene-2-sulfonamide (TJ-A7). Overall yield: 15.3%, purity: 99.5%. ¹H NMR (400 MHz, acetone- d_6): δ 8.22 (d, J = 9.2 Hz, 1H), 7.93 (dd, J = 8.0, 1.6 Hz, 1H), 7.82 (s, 1H), 7.69 (d, J = 2.4 Hz, 1H), 7.59–7.54 (m, 3H), 7.48–7.38 (m, 3H), 7.07 (s, 2H), 6.97–6.94 (m, 1H), 6.58 (s, 1H), 5.93–5.91 (m, 1H), 3.33–3.29 (m, 2H), 3.13–3.09 (m, 2H), 2.20 (s, 6H); ¹³C NMR (100 MHz, acetone- d_6): δ 162.1, 156.6, 151.0, 143.5, 143.3, 142.9, 141.2, 138.8, 132.4, 131.8, 130.8, 129.1, 127.9, 127.5, 126.5, 124.1, 122.9, 121.3, 116.9, 114.2, 45.1, 40.1, 21.5; ESI-MS: m/z 612.0 [M + H]⁺; ESI-HRMS C₂₇H₂₅N₅O₈S₂Na [M + Na]⁺ calcd, 634.1037; obs., 634.1061.

N-(2-(3-(4-Nitrophenyl)ureido)ethyl)-5-(2-(3,4-dinitrophenoxy)phenyl)thiophene-2-sulfonamide (TJ-A8). Overall yield: 2.6%, purity: 97.3%. ¹H NMR (400 MHz, acetone- d_6): δ 8.71 (s, 1H), 8.25 (d, J = 9.2 Hz, 1H), 8.13–8.10 (m, 2H), 7.94 (dd, J = 8.0, 1.6 Hz, 1H), 7.71–7.67 (m, 3H), 7.59–7.54 (m, 3H), 7.47–7.44 (m, 2H), 7.39 (t, J = 8.0 Hz, 1H), 6.88–6.85 (m, 1H), 6.20 (m, 1H), 3.38–3.34 (m, 2H), 3.18–3.13 (m, 2H); ¹³C NMR (100 MHz, acetone- d_6): δ 162.1, 155.6, 151.0, 147.8, 143.6, 142.9, 142.3, 137.3, 132.4, 131.8, 130.7, 129.1, 127.9,

127.5, 126.4, 125.7, 122.9, 121.2, 117.9, 117.9, 114.2, 44.4, 40.2; ESI-MS: m/z 627.0 [M - H]⁻; ESI-HRMS C₂₅H₁₉N₆O₁₀S₂ [M - H]⁻ calcd, 627.0610; obs., 627.0591.

N-(2-(3-(4-Methoxyphenyl)ureido)ethyl)-5-(2-(3,4-dinitrophenoxy)phenyl)thiophene-2-sulfonamide (TJ-A9). Overall yield: 21.1%, purity: 99.3%. ¹H NMR (400 MHz, acetone- d_6): δ 8.23 (d, J = 9.2 Hz, 1H), 7.94 (dd, J = 8.0, 1.2 Hz, 1H), 7.79 (s, 1H), 7.70 (d, J = 2.8 Hz, 1H), 7.58–7.54 (m, 3H), 7.49–7.41 (m, 3H), 7.39–7.34 (m, 2H), 7.01–6.98 (m, 1H), 6.81–6.79 (m, 2H), 5.88–5.85 (m, 1H), 3.73 (s, 3H), 3.31–3.30 (m, 2H), 3.11–3.10 (m, 2H); ¹³C NMR (100 MHz, acetone- d_6): δ 162.1, 157.0, 155.9, 151.0, 143.5, 142.9, 135.9, 134.3, 132.4, 131.8, 130.8, 129.1, 127.9, 127.5, 126.5, 122.9, 121.3, 121.1, 120.9, 114.7, 114.2, 55.6, 45.2, 40.2; ESI-MS: m/z 612.1 [M - H]⁻; ESI-HRMS C₂₆H₂₂N₅O₉S₂ [M - H]⁻ calcd, 612.0864; obs., 612.0846.

N-(2-(3-(3,5-Bis(trifluoromethyl)phenyl)ureido)ethyl)-5-(2-(3,4-dinitrophenoxy)phenyl)thiophene-2-sulfonamide (TJ-A10). Overall yield: 15.2%, purity: 97.1%. ¹H NMR (400 MHz, acetone- d_6): δ 8.69 (s, 1H), 8.24 (d, J = 9.2 Hz, 1H), 8.12 (s, 2H), 7.94 (dd, J = 8.0, 1.6 Hz, 1H), 7.71 (d, J = 2.8 Hz, 1H), 7.60–7.54 (m, 3H), 7.52 (s, 1H), 7.48–7.46 (m, 2H), 7.40 (dd, J = 8.0, 0.8 Hz, 1H), 6.88–6.85 (m, 1H), 6.23–6.22 (m, 1H), 3.39–3.35 (m, 2H), 3.18–3.13 (m, 2H); ¹³C NMR (100 MHz, acetone- d_6): δ 162.1, 155.8, 151.0, 143.6, 143.4, 142.9, 132.5, 132.4, 132.2, 131.8, 130.7, 129.1, 128.0, 127.5, 126.5, 125.8, 123.1, 122.9, 121.2, 118.4, 114.9, 114.2, 44.3, 40.3; ESI-MS: m/z 718.1 [M - H]⁻; ESI-HRMS C₂₇H₁₈N₅O₈F₆S₂ [M - H]⁻ calcd, 718.0506; obs., 718.0518.

N-(2-(3-(3,5-Bis(trifluoromethyl)phenyl)thioureido)ethyl)-4-(2-(3,4-dihydroxyphenoxy)phenyl)thiophene-2-sulfonamide (TJ-B1). Overall yield: 15.8%, purity: 97.9%. ¹H NMR (400 MHz, acetone- d_6): δ 9.37 (s, 1H), 8.18 (s, 2H), 7.96 (d, J = 1.2 Hz, 1H), 7.94 (s, 1H), 7.88 (d, J = 1.6 Hz, 1H), 7.69 (s, 1H), 7.62 (s, 1H), 7.58 (s, 1H), 7.55 (dd, J = 7.6, 1.6 Hz, 1H), 7.19 (dt, J = 7.8, 1.6 Hz, 1H), 7.03 (dt, J = 7.6, 0.8 Hz, 1H), 6.82–6.80 (m, 2H), 6.68 (d, J = 8.8 Hz, 1H), 6.40 (d, J = 2.8 Hz, 1H), 6.24 (dd, J = 8.8, 2.8 Hz, 1H), 3.72–3.67 (m, 2H), 3.20–3.15 (m, 2H); ¹³C NMR (100 MHz, acetone- d_6): δ 182.7, 155.7, 150.4, 146.9, 142.7, 142.3, 141.8, 139.0, 133.3, 132.4, 132.1, 131.7, 131.4, 130.7, 130.5, 130.1, 130.1, 128.4, 126.3, 125.7, 124.2, 123.6, 123.0, 119.6, 115.8, 117.7, 116.5, 110.6, 107.7, 44.6, 43.1; ESI-MS: m/z 677.8 [M + H]⁺, 699.8 [M + Na]⁺; MALDI-HRMS C₂₇H₂₂N₃O₅F₆S₃ [M + H]⁺ calcd, 678.0620; obs., 678.0630.

N-(2-(3-(3,5-Bis(trifluoromethyl)phenyl)ureido)ethyl)-4-(2-(3,4-dihydroxyphenoxy)phenyl)thiophene-2-sulfonamide (TJ-B2). Overall yield: 11.8%, purity: 98.4%. ¹H NMR (400 MHz, acetone- d_6): δ 8.59 (s, 1H), 8.00 (s, 2H), 7.94 (d, J = 1.2 Hz, 1H), 7.86 (d, J = 2.0 Hz, 1H), 7.54 (dd, J = 7.6, 1.6 Hz, 1H), 7.39 (s, 1H), 7.19 (dt, J = 7.6, 1.6 Hz,

1H), 7.03 (dt, $J = 7.6, 0.8$ Hz, 1H), 6.81 (d, $J = 8.4$ Hz, 1H), 7.34 (s, 1H), 6.66 (d, $J = 8.4$ Hz, 1H), 6.40 (d, $J = 2.8$ Hz, 1H), 6.21 (dd, $J = 8.4, 2.8$ Hz, 1H), 6.13–6.10 (m, 1H), 3.29–3.25 (m, 2H), 3.03–3.00 (m, 2H); ^{13}C NMR (100 MHz, acetone- d_6): δ 156.0, 155.6, 150.6, 147.0, 143.4, 142.0, 141.8, 138.9, 133.2, 132.8, 132.5, 132.2, 131.9, 130.7, 130.1, 130.0, 126.5, 125.8, 124.3, 123.1, 119.8, 118.5, 116.5, 114.9, 110.4, 107.6, 44.4, 40.3; ESI-MS: m/z 661.8 $[\text{M} + \text{H}]^+$, 683.7 $[\text{M} + \text{Na}]^+$; MALDI-HRMS $\text{C}_{27}\text{H}_{22}\text{N}_3\text{O}_6\text{F}_6\text{S}_2$ $[\text{M} + \text{H}]^+$ calcd, 662.0849; obs., 662.0848.

N-(2-(3-(3,5-Dichlorophenyl)ureido)ethyl)-4-(2-(3,4-dihydroxyphenoxy)phenyl)thiophene-2-sulfonamide (TJ-B3). Overall yield: 10.1%, purity: 97.2%. ^1H NMR (400 MHz, acetone- d_6): δ 8.25 (s, 1H), 7.95 (s, 1H), 7.92 (d, $J = 1.2$ Hz, 1H), 7.84 (d, $J = 1.2$ Hz, 1H), 7.66 (s, 1H), 7.53 (dd, $J = 7.6, 1.2$ Hz, 1H), 7.38 (d, $J = 1.6, 2\text{H}$), 7.18 (dt, $J = 7.8, 1.2$ Hz, 1H), 7.03 (t, $J = 7.6$ Hz, 1H), 6.84 (t, $J = 1.6$ Hz, 1H), 6.81 (d, $J = 8.4$ Hz, 1H), 6.74–6.71 (m, 1H), 6.66 (d, $J = 8.4$ Hz, 1H), 6.40 (d, $J = 2.8$ Hz, 1H), 6.20 (dd, $J = 8.4, 2.8$ Hz, 1H), 6.01–5.89 (m, 1H), 3.26–3.21 (m, 2H), 3.02–2.98 (m, 2H); ^{13}C NMR (100 MHz, acetone- d_6): δ 156.0, 155.6, 150.7, 147.0, 143.8, 142.3, 142.0, 139.0, 135.5, 133.2, 130.8, 130.2, 130.0, 126.6, 124.4, 121.6, 120.0, 117.0, 116.6, 110.5, 107.6, 44.6, 40.3; ESI-MS: m/z 594.0 $[\text{M} + \text{H}]^+$; MALDI-HRMS $\text{C}_{25}\text{H}_{21}\text{N}_3\text{O}_6\text{Cl}_2\text{S}_2\text{Na}$ $[\text{M} + \text{Na}]^+$ calcd, 616.0141; obs., 616.0146.

N-(2-(3-(3,5-Bis(trifluoromethyl)phenyl)thioureido)ethyl)-5-(2-(benzyloxy)phenyl)thiophene-2-sulfonamide (TJ-C1). Overall yield: 24.4%, purity: 98.4%. ^1H NMR (400 MHz, acetone- d_6): δ 9.54 (s, 1H), 8.33 (s, 2H), 7.81–7.77 (m, 2H), 7.71 (s, 1H), 7.62 (d, $J = 4.0$ Hz, 1H), 7.58 (d, $J = 4.0$ Hz, 1H), 7.54 (d, $J = 7.2$ Hz, 2H), 7.41 (t, $J = 7.6$ Hz, 2H), 7.34 (t, $J = 7.6$ Hz, 2H), 7.24 (d, $J = 8.4$ Hz, 1H), 7.04 (td, $J = 7.6, 1.2$ Hz, 1H), 6.87 (m, 1H), 5.35 (s, 2H), 3.87–3.82 (m, 2H), 3.34–3.30 (m, 2H); ^{13}C NMR (100 MHz, acetone- d_6): δ 182.6, 155.5, 146.0, 142.7, 141.1, 137.5, 132.1, 131.9, 131.8, 130.8, 129.4, 129.0, 128.9, 128.7, 125.7, 125.5, 123.5, 123.0, 122.5, 122.2, 117.6, 114.3, 71.4, 44.7, 43.1; ESI-MS: m/z 659.9 $[\text{M} + \text{H}]^+$, 681.8 $[\text{M} + \text{Na}]^+$; MALDI-HRMS $\text{C}_{28}\text{H}_{24}\text{N}_3\text{O}_3\text{F}_6\text{S}_3$ $[\text{M} + \text{H}]^+$ calcd, 660.0878; obs., 660.0881.

N-(2-(3-(3,5-Bis(trifluoromethyl)phenyl)ureido)ethyl)-5-(2-(benzyloxy)phenyl)thiophene-2-sulfonamide (TJ-C2). Overall yield: 32.9%, Purity: 99.1%. ^1H NMR (400 MHz, acetone- d_6): δ 8.72 (s, 1H), 8.13 (s, 2H), 7.79 (dd, $J = 8.0, 1.2$ Hz, 1H), 7.62 (d, $J = 4.0$ Hz, 1H), 7.56–7.52 (m, 4H), 7.41 (t, $J = 7.6$ Hz, 2H), 7.37–7.33 (m, 2H), 7.25 (d, $J = 8.4$ Hz, 1H), 7.04 (t, $J = 7.6$ Hz, 1H), 6.79–6.76 (m, 1H), 6.26–6.23 (m, 1H), 5.36 (s, 2H), 3.43–3.38 (m, 2H), 3.20–3.15 (m, 2H); ^{13}C NMR (100 MHz, acetone- d_6): δ 155.9, 155.5, 145.9, 143.5, 141.3, 137.5, 132.8, 132.5, 132.2, 131.8, 131.7, 130.8, 129.4, 128.9, 128.9, 128.7, 125.8, 125.5, 123.1, 122.6, 122.2, 118.4, 114.8, 114.3, 71.3, 44.4, 40.4; ESI-MS: m/z 643.9 $[\text{M} + \text{H}]^+$, 665.8 $[\text{M} + \text{Na}]^+$; ESI-HRMS $\text{C}_{28}\text{H}_{23}\text{N}_3\text{O}_4\text{F}_6\text{S}_2\text{Na}$ $[\text{M} + \text{Na}]^+$ calcd, 666.0926; obs., 666.0927.

N-(2-(3-(3-Chlorophenyl)thioureido)ethyl)-5-(2-(benzyloxy)phenyl)thiophene-2-sulfonamide (TJ-C3). Overall yield: 39.5%, purity: 98.7%. ^1H NMR (400 MHz, acetone- d_6): δ 9.09 (s, 1H), 7.82 (dd, $J = 7.6, 1.6$ Hz, 1H), 7.65 (s, 1H), 7.63 (d, $J = 4.0$ Hz, 1H), 7.57–7.54 (m, 3H), 7.49 (m, 1H), 7.42 (t, $J = 7.6$ Hz, 2H), 7.37–7.31 (m, 4H), 7.27 (t, $J = 7.6$ Hz, 1H), 7.15 (d, $J = 7.6$ Hz, 1H), 7.06 (t, $J = 7.6$ Hz, 1H), 6.90–6.87 (m, 1H), 5.37 (s, 2H), 3.84–3.79 (m, 2H), 3.31–3.27 (m, 2H); ^{13}C NMR (100 MHz, acetone- d_6): δ 182.6, 155.6, 145.9, 141.3, 137.5, 134.6, 131.8, 131.1, 130.8, 129.4, 129.0, 128.9, 128.7, 125.6, 125.4, 124.2, 122.8, 122.6, 122.2, 114.4, 71.4, 44.7, 43.5; ESI-MS: m/z 557.8 $[\text{M} + \text{H}]^+$, 579.8 $[\text{M} + \text{Na}]^+$; ESI-HRMS $\text{C}_{26}\text{H}_{24}\text{Cl}_1\text{N}_3\text{O}_3\text{S}_3\text{Na}$ $[\text{M} + \text{Na}]^+$ calcd, 580.0561; obs., 580.0574.

N-(2-(3-(3,5-Dimethylphenyl)ureido)ethyl)-5-(2-(benzyloxy)phenyl)thiophene-2-sulfonamide (TJ-C4). Overall yield: 32.4%, purity: 99.1%. ^1H NMR (400 MHz, acetone- d_6): δ 7.87 (s, 1H), 7.77 (dd, $J = 7.6, 1.6$ Hz, 1H), 7.57 (d, $J = 4.0$ Hz, 1H), 7.53–7.51 (m, 3H), 7.39 (t, $J = 7.6$ Hz, 2H), 7.35–7.31 (m, 2H), 7.22 (d, $J = 8.4$ Hz, 1H), 7.07 (s, 2H), 7.03 (t, $J = 7.6$ Hz, 1H), 6.90–6.87 (m, 1H), 6.56 (s, 1H), 5.98–5.95 (m, 1H), 5.31 (s, 2H), 3.38–3.33 (m, 2H), 3.15–3.11 (m, 2H), 2.18 (s, 6H); ^{13}C NMR (100 MHz, acetone- d_6): δ 156.7, 155.4, 145.8, 141.3, 141.1, 138.8, 137.5, 131.7, 130.7, 129.4, 129.0, 128.9, 128.7, 125.5, 124.2, 122.6, 122.2, 117.0, 114.3, 71.3, 45.1, 40.2, 21.5;

ESI-MS: m/z 536.0 $[\text{M} + \text{H}]^+$, 558.0 $[\text{M} + \text{Na}]^+$; ESI-HRMS $\text{C}_{28}\text{H}_{29}\text{N}_3\text{O}_4\text{S}_2\text{Na}$ $[\text{M} + \text{Na}]^+$ calcd, 558.1492; obs., 558.1491.

N-(2-(3-(3-Methoxyphenyl)ureido)ethyl)-5-(2-(benzyloxy)phenyl)thiophene-2-sulfonamide (TJ-C5). Overall yield: 33.8%, purity: 98.0%. ^1H NMR (400 MHz, acetone- d_6): δ 8.04 (s, 1H), 7.77 (dd, $J = 8.0, 1.6$ Hz, 1H), 7.58 (d, $J = 4.0$ Hz, 1H), 7.54–7.51 (m, 3H), 7.39 (t, $J = 7.6$ Hz, 2H), 7.34–7.31 (m, 2H), 7.25–7.21 (m, 2H), 7.09 (t, $J = 7.6$ Hz, 1H), 7.03 (t, $J = 7.6$ Hz, 1H), 6.92 (dd, $J = 8.0, 1.2$ Hz, 1H), 6.88–6.85 (m, 1H), 6.50 (dd, $J = 8.0, 1.6$ Hz, 1H), 6.00–5.97 (m, 1H), 5.32 (s, 2H), 3.71 (s, 3H), 3.39–3.34 (m, 2H), 3.16–3.12 (m, 2H); ^{13}C NMR (100 MHz, acetone- d_6): δ 161.1, 156.5, 155.4, 145.8, 142.5, 141.3, 137.5, 131.7, 130.7, 130.1, 129.4, 129.0, 128.9, 128.7, 125.5, 122.6, 122.2, 114.3, 111.3, 107.8, 104.9, 71.3, 55.3, 44.9, 40.2; ESI-MS: m/z 537.9 $[\text{M} + \text{H}]^+$, 560.0 $[\text{M} + \text{Na}]^+$; ESI-HRMS $\text{C}_{27}\text{H}_{27}\text{N}_3\text{O}_5\text{S}_2\text{Na}$ $[\text{M} + \text{Na}]^+$ calcd, 560.1284; obs., 560.1279.

N-(2-(3-(4-Chlorophenyl)thioureido)ethyl)-5-(2-(benzyloxy)phenyl)thiophene-2-sulfonamide (TJ-C6). Overall yield: 32.0%, purity: 97.5%. ^1H NMR (400 MHz, acetone- d_6): δ 9.03 (s, 1H), 7.81 (dd, $J = 7.6, 1.2$ Hz, 1H), 7.61 (d, $J = 4.0$ Hz, 1H), 7.56–7.53 (m, 3H), 7.46–7.29 (m, 9H), 7.24 (d, $J = 8.0$ Hz, 1H), 7.05 (t, $J = 7.2$ Hz, 1H), 6.90–6.87 (m, 1H), 5.35 (s, 2H), 3.84–3.79 (m, 2H), 3.31–3.26 (m, 2H); ^{13}C NMR (100 MHz, acetone- d_6): δ 182.6, 155.4, 145.8, 141.2, 138.4, 137.4, 131.8, 130.8, 130.4, 129.6, 129.4, 129.3, 129.0, 128.9, 128.7, 126.3, 125.5, 122.6, 122.2, 114.3, 71.3, 44.6, 43.6; ESI-MS: m/z 557.9 $[\text{M} + \text{H}]^+$, 579.8 $[\text{M} + \text{Na}]^+$; ESI-HRMS $\text{C}_{26}\text{H}_{24}\text{Cl}_1\text{N}_3\text{O}_3\text{S}_3\text{Na}$ $[\text{M} + \text{Na}]^+$ calcd, 580.0561; obs., 580.0540.

N-(2-(3-(3-Nitrophenyl)ureido)ethyl)-5-(2-(benzyloxy)phenyl)thiophene-2-sulfonamide (TJ-C7). Overall yield: 25.4%, purity: 98.9%. ^1H NMR (400 MHz, acetone- d_6): δ 8.56–8.53 (m, 2H), 7.78–7.71 (m, 3H), 7.59 (d, $J = 4.0$ Hz, 1H), 7.55–7.52 (m, 3H), 7.46 (d, $J = 8.4$ Hz, 1H), 7.43–7.48 (m, 2H), 7.33 (td, $J = 8.0, 1.6$ Hz, 2H), 7.21 (d, $J = 8.0$ Hz, 1H), 7.02 (t, $J = 7.6$ Hz, 1H), 6.84–6.81 (m, 1H), 6.17–6.14 (m, 1H), 5.32 (s, 2H), 3.43–3.39 (m, 2H), 3.20–3.16 (m, 2H); ^{13}C NMR (100 MHz, acetone- d_6): δ 156.1, 155.4, 149.5, 145.8, 142.7, 141.2, 137.5, 131.7, 130.7, 130.4, 129.4, 128.9, 128.9, 128.7, 125.5, 124.5, 122.5, 122.1, 116.7, 114.3, 113.0, 71.3, 44.6, 40.3; ESI-MS: m/z 553.0 $[\text{M} + \text{H}]^+$, 574.9 $[\text{M} + \text{Na}]^+$; ESI-HRMS $\text{C}_{26}\text{H}_{24}\text{N}_4\text{O}_6\text{S}_2\text{Na}$ $[\text{M} + \text{Na}]^+$ calcd, 575.1029; obs., 575.1028.

N-(2-(3-(4-Nitrophenyl)thioureido)ethyl)-5-(2-(benzyloxy)phenyl)thiophene-2-sulfonamide (TJ-C8). Overall yield: 41.8%, purity: 98.5%. ^1H NMR (400 MHz, acetone- d_6): δ 9.55 (s, 1H), 8.14–8.12 (m, 2H), 7.89–7.88 (m, 2H), 7.79 (dd, $J = 8.0, 1.2$ Hz, 1H), 7.75 (m, 1H), 7.61 (d, $J = 4.0$ Hz, 1H), 7.57 (d, $J = 4.0$ Hz, 1H), 7.54 (d, $J = 7.6$ Hz, 2H), 7.41 (t, $J = 7.6$ Hz, 2H), 7.33 (td, $J = 8.0, 1.6$ Hz, 2H), 7.22 (d, $J = 8.4$ Hz, 1H), 7.03 (t, $J = 7.2$ Hz, 1H), 6.88–6.86 (m, 1H), 5.34 (s, 2H), 3.87–3.82 (m, 2H), 3.35–3.31 (m, 2H); ^{13}C NMR (100 MHz, acetone- d_6): δ 182.1, 155.4, 146.6, 146.0, 143.8, 141.0, 137.5, 131.9, 130.8, 129.4, 128.9, 128.9, 128.9, 128.7, 125.5, 125.1, 122.5, 122.2, 122.0, 114.3, 71.3, 44.6, 43.2; ESI-MS: m/z 568.9 $[\text{M} + \text{H}]^+$, 590.9 $[\text{M} + \text{Na}]^+$; ESI-HRMS $\text{C}_{26}\text{H}_{24}\text{N}_4\text{O}_5\text{S}_3\text{Na}$ $[\text{M} + \text{Na}]^+$ calcd, 591.0801; obs., 591.0784.

N-(2-(3-(3-Nitrophenyl)thioureido)ethyl)-5-(2-(benzyloxy)phenyl)thiophene-2-sulfonamide (TJ-C9). Overall yield: 46.1%, purity: 96.5%. ^1H NMR (400 MHz, acetone- d_6): δ 9.41 (s, 1H), 8.62 (s, 1H), 7.94 (d, $J = 7.6$ Hz, 1H), 7.89 (d, $J = 8.0$ Hz, 1H), 7.79 (d, $J = 7.6$ Hz, 1H), 7.64–7.60 (m, 2H), 7.57–7.53 (m, 4H), 7.40 (t, $J = 7.6$ Hz, 2H), 7.35–7.31 (m, 2H), 7.22 (d, $J = 8.4$ Hz, 1H), 7.03 (t, $J = 7.6$ Hz, 1H), 6.88 (t, $J = 7.6$ Hz, 1H), 5.34 (s, 2H), 3.85–3.81 (m, 2H), 3.33–3.29 (m, 2H); ^{13}C NMR (100 MHz, acetone- d_6): δ 182.6, 155.4, 149.0, 145.9, 141.6, 141.1, 137.4, 131.8, 130.8, 130.4, 129.7, 129.4, 128.9, 128.9, 128.7, 125.5, 122.5, 122.2, 119.5, 118.4, 114.3, 71.3, 44.6, 43.3; ESI-MS: m/z 568.9 $[\text{M} + \text{H}]^+$, 591.0 $[\text{M} + \text{Na}]^+$; ESI-HRMS $\text{C}_{26}\text{H}_{24}\text{N}_4\text{O}_5\text{S}_3\text{Na}$ $[\text{M} + \text{Na}]^+$ calcd, 591.0801; obs., 591.0811.

N-(2-(3-(3,5-Dichlorophenyl)ureido)ethyl)-5-(2-(benzyloxy)phenyl)thiophene-2-sulfonamide (TJ-C10). Overall yield: 40.4%, purity: 99.6%. ^1H NMR (400 MHz, acetone- d_6): δ 8.38 (s, 1H), 7.78 (dd, $J = 8.0, 1.2$ Hz, 1H), 7.59 (d, $J = 4.0$ Hz, 1H), 7.55–7.51 (m, 5H), 7.40 (t, $J = 7.6$ Hz, 2H), 7.33 (td, $J = 8.0, 1.2$ Hz, 2H), 7.23 (d, $J = 8.0$ Hz, 1H), 7.04 (t, $J = 7.6$ Hz, 1H), 6.96 (t, $J = 1.6$ Hz, 1H), 6.78 (m, 1H), 6.13–6.10 (m, 1H), 5.33 (s, 2H), 3.40–3.36 (m, 2H), 3.18–3.14 (m,

2H); ^{13}C NMR (100 MHz, acetone- d_6): δ 155.8, 155.4, 145.9, 143.8, 141.2, 137.5, 135.4, 131.7, 130.8, 129.4, 128.9, 128.9, 128.7, 125.5, 122.5, 122.2, 121.5, 116.8, 114.3, 71.3, 44.5, 40.3; ESI-MS: m/z 597.8 $[\text{M} + \text{Na}]^+$; ESI-HRMS $\text{C}_{26}\text{H}_{23}\text{Cl}_2\text{N}_3\text{O}_4\text{S}_2\text{Na}$ $[\text{M} + \text{Na}]^+$ calcd, 598.0399; obs., 598.0385.

N-(2-(3-(4-Methoxyphenyl)ureido)ethyl)-5-(2-(benzyloxy)phenyl)thiophene-2-sulfonamide (TJ-C11). Overall yield: 46.1%, purity: 96.6%. ^1H NMR (400 MHz, acetone- d_6): δ 7.85 (s, 1H), 7.78 (dd, $J = 7.6, 1.2$ Hz, 1H), 7.58 (d, $J = 4.0$ Hz, 1H), 7.53–7.51 (m, 3H), 7.39 (t, $J = 7.2$ Hz, 2H), 7.34–7.32 (m, 3H), 7.22 (d, $J = 8.4$ Hz, 1H), 7.04 (t, $J = 7.6$ Hz, 1H), 6.92 (m, 1H), 6.79–6.77 (m, 2H), 5.92–5.90 (m, 1H), 5.32 (s, 2H), 3.71 (s, 3H), 3.37–3.32 (m, 2H), 3.14–3.10 (m, 2H); ^{13}C NMR (100 MHz, acetone- d_6): δ 157.1, 155.9, 155.4, 145.8, 141.3, 137.5, 134.2, 131.7, 130.7, 129.4, 129.0, 128.9, 128.6, 125.5, 122.6, 122.2, 121.2, 114.6, 114.3, 71.3, 55.6, 45.2, 40.3; ESI-MS: m/z 538.0 $[\text{M} + \text{H}]^+$, 560.0 $[\text{M} + \text{Na}]^+$; ESI-HRMS $\text{C}_{27}\text{H}_{27}\text{N}_3\text{O}_5\text{S}_2\text{Na}$ $[\text{M} + \text{Na}]^+$ calcd, 560.1284; obs., 560.1266.

N-(2-(3-(4-Chlorophenyl)ureido)ethyl)-5-(2-(4-aminophenoxy)phenyl)thiophene-2-sulfonamide (TJ-C12). Overall yield: 13.6%, purity: 95.7%. ^1H NMR (400 MHz, methanol- d_4): δ 7.69 (dd, $J = 8.0, 1.6$ Hz, 1H), 7.47 (d, $J = 4.0$ Hz, 1H), 7.46 (d, $J = 4.0$ Hz, 1H), 7.21–7.14 (m, 3H), 7.08–7.06 (m, 2H), 7.01 (t, $J = 7.2$ Hz, 1H), 6.73 (d, $J = 8.0$ Hz, 1H), 6.71–6.69 (m, 2H), 6.66–6.64 (m, 2H), 3.20–3.17 (m, 2H), 2.99–2.96 (m, 2H); ^{13}C NMR (100 MHz, methanol- d_4): δ 157.9, 156.1, 148.7, 146.4, 145.4, 141.2, 139.7, 132.5, 130.9, 129.6, 129.2, 128.0, 125.8, 124.2, 124.0, 121.6, 121.3, 118.6, 117.8, 44.4, 40.5; ESI-MS: m/z 541.0 $[\text{M} - \text{H}]^-$; ESI-HRMS calcd. for $\text{C}_{25}\text{H}_{22}\text{ClN}_4\text{O}_4\text{S}_2$ $[\text{M} - \text{H}]^-$ requires, 541.0776; found, 541.0795.

N-(2-(3-(3,5-Bis(trifluoromethyl)phenyl)ureido)ethyl)-5-(2-(4-aminophenoxy)phenyl)thiophene-2-sulfonamide (TJ-C13). Overall yield: 13.6%, purity: 98.7%. ^1H NMR (400 MHz, methanol- d_4): δ 7.94 (s, 2H), 7.72 (dd, $J = 8.0, 1.2$ Hz, 1H), 7.56 (d, $J = 4.0$ Hz, 1H), 7.53 (d, $J = 4.0$ Hz, 1H), 7.42 (s, 1H), 7.20 (td, $J = 7.6, 1.2$ Hz, 1H), 7.04 (t, $J = 7.6$ Hz, 1H), 6.79–6.73 (m, 5H), 3.32–3.30 (m, 2H), 3.12–3.09 (m, 2H); ^{13}C NMR (100 MHz, methanol- d_4): δ 157.3, 156.0, 148.8, 146.4, 145.4, 143.2, 141.2, 133.5, 133.1, 132.8, 132.6, 132.4, 130.9, 129.0, 126.1, 125.7, 124.1, 124.0, 123.4, 121.6, 118.8, 118.7, 117.8, 115.5, 44.1, 40.5; ESI-MS: m/z 643.0 $[\text{M} - \text{H}]^-$; ESI-HRMS calcd. for $\text{C}_{27}\text{H}_{21}\text{N}_4\text{O}_4\text{F}_6\text{S}_2$ $[\text{M} - \text{H}]^-$ requires, 643.0914; found, 643.0911.

N-(2-(3-(3,5-Dimethylphenyl)ureido)ethyl)-5-(2-(4-aminophenoxy)phenyl)thiophene-2-sulfonamide (TJ-C14). Overall yield: 19.0%, purity: 98.4%. ^1H NMR (400 MHz, methanol- d_4): δ 7.69 (dd, $J = 8.0, 1.2$ Hz, 1H), 7.47 (d, $J = 4.0$ Hz, 1H), 7.46 (d, $J = 4.0$ Hz, 1H), 7.16 (t, $J = 7.6$ Hz, 1H), 7.01 (t, $J = 7.6$ Hz, 1H), 6.83 (s, 2H), 6.74 (d, $J = 8.0$ Hz, 1H), 6.71–6.69 (m, 2H), 6.67–6.64 (m, 2H), 6.52 (s, 1H), 3.20–3.17 (m, 2H), 2.99–2.96 (m, 2H), 2.12 (s, 6H); ^{13}C NMR (100 MHz, methanol- d_4): δ 158.3, 156.0, 149.2, 146.3, 144.9, 141.3, 140.4, 139.4, 132.5, 130.9, 129.2, 125.9, 125.2, 124.3, 124.1, 121.5, 118.8, 118.2, 118.2, 44.5, 40.5, 21.5; ESI-MS: m/z 535.1 $[\text{M} - \text{H}]^-$; ESI-HRMS calcd for $\text{C}_{27}\text{H}_{27}\text{N}_4\text{O}_4\text{S}_2$ $[\text{M} - \text{H}]^-$ requires, 535.1479; found, 535.1480.

N-(2-(3-(3,5-Bis(trifluoromethyl)phenyl)thioureido)ethyl)-5-(2-(4-nitrophenoxy)phenyl)thiophene-2-sulfonamide (TJ-C15). Overall yield: 13.6%, purity: 98.4%. ^1H NMR (400 MHz, acetone- d_6): δ 9.48 (s, 1H), 8.31 (s, 2H), 8.29–8.25 (m, 2H), 7.97 (dd, $J = 8.0, 1.6$ Hz, 1H), 7.74 (m, 1H), 7.71 (s, 1H), 7.61 (d, $J = 4.0$ Hz, 1H), 7.58 (d, $J = 4.0$ Hz, 1H), 7.53 (td, $J = 7.6, 1.2$ Hz, 1H), 7.43 (td, $J = 7.6, 1.2$ Hz, 1H), 7.27 (d, $J = 8.0$ Hz, 1H), 7.21–7.18 (m, 2H), 7.17 (m, 1H), 3.80–3.76 (m, 2H), 3.30–3.26 (m, 2H); ^{13}C NMR (100 MHz, acetone- d_6): δ 182.7, 163.0, 151.7, 144.2, 144.1, 142.7, 142.5, 132.5, 132.4, 132.2, 131.8, 131.6, 130.3, 127.2, 127.1, 126.9, 126.4, 125.7, 123.6, 123.0, 122.8, 118.3, 117.7, 44.6, 43.0; ESI-MS: m/z 689.1 $[\text{M} - \text{H}]^-$; DART-HRMS $\text{C}_{27}\text{H}_{21}\text{N}_4\text{O}_5\text{F}_6\text{S}_3$ $[\text{M} + \text{H}]^+$ calcd, 691.0573; obs., 691.0553.

N-(2-(3-(3-Methoxyphenyl)thioureido)ethyl)-5-(2-(4-nitrophenoxy)phenyl)thiophene-2-sulfonamide (TJ-C16). Overall yield: 17.2%, purity: 97.6%. ^1H NMR (400 MHz, acetone- d_6): δ 8.90 (s, 1H), 8.28–8.26 (m, 2H), 7.98 (d, $J = 7.2$ Hz, 1H), 7.60 (d, $J = 4.0$ Hz, 1H), 7.56 (d, $J = 4.0$ Hz, 1H), 7.54–7.52 (m, 1H), 7.44 (t, $J = 7.6$ Hz, 1H), 7.34 (m, 1H), 7.28 (d, $J = 8.0$ Hz, 1H), 7.25–7.18 (m, 3H), 7.02 (s, 1H), 6.98–6.95 (m, 1H), 6.88 (d, $J = 8.0$ Hz, 1H), 6.74 (dd, $J =$

8.4, 2.0 Hz, 1H), 3.79–3.75 (m, 5H), 3.28–3.24 (m, 2H); ^{13}C NMR (100 MHz, acetone- d_6): δ 182.3, 163.0, 161.3, 151.7, 144.0, 142.6, 140.1, 132.3, 131.5, 130.8, 130.4, 127.2, 127.1, 126.9, 126.4, 122.8, 118.3, 116.8, 112.0, 110.4, 55.6, 44.6, 43.7; ESI-MS: m/z 583.0 $[\text{M} - \text{H}]^-$; ESI-HRMS $\text{C}_{26}\text{H}_{23}\text{N}_4\text{O}_6\text{S}_3$ $[\text{M} - \text{H}]^-$ calcd, 583.0785; obs., 583.0795.

N-(2-(3-(3-Chlorophenyl)thioureido)ethyl)-5-(2-(4-nitrophenoxy)phenyl)thiophene-2-sulfonamide (TJ-C17). Overall yield: 18.1%, purity: 98.0%. ^1H NMR (400 MHz, acetone- d_6): δ 9.05 (s, 1H), 8.29–8.25 (m, 2H), 7.98 (dd, $J = 8.0, 1.6$ Hz, 1H), 7.63 (s, 1H), 7.61 (d, $J = 4.0$ Hz, 1H), 7.57 (d, $J = 4.0$ Hz, 1H), 7.54 (td, $J = 8.0, 1.6$ Hz, 1H), 7.46–7.42 (m, 2H), 7.35–7.30 (m, 2H), 7.28 (dd, $J = 8.0, 1.2$ Hz, 1H), 7.21–7.17 (m, 2H), 7.16 (td, $J = 7.2, 2.0$ Hz, 1H), 6.95–6.92 (m, 1H), 3.79–3.74 (m, 2H), 3.29–3.24 (m, 2H); ^{13}C NMR (100 MHz, acetone- d_6): δ 182.6, 163.0, 151.7, 144.0, 142.6, 141.2, 134.6, 132.3, 131.6, 131.1, 130.3, 127.2, 127.1, 126.9, 126.4, 125.5, 124.3, 122.8, 122.8, 118.3, 44.6, 43.4; ESI-MS: m/z 587.0 $[\text{M} - \text{H}]^-$; ESI-HRMS $\text{C}_{25}\text{H}_{20}\text{ClN}_4\text{O}_5\text{S}_3$ $[\text{M} - \text{H}]^-$ calcd, 587.0290; obs., 587.0285.

N-(2-(3-(4-Methoxyphenyl)ureido)ethyl)-5-(2-(4-nitrophenoxy)phenyl)thiophene-2-sulfonamide (TJ-C18). Overall yield: 16.7%, purity: 96.6%. ^1H NMR (400 MHz, acetone- d_6): δ 8.27–8.25 (m, 2H), 7.95 (dd, $J = 8.0, 1.6$ Hz, 1H), 7.80 (s, 1H), 7.58 (d, $J = 4.0$ Hz, 1H), 7.54 (d, $J = 4.0$ Hz, 1H), 7.51 (m, 1H), 7.43 (td, $J = 7.2, 1.2$ Hz, 1H), 7.34–7.32 (m, 2H), 7.27 (dd, $J = 8.0, 1.2$ Hz, 1H), 7.18–7.16 (m, 2H), 6.98 (m, 1H), 6.81–6.79 (m, 2H), 5.87 (m, 1H), 3.74 (s, 3H), 3.31–3.28 (m, 2H), 3.10–3.08 (m, 2H); ^{13}C NMR (100 MHz, acetone- d_6): δ 163.0, 155.9, 151.7, 144.0, 142.7, 134.3, 132.3, 131.5, 130.4, 127.2, 127.1, 126.9, 122.8, 120.9, 118.3, 114.7, 55.6, 45.2, 40.1; ESI-MS: m/z 567.0 $[\text{M} - \text{H}]^-$; ESI-HRMS $\text{C}_{26}\text{H}_{23}\text{N}_4\text{O}_7\text{S}_2$ $[\text{M} - \text{H}]^-$ calcd, 567.1014; obs., 567.1031.

N-(2-(3-(4-Nitrophenyl)thioureido)ethyl)-5-(2-(3-hydroxybenzyl)oxy)phenyl)thiophene-2-sulfonamide (TJ-C19). Overall yield: 32.7%, Purity: 97.6%. ^1H NMR (400 MHz, acetone- d_6): δ 9.55 (s, 1H), 8.45 (s, 1H), 8.15–8.12 (m, 2H), 7.88–7.86 (m, 2H), 7.79 (dd, $J = 8.0, 1.6$ Hz, 1H), 7.75–7.74 (m, 1H), 7.63 (d, $J = 4.0$ Hz, 1H), 7.58 (d, $J = 4.0$ Hz, 1H), 7.31 (dd, $J = 8.0, 1.6$ Hz, 1H), 7.25–7.18 (m, 2H), 7.05–6.99 (m, 3H), 6.88 (m, 1H), 6.82 (td, $J = 7.6, 1.6$ Hz, 1H), 5.30 (s, 2H), 3.87–3.83 (m, 2H), 3.37–3.33 (m, 2H); ^{13}C NMR (100 MHz, acetone- d_6): δ 182.0, 158.4, 155.4, 146.6, 146.0, 143.8, 141.0, 139.1, 131.9, 130.8, 130.5, 128.9, 125.5, 125.1, 122.5, 122.1, 119.5, 115.8, 115.3, 114.3, 71.0, 44.6, 43.2; ESI-MS: m/z 583.1 $[\text{M} - \text{H}]^-$; ESI-HRMS $\text{C}_{26}\text{H}_{23}\text{N}_4\text{O}_6\text{S}_3$ $[\text{M} - \text{H}]^-$ calcd, 583.0774; obs., 584.0775.

N-(2-(3-(3-Nitrophenyl)thioureido)ethyl)-5-(2-(3-hydroxybenzyl)oxy)phenyl)thiophene-2-sulfonamide (TJ-C20). Overall yield: 38.8%, purity: 98.7%. ^1H NMR (400 MHz, acetone- d_6): δ 9.47 (s, 1H), 8.63 (s, 1H), 8.50 (s, 1H), 7.95–7.87 (m, 2H), 7.80 (d, $J = 7.6$ Hz, 1H), 7.71–7.52 (m, 4H), 7.32 (t, $J = 7.6$ Hz, 1H), 7.25–7.18 (m, 2H), 7.05–6.99 (m, 3H), 6.91 (m, 1H), 6.82 (d, $J = 7.2$ Hz, 1H), 5.30 (s, 2H), 3.86–3.81 (m, 2H), 3.35–3.31 (m, 2H); ^{13}C NMR (100 MHz, acetone- d_6): δ 158.5, 155.4, 149.0, 146.0, 141.7, 141.1, 139.1, 131.9, 130.8, 130.5, 130.4, 128.9, 125.5, 122.5, 122.1, 119.5, 118.3, 115.8, 115.3, 114.3, 71.1, 44.6, 43.3; ESI-MS: m/z 583.2 $[\text{M} - \text{H}]^-$; ESI-HRMS $\text{C}_{26}\text{H}_{23}\text{N}_4\text{O}_6\text{S}_3$ $[\text{M} - \text{H}]^-$ calcd, 583.0774; obs., 583.0775.

N-(2-(3-(3,5-Bis(trifluoromethyl)phenyl)ureido)ethyl)-5-(2-(3-hydroxybenzyl)oxy)phenyl)thiophene-2-sulfonamide (TJ-C21). Overall yield: 29.0%, purity: 96.9%. ^1H NMR (400 MHz, acetone- d_6): δ 8.74 (s, 1H), 8.47 (s, 1H), 8.12 (s, 2H), 7.77 (d, $J = 7.2$ Hz, 1H), 7.60 (d, $J = 4.0$ Hz, 1H), 7.56 (d, $J = 4.0$ Hz, 1H), 7.50 (s, 1H), 7.32 (t, $J = 7.6$ Hz, 1H), 7.23–7.18 (m, 2H), 7.04–6.98 (m, 3H), 6.83–6.76 (m, 2H), 6.27 (m, 1H), 5.28 (s, 2H), 3.44–3.40 (m, 2H), 3.23–3.18 (m, 2H); ^{13}C NMR (100 MHz, acetone- d_6): δ 158.5, 156.0, 155.4, 145.9, 143.4, 141.3, 139.1, 132.8, 132.5, 132.1, 131.8, 131.8, 130.7, 130.5, 128.9, 125.5, 122.5, 122.1, 119.5, 118.4, 115.9, 115.4, 114.8, 114.3, 71.1, 44.4, 40.4; ESI-MS: m/z 658.0 $[\text{M} - \text{H}]^-$; DART-HRMS $\text{C}_{28}\text{H}_{24}\text{N}_3\text{O}_5\text{F}_6\text{S}_2$ $[\text{M} + \text{H}]^+$ calcd, 660.1056; obs., 660.1045.

N-(2-(3-(3,5-Dichlorophenyl)ureido)ethyl)-5-(2-(3-hydroxybenzyl)oxy)phenyl)thiophene-2-sulfonamide (TJ-C22). Overall yield: 21.5%, purity: 98.7%. ^1H NMR (400 MHz, DMSO-

d_6): δ 9.46 (s, 1H), 9.02 (s, 1H), 7.91–7.88 (m, 1H), 7.83 (dd, $J = 7.6$, 1.6 Hz, 1H), 7.67 (d, $J = 4.0$ Hz, 1H), 7.56 (d, $J = 4.0$ Hz, 1H), 7.44 (d, $J = 2.0$ Hz, 2H), 7.33 (td, $J = 7.6$, 1.6 Hz, 1H), 7.21–7.15 (m, 2H), 7.05–7.01 (m, 2H), 6.90 (t, $J = 7.6$ Hz, 1H), 6.85 (m, 1H), 6.70 (dd, $J = 8.0$, 1.6 Hz, 1H), 6.42–6.39 (m, 1H), 5.28 (s, 2H), 3.21–3.16 (m, 2H), 2.96–2.92 (m, 2H); ^{13}C NMR (100 MHz, DMSO- d_6): δ 157.5, 154.7, 153.9, 144.0, 142.9, 139.9, 137.9, 133.9, 130.8, 129.9, 129.5, 127.9, 124.8, 121.2, 121.0, 120.1, 118.0, 115.6, 114.9, 114.3, 113.5, 69.8, 42.8; ESI-MS: m/z 591.8 [M + H] $^+$; DART-HRMS $\text{C}_{26}\text{H}_{24}\text{Cl}_2\text{N}_3\text{O}_5\text{S}_2$ [M + H] $^+$ calcd, 592.0529; obs., 592.0517.

N-(2-(3-(4-Methoxyphenyl)ureido)ethyl)-5-(2-((3-hydroxybenzyl)oxy)phenyl)thiophene-2-sulfonamide (TJ-C23). Overall yield: 23.8%, purity: 96.3%. ^1H NMR (400 MHz, acetone- d_6): δ 8.66 (s, 1H), 7.87 (s, 1H), 7.79 (dd, $J = 8.0$, 1.6 Hz, 1H), 7.60 (d, $J = 4.0$ Hz, 1H), 7.53 (d, $J = 4.0$ Hz, 1H), 7.35–7.27 (m, 3H), 7.23–7.19 (m, 2H), 7.05–7.01 (m, 2H), 6.97 (d, $J = 7.6$ Hz, 1H), 6.89–6.86 (m, 1H), 6.80 (dd, $J = 8.0$, 1.6 Hz, 1H), 6.78–6.74 (m, 2H), 5.99–5.96 (m, 1H), 5.26 (s, 2H), 3.71 (s, 3H), 3.39–3.34 (m, 2H), 3.18–3.13 (m, 2H); ^{13}C NMR (100 MHz, acetone- d_6): δ 158.6, 157.3, 156.1, 155.4, 145.8, 141.3, 139.0, 133.9, 131.6, 130.7, 130.4, 128.9, 125.4, 122.6, 122.1, 121.6, 119.5, 116.0, 115.5, 114.7, 114.2, 71.1, 55.6, 45.2, 40.3; ESI-MS: m/z 575.9 [M + Na] $^+$; ESI-HRMS $\text{C}_{27}\text{H}_{28}\text{N}_3\text{O}_6\text{S}_2$ [M + H] $^+$ calcd, 554.1414; obs., 554.1401.

N-(2-(3-(3,5-Dimethylphenyl)ureido)ethyl)-5-(2-((3-hydroxybenzyl)oxy)phenyl)thiophene-2-sulfonamide (TJ-C24). Overall yield: 25.7%, purity: 95.3%. ^1H NMR (400 MHz, acetone- d_6): δ 8.60 (s, 1H), 7.89 (s, 1H), 7.76 (dd, $J = 7.6$, 1.6 Hz, 1H), 7.57 (d, $J = 4.0$ Hz, 1H), 7.53 (d, $J = 4.0$ Hz, 1H), 7.32 (td, $J = 7.6$, 1.6 Hz, 1H), 7.22–7.17 (m, 2H), 7.04–7.00 (m, 4H), 6.96 (d, $J = 7.6$ Hz, 1H), 6.85–6.80 (m, 2H), 6.56 (s, 1H), 6.03–6.02 (m, 1H), 5.24 (s, 2H), 3.39–3.34 (m, 2H), 3.18–3.14 (m, 2H), 2.16 (s, 6H); ^{13}C NMR (100 MHz, acetone- d_6): δ 158.6, 156.9, 155.4, 145.8, 141.3, 140.9, 139.0, 138.8, 131.6, 130.7, 130.4, 128.9, 125.4, 124.3, 122.6, 122.1, 119.5, 117.2, 115.9, 115.5, 114.2, 71.1, 45.1, 40.2, 21.5; ESI-MS: m/z 551.6 [M + H] $^+$; ESI-HRMS $\text{C}_{28}\text{H}_{28}\text{N}_3\text{O}_5\text{S}_2$ [M + H] $^+$ calcd, 550.1465; obs., 550.1465.

N-(2-(3-(3,5-Bis(trifluoromethyl)phenyl)thioureido)ethyl)-5-(2-((3-hydroxybenzyl)oxy)phenyl)thiophene-2-sulfonamide (TJ-C25). Overall yield: 37.4%, purity: 96.3%. ^1H NMR (400 MHz, acetone- d_6): δ 9.64 (s, 1H), 8.52 (s, 1H), 8.33 (s, 2H), 7.84–7.79 (m, 2H), 7.71 (s, 1H), 7.63 (d, $J = 4.0$ Hz, 1H), 7.59 (d, $J = 4.0$ Hz, 1H), 7.32 (td, $J = 7.6$, 1.6 Hz, 1H), 7.25–7.19 (m, 2H), 7.05–6.99 (m, 3H), 6.93–6.90 (m, 1H), 6.82 (dd, $J = 8.0$, 1.6 Hz, 1H), 5.30 (s, 2H), 3.87–3.82 (m, 2H), 3.36–3.31 (m, 2H); ^{13}C NMR (100 MHz, acetone- d_6): δ 182.6, 158.5, 155.4, 146.1, 142.7, 141.0, 139.1, 132.1, 131.9, 131.8, 130.8, 130.5, 128.9, 125.7, 125.5, 123.5, 123.0, 122.5, 122.1, 119.5, 117.6, 115.8, 115.3, 114.3, 71.1, 44.7, 43.1; ESI-MS: m/z 673.9 [M + H] $^+$; DART-HRMS $\text{C}_{28}\text{H}_{24}\text{N}_3\text{O}_4\text{F}_6\text{S}_3$ [M + H] $^+$ calcd, 676.0828; obs., 676.0812.

N-(2-(3-(3-Chlorophenyl)thioureido)ethyl)-5-(2-((3-hydroxybenzyl)oxy)phenyl)thiophene-2-sulfonamide (TJ-C26). Overall yield: 38.8%, purity: 95.1%. ^1H NMR (400 MHz, acetone- d_6): δ 9.14 (s, 1H), 8.50 (s, 1H), 7.81 (dd, $J = 7.6$, 1.2 Hz, 1H), 7.66 (d, $J = 2.0$ Hz, 1H), 7.63 (d, $J = 4.0$ Hz, 1H), 7.57 (d, $J = 4.0$ Hz, 1H), 7.54–7.51 (m, 1H), 7.36–7.19 (m, 5H), 7.14 (d, $J = 8.0$ Hz, 1H), 7.06–6.99 (m, 3H), 6.94–6.91 (m, 1H), 6.82 (dd, $J = 7.6$, 2.0 Hz, 1H), 5.30 (s, 2H), 3.85–3.80 (m, 2H), 3.33–3.29 (m, 2H); ^{13}C NMR (100 MHz, acetone- d_6): δ 182.5, 158.4, 155.4, 145.9, 141.1, 139.0, 134.5, 131.8, 131.0, 130.7, 130.5, 128.9, 125.5, 125.4, 124.2, 122.7, 122.5, 122.1, 119.5, 115.8, 115.3, 114.3, 71.0, 44.7, 43.5; ESI-MS: m/z 572.0 [M + H] $^+$; ESI-HRMS $\text{C}_{26}\text{H}_{25}\text{Cl}_1\text{N}_3\text{O}_4\text{S}_3$ [M + H] $^+$ calcd, 574.0690; obs., 574.0686.

N-(2-(3-(3,5-Bis(trifluoromethyl)phenyl)ureido)ethyl)-5-(2-(((1*r*,4*r*)-4-hydroxycyclohexyl)oxy)phenyl)thiophene-2-sulfonamide (TJ-C27). Overall yield: 27.0%, purity: 98.8%. ^1H NMR (400 MHz, acetone- d_6): δ 8.79 (s, 1H), 8.13 (s, 2H), 7.79 (dd, $J = 8.0$, 1.6 Hz, 1H), 7.60 (d, $J = 4.0$ Hz, 1H), 7.57 (d, $J = 4.0$ Hz, 1H), 7.51 (s, 1H), 7.33 (td, $J = 7.6$, 1.6 Hz, 1H), 7.20 (d, $J = 8.0$ Hz, 1H), 7.00 (td, $J = 7.6$, 0.8 Hz, 1H), 6.86–6.83 (m, 1H), 6.30–6.28 (m, 1H), 4.61–4.59 (m, 1H), 3.76–3.66 (m, 2H), 3.45–3.40 (m, 2H), 3.24–3.20 (m, 2H), 2.21–

2.17 (m, 2H), 2.02–1.98 (m, 2H), 1.69–1.63 (m, 2H), 1.52–1.46 (m, 2H); ^{13}C NMR (100 MHz, acetone- d_6): δ 155.9, 154.6, 146.1, 143.5, 141.1, 132.8, 132.5, 132.1, 131.8, 131.7, 130.7, 128.8, 125.8, 125.1, 123.1, 122.9, 121.7, 118.4, 114.8, 77.0, 68.9, 44.4, 40.4, 33.0, 29.6; ESI-MS: m/z 650.1 [M + H] $^+$; ESI-HRMS $\text{C}_{27}\text{H}_{28}\text{N}_3\text{O}_5\text{F}_6\text{S}_2$ [M + H] $^+$ calcd, 652.1369; obs., 652.1373.

N-(2-(3-(3,5-Dichlorophenyl)ureido)ethyl)-5-(2-(((1*r*,4*r*)-4-hydroxycyclohexyl)oxy)phenyl)thiophene-2-sulfonamide (TJ-C28). Overall yield: 25.8%, purity: 95.2%. ^1H NMR (400 MHz, acetone- d_6): δ 8.39 (s, 1H), 7.79 (dd, $J = 8.0$, 1.6 Hz, 1H), 7.60 (d, $J = 4.0$ Hz, 1H), 7.56 (d, $J = 4.0$ Hz, 1H), 7.51 (d, $J = 2.0$ Hz, 2H), 7.34 (t, $J = 7.2$ Hz, 1H), 7.20 (d, $J = 8.0$ Hz, 1H), 7.01 (t, $J = 7.6$ Hz, 1H), 6.96 (t, $J = 2.0$ Hz, 1H), 6.82 (m, 1H), 6.12 (m, 1H), 4.60 (m, 1H), 3.75–3.72 (m, 2H), 3.41–3.37 (m, 2H), 3.22–3.17 (m, 2H), 2.21–2.15 (m, 2H), 2.02–1.98 (m, 2H), 1.68–1.65 (m, 2H), 1.50–1.46 (m, 2H); ^{13}C NMR (100 MHz, acetone- d_6): δ 155.9, 154.6, 146.1, 143.8, 141.0, 135.4, 131.6, 130.7, 128.8, 125.0, 122.9, 121.7, 121.5, 116.9, 114.8, 77.0, 68.9, 44.6, 40.3, 33.0, 29.6; ESI-MS: m/z 582.0 [M + H] $^+$; ESI-HRMS $\text{C}_{25}\text{H}_{28}\text{Cl}_2\text{N}_3\text{O}_5\text{S}_2$ [M + H] $^+$ calcd, 584.0842; obs., 584.0843.

N-(2-(3-(4-Nitrophenyl)thioureido)ethyl)-5-(2-(((1*r*,4*r*)-4-hydroxycyclohexyl)oxy)phenyl)thiophene-2-sulfonamide (TJ-C29). Overall yield: 21.9%, purity: 98.1%. ^1H NMR (400 MHz, acetone- d_6): δ 9.56 (s, 1H), 8.15–8.13 (m, 2H), 7.90–7.87 (m, 2H), 7.81–7.79 (m, 2H), 7.61 (d, $J = 4.0$ Hz, 1H), 7.59 (d, $J = 4.0$ Hz, 1H), 7.34 (td, $J = 7.6$, 1.6 Hz, 1H), 7.21 (d, $J = 8.0$ Hz, 1H), 7.01 (t, $J = 7.6$ Hz, 1H), 6.92–6.89 (m, 1H), 4.64–4.58 (m, 1H), 3.87–3.83 (m, 2H), 3.75–3.71 (m, 2H), 3.39–3.35 (m, 2H), 2.22–2.18 (m, 2H), 2.02–1.98 (m, 2H), 1.70–1.66 (m, 2H), 1.49–1.46 (m, 2H); ^{13}C NMR (100 MHz, acetone- d_6): δ 182.1, 154.6, 146.7, 146.2, 143.9, 140.9, 131.8, 130.7, 128.8, 125.2, 125.1, 122.9, 122.1, 121.7, 114.8, 77.0, 68.9, 44.6, 43.2, 33.1, 29.7; ESI-MS: m/z 575.1 [M + H] $^+$; ESI-HRMS $\text{C}_{25}\text{H}_{29}\text{N}_4\text{O}_6\text{S}_3$ [M + H] $^+$ calcd, 577.1244; obs., 577.1244.

N-(2-(3-(4-Nitrophenyl)ureido)ethyl)-5-(2-(((1*r*,4*r*)-4-hydroxycyclohexyl)oxy)phenyl)thiophene-2-sulfonamide (TJ-C30). Overall yield: 15.0%, purity: 99.5%. ^1H NMR (400 MHz, acetone- d_6): δ 8.73 (s, 1H), 8.11–8.08 (m, 2H), 7.79 (dd, $J = 7.6$, 1.6 Hz, 1H), 7.68–7.66 (m, 2H), 7.59 (d, $J = 4.0$ Hz, 1H), 7.56 (d, $J = 4.0$ Hz, 1H), 7.33 (td, $J = 7.6$, 1.6 Hz, 1H), 7.20 (d, $J = 8.0$ Hz, 1H), 7.00 (td, $J = 7.6$, 0.8 Hz, 1H), 6.83–6.80 (m, 1H), 6.25–6.22 (m, 1H), 4.62–4.56 (m, 1H), 3.75–3.69 (m, 2H), 3.44–3.39 (m, 2H), 3.24–3.20 (m, 2H), 2.21–2.17 (m, 2H), 2.02–1.97 (m, 2H), 1.71–1.51 (m, 2H), 1.51–1.42 (m, 2H); ^{13}C NMR (100 MHz, acetone- d_6): δ 155.6, 154.6, 147.8, 146.1, 142.3, 141.1, 131.6, 130.7, 128.8, 125.7, 125.0, 122.9, 121.7, 117.9, 114.8, 77.0, 68.9, 44.5, 40.3, 33.0, 29.7; ESI-MS: m/z 559.1 [M + H] $^+$; ESI-HRMS $\text{C}_{25}\text{H}_{29}\text{N}_4\text{O}_7\text{S}_2$ [M + H] $^+$ calcd, 561.1472; obs., 561.1473.

N-(2-(3-(3,5-Bis(trifluoromethyl)phenyl)thioureido)ethyl)-5-(2-(((1*s*,4*s*)-4-hydroxycyclohexyl)oxy)phenyl)thiophene-2-sulfonamide (TJ-C31). Overall yield: 21.4%, purity: 96.1%. ^1H NMR (400 MHz, acetone- d_6): δ 9.54 (s, 1H), 8.32 (s, 2H), 7.82–7.79 (m, 2H), 7.71 (s, 1H), 7.62 (d, $J = 4.0$ Hz, 1H), 7.60 (d, $J = 4.0$ Hz, 1H), 7.35 (td, $J = 7.6$, 1.6 Hz, 1H), 7.20 (d, $J = 8.0$ Hz, 1H), 7.01 (td, $J = 7.6$, 0.8 Hz, 1H), 6.95–6.92 (m, 1H), 4.71–4.70 (m, 1H), 3.94–3.93 (m, 1H), 3.86–3.81 (m, 3H), 3.39–3.34 (m, 2H), 2.14–2.07 (m, 2H), 1.85–1.73 (m, 6H); ^{13}C NMR (100 MHz, acetone- d_6): δ 182.7, 154.6, 146.3, 142.8, 141.0, 132.4, 132.1, 131.8, 131.8, 131.5, 130.8, 129.2, 125.7, 125.3, 123.5, 123.0, 121.7, 117.6, 114.8, 75.4, 67.6, 44.6, 43.2, 31.4, 28.0; ESI-MS: m/z 668.0 [M + H] $^+$; ESI-HRMS $\text{C}_{27}\text{H}_{28}\text{N}_3\text{O}_4\text{F}_6\text{S}_3$ [M + H] $^+$ calcd, 668.1141; obs., 668.1141.

N-(2-(3-(3,5-Bis(trifluoromethyl)phenyl)ureido)ethyl)-5-(2-(((1*s*,4*s*)-4-hydroxycyclohexyl)oxy)phenyl)thiophene-2-sulfonamide (TJ-C32). Overall yield: 18.0%, purity: 95.7%. ^1H NMR (400 MHz, acetone- d_6): δ 8.73 (s, 1H), 8.12 (s, 2H), 7.78 (dd, $J = 8.0$, 1.6 Hz, 1H), 7.59 (d, $J = 4.0$ Hz, 1H), 7.57 (d, $J = 4.0$ Hz, 1H), 7.51 (s, 1H), 7.34 (td, $J = 7.6$, 1.6 Hz, 1H), 7.19 (d, $J = 8.0$ Hz, 1H), 7.00 (td, $J = 7.6$, 0.8 Hz, 1H), 6.85–6.82 (m, 1H), 6.29 (m, 1H), 4.71–4.68 (m, 1H), 3.96–3.95 (m, 1H), 3.86–3.85 (m, 1H), 3.44–3.39 (m, 2H), 3.26–3.21 (m, 2H), 2.13–2.06 (m, 2H), 1.84–1.70 (m, 6H); ^{13}C NMR (100 MHz, acetone- d_6): δ 155.9, 154.6, 146.2, 143.5, 141.2, 132.8, 132.5, 132.2, 131.9, 131.8, 130.8, 129.2, 125.9, 125.3, 123.1, 123.0, 121.6, 118.4, 114.8, 75.4, 67.6, 44.5, 40.3, 31.4, 28.0; ESI-MS: m/z 650.1 [M +

H⁻; ESI-HRMS C₂₇H₂₈N₃O₃F₆S₂ [M + H]⁺ calcd, 652.1369; obs., 652.1371.

N-(2-(3-(4-Nitrophenyl)thioureido)ethyl)-5-(2-(((1*s*,4*s*)-4-hydroxycyclohexyloxy)phenyl)thiophene-2-sulfonamide (TJ-C33). Overall yield: 21.7%, purity: 95.7%. ¹H NMR (400 MHz, acetone-*d*₆): δ 9.55 (s, 1H), 8.16–8.13 (m, 2H), 7.90–7.88 (m, 2H), 7.81–7.79 (m, 2H), 7.61 (d, *J* = 4.0 Hz, 1H), 7.60 (d, *J* = 4.0 Hz, 1H), 7.34 (td, *J* = 7.6, 1.6 Hz, 1H), 7.19 (d, *J* = 8.0 Hz, 1H), 7.01 (t, *J* = 7.6 Hz, 1H), 6.94–6.91 (m, 1H), 4.71–4.67 (m, 1H), 3.92–3.91 (m, 1H), 3.87–3.82 (m, 3H), 3.40–3.35 (m, 2H), 2.13–2.06 (m, 2H), 1.86–1.70 (m, 6H); ¹³C NMR (100 MHz, acetone-*d*₆): δ 182.1, 154.5, 146.7, 146.2, 143.9, 140.9, 131.8, 130.8, 129.1, 125.3, 125.1, 122.9, 122.1, 121.6, 114.7, 75.4, 67.5, 44.5, 43.3, 31.4, 27.9; ESI-MS: *m/z* 575.0 [M – H]⁻; ESI-HRMS C₂₅H₂₉N₄O₆S₃ [M + H]⁺ calcd, 577.1244; obs., 577.1247.

N-(2-(3-(4-Nitrophenyl)ureido)ethyl)-5-(2-(((1*s*,4*s*)-4-hydroxycyclohexyloxy)phenyl)thiophene-2-sulfonamide (TJ-C34). Overall yield: 19.4%, purity: 99.3%. ¹H NMR (400 MHz, acetone-*d*₆): δ 8.75 (s, 1H), 8.11–8.09 (m, 2H), 7.77 (dd, *J* = 8.0, 1.6 Hz, 1H), 7.68–7.65 (m, 2H), 7.57 (m, 2H), 7.33 (td, *J* = 7.6, 1.6 Hz, 1H), 7.18 (d, *J* = 8.0 Hz, 1H), 7.00 (t, *J* = 7.6 Hz, 1H), 6.86–6.83 (m, 1H), 6.30–6.27 (m, 1H), 4.69–4.66 (m, 1H), 3.96–3.95 (m, 1H), 3.86–3.85 (m, 1H), 3.43–3.39 (m, 2H), 3.26–3.22 (m, 2H), 2.10–2.07 (m, 2H), 1.84–1.73 (m, 6H); ¹³C NMR (100 MHz, acetone-*d*₆): δ 155.7, 154.5, 147.7, 146.1, 142.3, 141.1, 131.7, 130.7, 129.2, 125.6, 125.2, 123.0, 121.6, 118.0, 114.7, 75.4, 67.5, 44.6, 40.2, 31.4, 28.0; ESI-MS: *m/z* 559.0 [M – H]⁻; ESI-HRMS C₂₅H₂₉N₄O₇S₂ [M + H]⁺ calcd, 561.1472; obs., 561.1477.

N-(2-(3-(3,5-Bis(trifluoromethyl)phenyl)thioureido)ethyl)-3-(2-(3,4-dihydroxyphenoxy)-4-methylphenyl)thiophene-2-sulfonamide (FWJ-D1). Overall yield: 19.1%, purity: 96.1%. ¹H NMR (400 MHz, CDCl₃): δ 7.82 (s, 2H), 7.68 (s, 1H), 7.55 (d, *J* = 5.1 Hz, 1H), 7.23 (d, *J* = 7.7 Hz, 1H), 7.10 (d, *J* = 5.0 Hz, 1H), 6.93 (d, *J* = 7.5 Hz, 1H), 6.78–6.72 (m, 2H), 6.51 (d, *J* = 2.3 Hz, 1H), 6.33–6.27 (m, 1H), 3.70 (s, 2H), 3.15 (s, 2H), 2.29 (s, 3H); ¹³C NMR (100 MHz, CDCl₃): δ 179.52, 152.03, 149.94, 148.42, 140.44, 138.15, 137.74, 136.85, 133.94, 131.66, 129.42, 128.45, 126.96, 125.78, 124.44, 122.60, 122.02, 119.16, 118.43, 116.86, 112.81, 106.63, 45.47, 42.32, 21.64; ESI-MS: *m/z* 690.00 [M – H]⁻; ESI-HRMS calcd for C₂₈H₂₂O₃N₃F₆S₃ [M – H]⁻, 690.0641.

N-(2-(3-(3,5-Bis(trifluoromethyl)phenyl)thioureido)ethyl)-3-(2-(3,4-dihydroxyphenoxy)-5-isopropylphenyl)thiophene-2-sulfonamide (FWJ-D2). Overall yield: 14.1%, purity: 98.0%. ¹H NMR (400 MHz, acetone-*d*₆): δ 9.51 (s, 1H), 8.31 (s, 2H), 8.01 (s, 1H), 7.80 (s, 1H), 7.77 (d, *J* = 5.1 Hz, 1H), 7.71 (d, *J* = 11.3 Hz, 2H), 7.40 (d, *J* = 2.2 Hz, 1H), 7.24–7.18 (m, 2H), 6.78 (t, *J* = 8.3 Hz, 2H), 6.56 (d, *J* = 2.8 Hz, 1H), 6.48–6.34 (m, 2H), 3.73 (dd, *J* = 11.9, 5.9 Hz, 2H), 3.16 (q, *J* = 6.1 Hz, 2H), 2.93 (dd, *J* = 13.8, 6.9 Hz, 1H), 1.25 (d, *J* = 6.9 Hz, 6H); ¹³C NMR (100 MHz, acetone-*d*₆): δ 181.7, 153.6, 149.7, 145.8, 142.3, 141.8, 141.3, 141.2, 137.1, 132.1, 131.1, 130.8, 130.0, 128.8, 127.7, 124.5, 117.1, 115.4, 110.2, 107.2, 43.7, 42.0, 33.1, 23.4; ESI-MS: *m/z* 718.05 [M – H]⁻; ESI-HRMS calcd for C₃₀H₂₆O₃N₃F₆S₃ [M – H]⁻, 718.0955.

N-(2-(3-(3,5-Bis(trifluoromethyl)phenyl)thioureido)ethyl)-3-(2-(3,4-dimethoxyphenoxy)-5-isopropylphenyl)thiophene-2-sulfonamide (FWJ-D3). Overall yield: 14.4%, purity: 96.7%. ¹H NMR (400 MHz, acetone-*d*₆): δ 9.48 (s, 1H), 8.30 (s, 2H), 7.77 (d, *J* = 5.1 Hz, 1H), 7.71 (d, *J* = 10.4 Hz, 2H), 7.42 (d, *J* = 2.3 Hz, 1H), 7.23 (q, *J* = 2.7 Hz, 2H), 6.87 (d, *J* = 8.7 Hz, 1H), 6.79 (d, *J* = 8.5 Hz, 1H), 6.72 (d, *J* = 2.7 Hz, 1H), 6.54 (dd, *J* = 8.7, 2.7 Hz, 1H), 6.48 (s, 1H), 3.74 (dd, *J* = 9.9, 5.6 Hz, 8H), 3.18 (q, *J* = 6.1 Hz, 2H), 2.93 (dd, *J* = 13.8, 6.9 Hz, 1H), 1.25 (d, *J* = 6.9 Hz, 6H); ¹³C NMR (101 MHz, acetone-*d*₆): δ 182.4, 154.2, 151.3, 151.1, 146.5, 143.2, 142.4, 141.8, 137.8, 132.9, 131.9, 131.5, 130.7, 129.5, 128.4, 125.3, 123.3, 122.7, 117.8, 117.4, 113.1, 111.0, 105.3, 56.3, 55.9, 44.4, 42.7, 33.8, 24.1; ESI-MS: *m/z* 746.10 [M – H]⁻; ESI-HRMS calcd for C₃₂H₃₂O₅N₃F₆S₃ [M + H]⁺, 748.1401.

N-(2-(3-(3,5-Bis(trifluoromethyl)phenyl)ureido)ethyl)-3-(2-(3,4-dihydroxyphenoxy)-4-methylphenyl)thiophene-2-sulfonamide (FWJ-D4). Overall yield: 18.7%, purity: 97.9%. ¹H NMR (400 MHz, CDCl₃): δ 7.66 (s, 2H), 7.53–7.42 (m, 4H), 7.24 (s, 1H), 7.12 (d, *J* = 5.1 Hz, 1H), 6.88 (d, *J* = 7.7 Hz, 1H), 6.77–6.67 (m, 2H), 6.50 (d, *J* = 2.7 Hz, 1H), 6.29 (dd, *J* = 8.6, 2.7 Hz, 1H), 5.88 (s, 1H), 5.80 (s, 1H),

5.40 (s, 1H), 3.31 (d, *J* = 5.1 Hz, 2H), 3.06 (d, *J* = 5.3 Hz, 2H), 2.19 (s, 3H); ¹³C NMR (100 MHz, CDCl₃): δ 171.29, 155.45, 154.49, 149.15, 144.68, 142.13, 141.18, 141.10, 139.93, 133.84, 132.67, 132.22, 131.89, 131.56, 131.11, 129.98, 124.41, 123.99, 121.60, 118.67, 115.58, 110.57, 106.47, 43.41, 39.71, 21.22; ESI-MS: *m/z* 698.00 [M + Na]⁺; ESI-HRMS calcd for C₂₈H₂₄O₆N₃F₆S₂ [M + H]⁺, 676.1004.

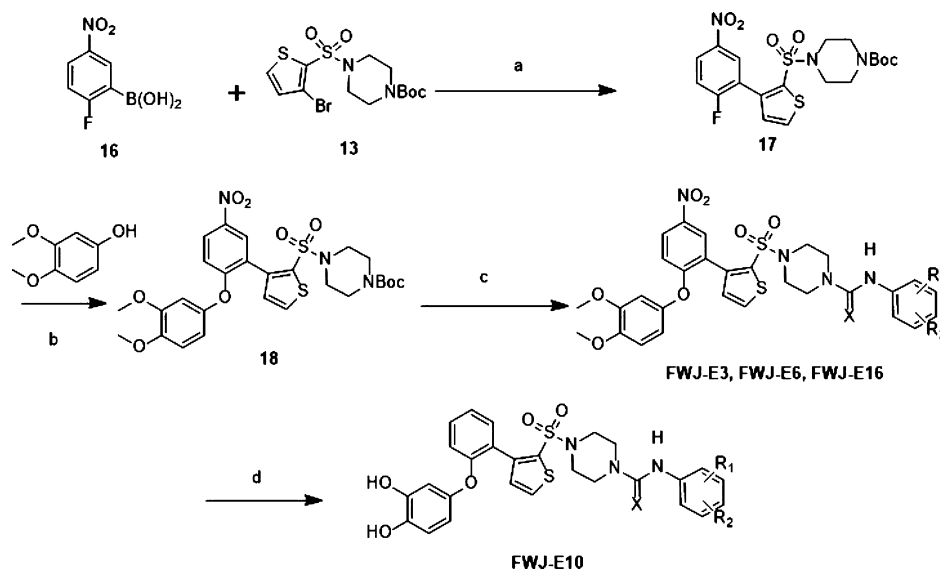
N-(2-(3-(3,5-Bis(trifluoromethyl)phenyl)ureido)ethyl)-3-(2-(3,4-dimethoxyphenoxy)-4-methylphenyl)thiophene-2-sulfonamide (FWJ-D5). Overall yield: 18.9%, purity: 98.7%. ¹H NMR (400 MHz, acetone-*d*₆): δ 8.68 (s, 1H), 8.14 (s, 2H), 7.75 (d, *J* = 5.1 Hz, 1H), 7.54 (s, 1H), 7.38 (d, *J* = 7.7 Hz, 1H), 7.19 (d, *J* = 5.1 Hz, 1H), 6.92 (d, *J* = 7.7 Hz, 1H), 6.86 (d, *J* = 8.7 Hz, 1H), 6.76–6.65 (m, 2H), 6.55 (dd, *J* = 8.7, 2.7 Hz, 1H), 6.46 (t, *J* = 5.8 Hz, 1H), 6.19 (s, 1H), 3.75 (s, 6H), 3.34 (q, *J* = 5.9 Hz, 2H), 3.09 (q, *J* = 6.0 Hz, 2H); ¹³C NMR (100 MHz, acetone-*d*₆): δ 156.17, 155.65, 151.18, 146.62, 143.29, 141.52, 140.73, 137.91, 133.01, 132.33, 132.00, 129.51, 125.66, 123.76, 122.86, 118.47, 118.23, 114.70, 113.14, 111.30, 105.46, 56.27, 55.93, 43.96, 40.30, 21.15; ESI-MS: *m/z* 726.10 [M + Na]⁺; ESI-HRMS calcd for C₃₀H₂₈O₆N₃F₆S₂ [M + H]⁺, 704.1310.

N-(2-(3-(3,5-Bis(trifluoromethyl)phenyl)ureido)ethyl)-3-(2-(3,4-dihydroxyphenoxy)-5-isopropylphenyl)thiophene-2-sulfonamide (FWJ-D6). Overall yield: 18.0%, purity: 99.0%. ¹H NMR (400 MHz, acetone-*d*₆): δ 8.72 (s, 1H), 8.09 (d, *J* = 23.2 Hz, 3H), 7.74 (d, *J* = 5.1 Hz, 2H), 7.54 (s, 1H), 7.41 (d, *J* = 1.6 Hz, 1H), 7.23–7.14 (m, 2H), 6.77 (dd, *J* = 8.5, 4.1 Hz, 2H), 6.56 (d, *J* = 2.5 Hz, 1H), 6.39 (dd, *J* = 8.5, 2.6 Hz, 1H), 6.33 (t, *J* = 5.7 Hz, 1H), 6.19 (s, 1H), 3.31 (dd, *J* = 11.3, 5.6 Hz, 2H), 3.02 (dd, *J* = 11.9, 6.0 Hz, 2H), 2.89 (dd, *J* = 13.8, 6.8 Hz, 1H), 1.24 (d, *J* = 6.9 Hz, 6H); ¹³C NMR (100 MHz, acetone-*d*₆): δ 155.4, 154.1, 150.3, 146.3, 142.9, 141.8, 141.6, 137.7, 132.7, 132.1, 131.8, 130.5, 129.3, 128.2, 125.5, 125.0, 122.8, 118.0, 117.6, 115.9, 114.5, 110.8, 107.7, 43.8, 39.9, 33.7, 23.9; ESI-MS: *m/z* 704.15 [M + H]⁺; ESI-HRMS calcd for C₃₀H₂₈O₆N₃F₆S₂ [M + H]⁺, 704.1320.

N-(2-(3-(3,5-Bis(trifluoromethyl)phenyl)ureido)ethyl)-3-(2-(3,4-dimethoxyphenoxy)-5-isopropylphenyl)thiophene-2-sulfonamide (FWJ-D7). Overall yield: 18.0%, purity: 97.1%. ¹H NMR (400 MHz, acetone-*d*₆): δ 8.13 (s, 2H), 7.75 (d, *J* = 5.1 Hz, 1H), 7.53 (s, 1H), 7.42 (d, *J* = 2.1 Hz, 1H), 7.20 (dd, *J* = 12.2, 3.6 Hz, 2H), 6.86 (d, *J* = 8.7 Hz, 1H), 6.77 (d, *J* = 8.5 Hz, 1H), 6.72 (d, *J* = 2.6 Hz, 1H), 6.54 (dd, *J* = 8.7, 2.7 Hz, 1H), 3.74 (d, *J* = 2.2 Hz, 6H), 3.30 (t, *J* = 5.7 Hz, 2H), 3.04 (t, *J* = 6.0 Hz, 2H), 2.92 (dd, *J* = 13.8, 6.9 Hz, 1H), 1.24 (d, *J* = 6.9 Hz, 6H); ¹³C NMR (101 MHz, acetone-*d*₆): δ 155.6, 154.2, 151.2, 146.53, 143.2, 141.6, 138.1, 132.8, 132.2, 131.9, 130.7, 128.4, 125.6, 125.2, 122.9, 118.1, 117.7, 114.5, 113.1, 111.1, 105.3, 56.2, 55.9, 43.9, 40.2, 33.83, 24.0; ESI-MS: *m/z* 770.15 (M + K)⁺; ESI-HRMS calcd for C₃₂H₃₂O₆N₃F₆S₂ [M + H]⁺, 732.1628.

N-(2-(3-(3,5-Dichlorophenyl)ureido)ethyl)-3-(2-(3,4-dihydroxyphenoxy)-4-methylphenyl)thiophene-2-sulfonamide (FWJ-D8). Overall yield: 18.2%, purity: 95.0%. ¹H NMR (400 MHz, acetone-*d*₆): δ 8.37 (s, 1H), 8.06 (s, 1H), 7.78–7.72 (m, 2H), 7.53 (d, *J* = 1.7 Hz, 2H), 7.35 (d, *J* = 7.7 Hz, 1H), 7.17 (d, *J* = 5.1 Hz, 1H), 7.00 (s, 1H), 6.90 (d, *J* = 7.7 Hz, 1H), 6.78 (d, *J* = 8.6 Hz, 1H), 6.67 (s, 1H), 6.57 (d, *J* = 2.7 Hz, 1H), 6.40 (dt, *J* = 11.7, 4.3 Hz, 2H), 6.07 (s, 1H), 3.30 (q, *J* = 5.9 Hz, 2H), 3.04 (q, *J* = 5.9 Hz, 2H), 2.26 (s, 3H); ¹³C NMR (100 MHz, acetone-*d*₆): δ 155.67, 155.02, 149.54, 145.94, 142.98, 141.58, 140.90, 139.98, 137.13, 134.57, 132.30, 131.64, 128.78, 122.88, 122.03, 120.73, 117.69, 116.16, 115.52, 110.60, 107.50, 43.47, 39.53, 20.49; ESI-MS: *m/z* 606.05 [M – H]⁻; ESI-HRMS calcd for C₂₆H₂₄O₆N₃Cl₂S₂ [M + H]⁺, 608.0478.

N-(2-(3-(3,5-Dichlorophenyl)ureido)ethyl)-3-(2-(3,4-dihydroxyphenoxy)-5-isopropylphenyl)thiophene-2-sulfonamide (FWJ-D9). Overall yield: 16.1%, purity: 96.5%. ¹H NMR (400 MHz, acetone-*d*₆): δ 7.74 (d, *J* = 5.1 Hz, 1H), 7.52 (d, *J* = 1.8 Hz, 2H), 7.41 (d, *J* = 2.2 Hz, 1H), 7.20 (d, *J* = 5.1 Hz, 1H), 7.16 (dd, *J* = 8.5, 2.2 Hz, 1H), 7.01 (t, *J* = 1.8 Hz, 1H), 6.80–6.73 (m, 2H), 6.60 (d, *J* = 2.7 Hz, 1H), 6.39 (dd, *J* = 8.6, 2.8 Hz, 1H), 3.28 (t, *J* = 6.0 Hz, 2H), 2.99 (t, *J* = 6.0 Hz, 2H), 2.91 (dt, *J* = 13.8, 6.9 Hz, 1H), 1.25 (d, *J* = 6.9 Hz, 6H); ¹³C NMR (100 MHz, acetone-*d*₆): δ 155.5, 154.1, 150.1, 146.4, 143.3, 142.8, 141.8, 141.5, 137.7, 135.0, 132.6, 130.5, 129.2, 128.2, 124.9, 121.1, 117.5, 116.5, 115.8, 107.7, 43.9, 39.8, 33.7, 23.9; ESI-MS: *m/z* 658.10 [M + Na]⁺; ESI-HRMS calcd for C₂₈H₂₈O₆N₃Cl₂S₂ [M + H]⁺, 636.0788.

Scheme 3. Synthesis of Compounds FWJ-E3, FWJ-E6, FWJ-E10, and FWJ-E16^a

^aReagents and conditions: (a) Pd(OAc)₂, K₃PO₄, Ph₂Pcy, THF; (b) Cs₂CO₃, DMSO; (c) (i) TFA, DCM, (ii) aryl isothiocyanate, DCM; (d) BBr₃, DCM.

N-(2-(3-(3,5-Dichlorophenyl)ureido)ethyl)-3-(2-(3,4-dimethoxyphenoxy)-5-isopropylphenyl)thiophene-2-sulfonamide (**FWJ-D10**). Overall yield: 16.1%, purity: 97.3%. ¹H NMR (400 MHz, acetone-*d*₆): δ 8.39 (s, 1H), 7.75 (d, *J* = 5.1 Hz, 1H), 7.52 (d, *J* = 1.8 Hz, 2H), 7.42 (d, *J* = 2.3 Hz, 1H), 7.24–7.17 (m, 2H), 6.99 (t, *J* = 1.8 Hz, 1H), 6.86 (d, *J* = 8.7 Hz, 1H), 6.74 (dd, *J* = 14.6, 5.6 Hz, 2H), 6.54 (dd, *J* = 8.7, 2.7 Hz, 1H), 6.38 (t, *J* = 5.6 Hz, 1H), 6.09 (t, *J* = 5.5 Hz, 1H), 3.75 (d, *J* = 3.2 Hz, 6H), 3.27 (q, *J* = 5.9 Hz, 2H), 3.02 (q, *J* = 5.9 Hz, 2H), 2.93 (dd, *J* = 13.8, 6.9 Hz, 1H), 1.24 (t, *J* = 7.1 Hz, 6H). ¹³C NMR (100 MHz, acetone-*d*₆): δ 155.6, 154.2, 151.3, 151.1, 146.5, 143.6, 143.1, 141.6, 138.1, 135.1, 132.8, 130.7, 129.4, 128.4, 125.2, 121.2, 117.6, 116.6, 113.1, 111.1, 105.4, 56.2, 55.9, 44.1, 40.2, 33.8, 24.2; ESI-MS: *m/z* 662.05 [M – H][–]; ESI-HRMS calcd for C₃₀H₃₂O₆N₃Cl₂S₂ [M + H]⁺, 664.1103.

N-(2-(3-(3-Nitrophenyl)thioureido)ethyl)-3-(2-(3,4-dihydroxyphenoxy)-4-methylphenyl)thiophene-2-sulfonamide (**FWJ-D11**). Overall yield: 18.2%, purity: 96.3%. ¹H NMR (400 MHz, acetone-*d*₆): δ 9.33 (s, 1H), 8.62 (s, 1H), 8.01 (s, 1H), 7.98 (d, *J* = 8.1 Hz, 1H), 7.90 (d, *J* = 7.4 Hz, 1H), 7.81 (s, 1H), 7.76 (d, *J* = 5.1 Hz, 1H), 7.59 (t, *J* = 8.1 Hz, 1H), 7.54 (s, 1H), 7.36 (d, *J* = 7.7 Hz, 1H), 7.18 (d, *J* = 5.1 Hz, 1H), 6.91 (d, *J* = 7.6 Hz, 1H), 6.78 (d, *J* = 8.5 Hz, 1H), 6.68 (s, 1H), 6.57 (d, *J* = 2.8 Hz, 1H), 6.48 (s, 1H), 6.41 (dd, *J* = 8.6, 2.8 Hz, 1H), 3.75 (dd, *J* = 11.7, 5.8 Hz, 2H), 3.19 (dd, *J* = 12.1, 6.1 Hz, 2H), 2.28 (s, 3H); ¹³C NMR (100 MHz, acetone-*d*₆): δ 182.2, 156.1, 149.9, 148.6, 146.3, 142.0, 141.4, 141.2, 140.4, 137.3, 132.7, 132.0, 130.1, 129.5, 129.4, 123.3, 122.4, 119.2, 118.1, 116.0, 111.1, 108.0, 44.2, 42.7, 21.0; ESI-MS: *m/z* 622.90 [M + Na]⁺; ESI-HRMS calcd for C₂₆H₂₄O₇N₄NaS₃ [M + Na]⁺, 623.0698.

N-(2-(3-(3-Nitrophenyl)ureido)ethyl)-3-(2-(3,4-dihydroxyphenoxy)-4-methylphenyl)thiophene-2-sulfonamide (**FWJ-D12**). Overall yield: 18.7%, purity: 95.7%. ¹H NMR (400 MHz, acetone-*d*₆): δ 8.57 (t, *J* = 2.1 Hz, 1H), 8.52 (s, 1H), 8.06 (s, 1H), 7.82–7.77 (m, 1H), 7.74 (d, *J* = 5.9 Hz, 3H), 7.51 (t, *J* = 8.2 Hz, 1H), 7.36 (d, *J* = 7.8 Hz, 1H), 7.17 (d, *J* = 5.1 Hz, 1H), 6.91 (d, *J* = 7.5 Hz, 1H), 6.77 (d, *J* = 8.6 Hz, 1H), 6.67 (s, 1H), 6.57 (d, *J* = 2.8 Hz, 1H), 6.44–6.37 (m, 2H), 6.10 (s, 1H), 3.33 (dd, *J* = 11.9, 5.9 Hz, 2H), 3.06 (dd, *J* = 12.0, 6.0 Hz, 2H), 2.25 (s, 3H); ¹³C NMR (100 MHz, acetone-*d*₆): δ 155.66, 155.24, 149.53, 148.75, 145.94, 141.87, 141.58, 140.90, 139.97, 137.17, 132.29, 131.66, 129.65, 128.76, 123.78, 122.88, 122.04, 117.67, 115.90, 115.51, 112.33, 110.59, 107.51, 43.51, 39.54, 20.48; ESI-MS: *m/z* 583.10 [M – H][–]; ESI-HRMS calcd for C₂₆H₂₃O₈N₄S₂ [M – H][–], 583.0961.

N-(2-(3-(4-Nitrophenyl)thioureido)ethyl)-3-(2-(3,4-dihydroxyphenoxy)-4-methylphenyl)thiophene-2-sulfonamide (**FWJ-D13**). Over-

all yield: 18.0%, purity: 97.1%. ¹H NMR (400 MHz, acetone-*d*₆): δ 9.51 (s, 1H), 8.19 (d, *J* = 9.2 Hz, 2H), 8.01 (s, 1H), 7.90 (d, *J* = 9.2 Hz, 2H), 7.82 (s, 1H), 7.76 (d, *J* = 5.1 Hz, 1H), 7.67 (s, 1H), 7.36 (d, *J* = 7.7 Hz, 1H), 7.18 (d, *J* = 5.1 Hz, 1H), 6.92 (d, *J* = 7.5 Hz, 1H), 6.78 (d, *J* = 8.6 Hz, 1H), 6.68 (s, 1H), 6.57 (d, *J* = 2.8 Hz, 1H), 6.49 (s, 1H), 6.41 (dd, *J* = 8.6, 2.8 Hz, 1H), 3.76 (dd, *J* = 11.7, 5.8 Hz, 2H), 3.20 (dd, *J* = 12.0, 6.0 Hz, 2H), 2.28 (s, 3H); ¹³C NMR (100 MHz, acetone-*d*₆): δ 181.8, 156.3, 150.1, 146.6, 146.5, 143.7, 142.1, 141.6, 140.6, 137.5, 132.9, 132.2, 129.6, 124.9, 123.5, 122.5, 122.0, 118.2, 116.1, 111.2, 108.2, 44.5, 42.7, 21.1; ESI-MS: *m/z* 623.05 [M + Na]⁺; ESI-HRMS calcd for C₂₆H₂₄O₇N₄NaS₃ [M + Na]⁺, 623.0698.

N-(2-(3-(4-Nitrophenyl)thioureido)ethyl)-3-(2-(3,4-dihydroxyphenoxy)-5-isopropylphenyl)thiophene-2-sulfonamide (**FWJ-D14**). Overall yield: 14.3%, purity: 97.6%. ¹H NMR (400 MHz, acetone-*d*₆): δ 9.62 (s, 1H), 8.18 (d, *J* = 9.0 Hz, 2H), 8.05 (s, 1H), 7.92 (d, *J* = 8.9 Hz, 2H), 7.77 (dd, *J* = 14.0, 5.5 Hz, 3H), 7.40 (s, 1H), 7.21 (t, *J* = 7.1 Hz, 2H), 6.78 (dd, *J* = 8.5, 3.7 Hz, 2H), 6.58 (d, *J* = 2.4 Hz, 1H), 6.47–6.33 (m, 2H), 3.74 (d, *J* = 5.4 Hz, 2H), 3.22–3.13 (m, 2H), 2.91 (dd, *J* = 13.7, 6.8 Hz, 1H), 1.25 (d, *J* = 6.9 Hz, 6H); ¹³C NMR (100 MHz, acetone-*d*₆): δ 181.3, 153.6, 149.7, 145.8, 142.3, 141.1, 132.1, 130.0, 128.8, 127.7, 124.5, 124.2, 121.1, 117.1, 115.4, 110.2, 107.3, 43.7, 42.0, 33.1, 23.4; ESI-MS: *m/z* 629.10 [M + H]⁺; ESI-HRMS calcd for C₂₈H₂₉O₇N₄S₃ [M + H]⁺, 629.1190.

N-(2-(3-(4-Nitrophenyl)thioureido)ethyl)-3-(2-(3,4-dimethoxyphenoxy)-5-isopropylphenyl)thiophene-2-sulfonamide (**FWJ-D15**). Overall yield: 15.9%, purity: 97.9%. ¹H NMR (400 MHz, acetone-*d*₆): δ 9.52 (s, 1H), 8.18 (d, *J* = 9.1 Hz, 2H), 7.89 (d, *J* = 9.1 Hz, 2H), 7.80–7.73 (m, 1H), 7.69 (s, 1H), 7.41 (s, 1H), 7.23 (d, *J* = 5.1 Hz, 2H), 6.88 (d, *J* = 8.7 Hz, 1H), 6.79 (d, *J* = 8.5 Hz, 1H), 6.72 (d, *J* = 2.4 Hz, 1H), 6.57–6.45 (m, 2H), 3.75 (d, *J* = 4.9 Hz, 8H), 3.18 (dd, *J* = 11.8, 5.9 Hz, 2H), 2.92 (dt, *J* = 14.0, 7.0 Hz, 1H), 1.25 (d, *J* = 6.9 Hz, 6H); ¹³C NMR (101 MHz, acetone-*d*₆): δ 181.8, 154.2, 151.3, 151.1, 146.5, 143.2, 141.8, 137.9, 132.9, 130.7, 129.6, 128.4, 125.2, 125.0, 121.9, 117.8, 113.1, 111.0, 105.3, 56.3, 56.0, 44.5, 42.7, 33.8, 24.1; ESI-MS: *m/z* 657.15 [M + H]⁺; ESI-HRMS calcd for C₃₀H₃₃O₇N₄S₃ [M + H]⁺, 658.1504.

N-(2-(3-(4-Nitrophenyl)ureido)ethyl)-3-(2-(3,4-dihydroxyphenoxy)-4-methylphenyl)thiophene-2-sulfonamide (**FWJ-D16**). Overall yield: 17.8%, purity: 93.6%. ¹H NMR (400 MHz, acetone-*d*₆): δ 8.72 (s, 1H), 8.15 (d, *J* = 9.2 Hz, 2H), 8.05 (s, 1H), 7.79 (s, 1H), 7.74 (d, *J* = 5.1 Hz, 1H), 7.71 (d, *J* = 9.2 Hz, 2H), 7.36 (d, *J* = 7.7 Hz, 1H), 7.18 (d, *J* = 5.1 Hz, 1H), 6.90 (d, *J* = 7.7 Hz, 1H), 6.77 (d, *J* = 8.6 Hz, 1H), 6.66 (s, 1H), 6.58 (d, *J* = 2.8 Hz, 1H), 6.41 (dd, *J* = 8.5, 2.7 Hz, 2H), 6.17 (s,

1H), 3.33 (dd, $J = 11.8, 5.9$ Hz, 2H), 3.05 (q, $J = 5.9$ Hz, 2H), 2.25 (s, 3H); ^{13}C NMR (100 MHz, acetone- d_6): δ 156.68, 155.73, 150.49, 147.89, 146.94, 142.58, 142.52, 141.89, 140.97, 138.14, 133.30, 132.66, 129.78, 125.82, 123.83, 122.97, 118.60, 118.24, 116.50, 111.62, 108.59, 44.33, 40.58, 21.49; ESI-MS: m/z 607.15 $[\text{M} + \text{Na}]^+$; ESI-HRMS calcd for $\text{C}_{26}\text{H}_{25}\text{O}_8\text{N}_4\text{S}_2$ $[\text{M} + \text{H}]^+$, 585.1109.

N-(2-(3-(3-Methoxyphenyl)thioureido)ethyl)-3-(2-(3,4-dihydroxyphenoxy)-4-methylphenyl)thiophene-2-sulfonamide (FWJ-D17). Overall yield: 17.6%, purity: 97.3%. ^1H NMR (400 MHz, acetone- d_6): δ 8.92 (s, 1H), 8.05 (s, 1H), 7.76 (dd, $J = 14.7, 5.1$ Hz, 2H), 7.34 (dd, $J = 14.1, 6.4$ Hz, 2H), 7.24 (t, $J = 8.1$ Hz, 1H), 7.17 (d, $J = 5.1$ Hz, 1H), 7.03 (s, 1H), 6.90 (t, $J = 6.7$ Hz, 2H), 6.77 (dd, $J = 15.7, 8.9$ Hz, 2H), 6.67 (s, 1H), 6.58 (d, $J = 2.6$ Hz, 1H), 6.49–6.36 (m, 2H), 3.82–3.70 (m, 5H), 3.17 (dd, $J = 12.0, 6.1$ Hz, 2H), 2.28 (s, 3H); ESI-MS: m/z 584.05 $[\text{M} - \text{H}]^-$; ESI-HRMS calcd for $\text{C}_{27}\text{H}_{26}\text{O}_6\text{N}_3\text{S}_3$ $[\text{M} - \text{H}]^-$, 584.0991.

N-(2-(3-(3-Methoxyphenyl)ureido)ethyl)-3-(2-(3,4-dihydroxyphenoxy)-4-methylphenyl)thiophene-2-sulfonamide (FWJ-D18). Overall yield: 17.6%, purity: 95.2%. ^1H NMR (400 MHz, acetone- d_6): δ 8.16 (s, 1H), 8.02 (s, 1H), 7.73 (d, $J = 5.1$ Hz, 1H), 7.68 (s, 1H), 7.36 (d, $J = 7.7$ Hz, 1H), 7.22 (s, 1H), 7.17 (d, $J = 5.1$ Hz, 1H), 7.11 (t, $J = 8.1$ Hz, 1H), 6.90 (d, $J = 7.7$ Hz, 2H), 6.77 (d, $J = 8.6$ Hz, 1H), 6.67 (s, 1H), 6.58 (d, $J = 2.8$ Hz, 1H), 6.52 (dd, $J = 8.2, 2.1$ Hz, 1H), 6.45–6.34 (m, 2H), 5.96 (s, 1H), 3.74 (s, 3H), 3.31 (q, $J = 5.9$ Hz, 2H), 3.02 (q, $J = 6.0$ Hz, 2H), 2.25 (s, 3H); ^{13}C NMR (100 MHz, acetone- d_6): δ 160.9, 156.3, 156.2, 150.1, 146.5, 142.2, 142.1, 141.5, 140.6, 137.8, 132.9, 132.3, 129.9, 129.3, 123.5, 122.6, 118.3, 116.2, 111.3, 111.2, 108.1, 108.0, 104.9, 55.1, 44.4, 40.1, 21.1; ESI-MS: m/z 592.15 $[\text{M} + \text{Na}]^+$.

N-(2-(3-(4-Methoxyphenyl)thioureido)ethyl)-3-(2-(3,4-dihydroxyphenoxy)-4-methylphenyl)thiophene-2-sulfonamide (FWJ-D19). Overall yield: 18.7%, purity: 91.8%. ^1H NMR (400 MHz, acetone- d_6): δ 8.75 (s, 1H), 8.13 (s, 2H), 7.73 (d, $J = 5.1$ Hz, 1H), 7.36 (d, $J = 7.7$ Hz, 1H), 7.19 (dd, $J = 17.6, 7.0$ Hz, 3H), 7.06 (d, $J = 5.3$ Hz, 1H), 6.94–6.87 (m, 3H), 6.79 (d, $J = 8.6$ Hz, 1H), 6.67 (s, 1H), 6.58 (d, $J = 2.8$ Hz, 1H), 6.46 (s, 1H), 6.41 (dd, $J = 8.6, 2.8$ Hz, 1H), 3.79 (s, 3H), 3.73 (q, $J = 6.1$ Hz, 2H), 3.15 (q, $J = 6.1$ Hz, 2H), 2.28 (s, 3H); ESI-MS: m/z 584.05 $[\text{M} - \text{H}]^-$; ESI-HRMS calcd for $\text{C}_{27}\text{H}_{26}\text{O}_6\text{N}_3\text{S}_3$ $[\text{M} - \text{H}]^-$, 584.0989.

N-(2-(3-(4-Methoxyphenyl)ureido)ethyl)-3-(2-(3,4-dihydroxyphenoxy)-4-methylphenyl)thiophene-2-sulfonamide (FWJ-D20). Overall yield: 18.2%, purity: 98.3%. ^1H NMR (400 MHz, acetone- d_6): δ 8.26 (s, 1H), 7.81 (s, 1H), 7.72 (d, $J = 5.1$ Hz, 1H), 7.61 (s, 1H), 7.36 (d, $J = 7.8$ Hz, 1H), 7.31 (d, $J = 9.0$ Hz, 2H), 7.18 (d, $J = 5.1$ Hz, 1H), 6.89 (d, $J = 7.8$ Hz, 1H), 6.82 (d, $J = 9.0$ Hz, 2H), 6.76 (d, $J = 8.6$ Hz, 1H), 6.67 (s, 1H), 6.59 (d, $J = 2.8$ Hz, 1H), 6.45–6.37 (m, 2H), 5.90 (s, 1H), 3.74 (s, 3H), 3.30 (q, $J = 6.0$ Hz, 2H), 3.01 (q, $J = 6.0$ Hz, 2H), 2.25 (s, 3H); ^{13}C NMR (100 MHz, acetone- d_6): δ 156.18, 155.58, 149.34, 145.89, 141.64, 140.75, 139.90, 133.05, 132.29, 131.64, 128.64, 122.82, 121.93, 120.72, 117.59, 115.38, 113.79, 110.51, 107.46, 54.69, 43.89, 39.49, 20.48; ESI-MS: m/z 592.15 $[\text{M} + \text{Na}]^+$; ESI-HRMS calcd for $\text{C}_{27}\text{H}_{28}\text{O}_7\text{N}_3\text{S}_2$ $[\text{M} + \text{H}]^+$, 570.1362.

The general procedure for the synthesis of compounds FWJ-E1–FWJ-E18 (see Schemes 2 and 3) is described as follows:

Compound 12 (2.93 mmol), 13 (2.44 mmol), palladium acetate (0.49 mmol), diphenylcyclohexylphosphine (0.98 mmol), and potassium phosphate (7.32 mmol) were added into a 100 mL flask. After full deoxidation, THF (25 mL) and water (5 mL) were added to dissolve the reactants. The solution was then heated under reflux for 6 h. The residue was concentrated and extracted by water (20 mL) and ethyl acetate (20 mL) three times. It was further purified by chromatography (EtOAc/petroleum ether 1:10) to obtain compound 14.

Compound 14 (1.7 mmol) reacted with DCM (10 mL) and TFA (1.7 mL) at room temperature for 10 h. The residue was treated with potassium carbonate saturated solution and extracted by 15 mL of water and 20 mL of CH_2Cl_2 three times to obtain compound 15.

Compound 15 (~50 mg), CH_2Cl_2 (3 mL), and isocyanate or 1.1 equiv of isocyanate or isothiocyanate were added into a 25 mL flask. The mixture was stirred at room temperature until the reaction is complete. The residue was purified by chromatography (EtOAc/petroleum ether 1:3) to obtain compounds FWJ-E2, FWJ-E5, FWJ-E8,

FWJ-E11, FWJ-E13, FWJ-E15, and FWJ-E18. These compounds were dissolved in 3 mL of DCM. Then, 10 equiv of BBr_3 was added dropwise in an ice-water bath. The mixture was stirred for 1 h. After that, water was slowly added to quench the reaction. 3 mL of CH_2Cl_2 was used to extract the residue three times. The demethylated products were collected via evaporation, filtration, and concentration, that is, FWJ-E1, FWJ-E4, FWJ-E7, FWJ-E9, FWJ-E12, FWJ-E14, and FWJ-E17.

Using a similar synthetic route, compound 16 (55 mg, 0.2927 mmol) reacted with compound 13 (100 mg, 0.2439 mmol) to obtain the mediate product 17. 3,4-dimethoxyphenol (16 mg, 0.1018 mmol), 17 (40 mg, 0.0849 mmol), and DMSO (1 mL) were added to the flask. Then, cesium carbonate (33 mg, 0.1018 mmol) was added, and the solution was heated and stirred at 110 °C for 1 h. After that, water (3 mL) and dichloromethane (3 mL) were added to extract three times. It was further purified by chromatography (EtOAc/petroleum ether 1:5) to obtain 18 as a yellow solid.

Compound 18 (1.4 mmol) reacted with DCM (10 mL) and TFA (1.5 mL) at room temperature for 5 h. The residue was treated with potassium carbonate saturated solution and extracted by 10 mL of water and 10 mL of CH_2Cl_2 three times. The intermediate compound reacted with isocyanate or 1.1 equiv of isocyanate or isothiocyanate to produce FWJ-E3, FWJ-E6, and FWJ-E16. The demethylated product FWJ-E10 was obtained as the previous protocol.

N-(4-Nitrophenyl)-4-((3-(2-(3,4-dihydroxyphenoxy)phenyl)thiophen-2-yl)sulfonyl)piperazine-1-carbothioamide (FWJ-E1). Overall yield: 31.4%, purity: 96.4%. ^1H NMR (400 MHz, acetone- d_6): δ 8.15 (d, $J = 9.1$ Hz, 2H), 7.89 (d, $J = 5.1$ Hz, 1H), 7.68–7.61 (m, 2H), 7.48 (dd, $J = 7.6, 1.6$ Hz, 1H), 7.37–7.30 (m, 1H), 7.29 (d, $J = 5.1$ Hz, 1H), 7.09 (t, $J = 7.1$ Hz, 1H), 6.79 (t, $J = 8.1$ Hz, 2H), 6.63 (d, $J = 2.8$ Hz, 1H), 6.45 (dd, $J = 8.6, 2.8$ Hz, 1H), 4.07–4.01 (m, 4H), 3.09–3.00 (m, 4H); ^{13}C NMR (101 MHz, Acetone- d_6): δ 182.7, 157.1, 149.2, 148.0, 146.8, 142.9, 142.7, 134.3, 133.4, 130.9, 130.7, 124.8, 124.5, 123.6, 123.5, 122.0, 116.3, 116.2, 112.0, 108.8, 48.9, 46.1; ESI-MS: m/z 611.00 $[\text{M} - \text{H}]^-$; ESI-HRMS calcd for $\text{C}_{27}\text{H}_{23}\text{O}_7\text{N}_4\text{S}_3$ $[\text{M} - \text{H}]^-$, 611.0724.

N-(4-Nitrophenyl)-4-((3-(2-(3,4-dimethoxyphenoxy)phenyl)thiophen-2-yl)sulfonyl)piperazine-1-carbothioamide (FWJ-E2). Overall yield: 31.4%, purity: 98.0%. ^1H NMR (400 MHz, acetone- d_6): δ 9.23 (s, 1H), 8.15 (d, $J = 9.1$ Hz, 2H), 7.90 (d, $J = 5.1$ Hz, 1H), 7.63 (d, $J = 9.1$ Hz, 2H), 7.49 (dd, $J = 7.6, 1.5$ Hz, 1H), 7.38–7.29 (m, 2H), 7.12 (t, $J = 7.2$ Hz, 1H), 6.90–6.76 (m, 3H), 6.60 (dd, $J = 8.7, 2.7$ Hz, 1H), 4.10–3.99 (m, 4H), 3.77 (s, 3H), 3.74 (s, 3H), 3.12–3.03 (m, 4H); ^{13}C NMR (100 MHz, acetone- d_6): δ 182.83, 156.85, 151.33, 150.48, 148.02, 147.06, 142.95, 133.47, 133.38, 130.98, 130.73, 125.17, 124.55, 123.33, 122.30, 116.75, 113.36, 111.98, 106.07, 56.15, 48.83, 46.07; ESI-MS: m/z 639.05 $[\text{M} - \text{H}]^-$; ESI-HRMS calcd for $\text{C}_{29}\text{H}_{27}\text{O}_7\text{N}_4\text{S}_3$ $[\text{M} - \text{H}]^-$, 639.1066.

N-(4-Nitrophenyl)-4-((3-(2-(3,4-dimethoxyphenoxy)-5-nitrophenyl)thiophen-2-yl)sulfonyl)piperazine-1-carbothioamide (FWJ-E3). Overall yield: 72.1%, purity: 96.5%. ^1H NMR (400 MHz, acetone- d_6): δ 9.25 (s, 1H), 8.38 (d, $J = 2.8$ Hz, 1H), 8.25 (dd, $J = 9.2, 2.8$ Hz, 1H), 8.15 (d, $J = 9.1$ Hz, 2H), 8.04 (d, $J = 5.1$ Hz, 1H), 7.62 (d, $J = 9.1$ Hz, 2H), 7.47 (d, $J = 5.1$ Hz, 1H), 6.98–6.88 (m, 3H), 6.75 (dd, $J = 8.7, 2.7$ Hz, 1H), 4.13–4.07 (m, 4H), 3.79 (s, 3H), 3.78 (s, 3H), 3.16–3.10 (m, 4H); ^{13}C NMR (100 MHz, acetone- d_6): δ 182.96, 162.55, 151.62, 148.71, 148.20, 148.05, 142.27, 140.67, 134.71, 133.12, 131.96, 128.95, 126.56, 125.21, 124.63, 123.38, 115.81, 113.36, 113.01, 106.54, 56.35, 48.86, 46.26; ESI-MS: m/z 683.95 $[\text{M} - \text{H}]^-$; ESI-HRMS calcd for $\text{C}_{29}\text{H}_{26}\text{O}_9\text{N}_5\text{S}_3$ $[\text{M} - \text{H}]^-$, 684.0896.

N-(4-Nitrophenyl)-4-((3-(2-(3,4-dihydroxyphenoxy)phenyl)thiophen-2-yl)sulfonyl)piperazine-1-carboxamide (FWJ-E4). Overall yield: 30.4%, purity: 94.5%. ^1H NMR (400 MHz, acetone- d_6): δ 8.14 (d, $J = 9.3$ Hz, 2H), 7.87 (d, $J = 5.1$ Hz, 1H), 7.73 (d, $J = 9.3$ Hz, 2H), 7.48 (dd, $J = 7.6, 1.6$ Hz, 1H), 7.37–7.31 (m, 1H), 7.28 (d, $J = 5.1$ Hz, 1H), 7.09 (t, $J = 7.5$ Hz, 1H), 6.77 (t, $J = 8.7$ Hz, 2H), 6.58 (d, $J = 2.7$ Hz, 1H), 6.42 (dd, $J = 8.6, 2.8$ Hz, 1H), 3.64–3.56 (m, 4H), 2.99–2.93 (m, 4H); ^{13}C NMR (100 MHz, acetone- d_6): δ 157.04, 154.52, 149.00, 147.40, 146.71, 142.66, 142.55, 134.15, 133.37, 133.22, 130.65, 130.51, 125.04, 124.69, 121.79, 119.19, 119.11, 116.13, 116.07, 111.79, 108.66,

46.17, 44.28; ESI-MS: m/z 619.10 $[M + Na]^+$; ESI-HRMS calcd for $C_{27}H_{23}O_8N_4S_2 [M - H]^-$, 595.0872.

N-(4-Nitrophenyl)-4-((3-(2-(3,4-dimethoxyphenoxy)phenyl)thiophen-2-yl)sulfonyl)piperazine-1-carboxamide (FWJ-E5). Overall yield: 30.4%, purity: 97.2%. 1H NMR (400 MHz, acetone- d_6): δ 8.65 (s, 1H), 8.18–8.10 (m, 2H), 7.88 (d, $J = 5.1$ Hz, 1H), 7.75 (dd, $J = 7.2, 5.1$ Hz, 2H), 7.49 (dd, $J = 7.6, 1.6$ Hz, 1H), 7.40–7.27 (m, 2H), 7.12 (t, $J = 7.1$ Hz, 1H), 6.81 (dd, $J = 13.6, 8.5$ Hz, 2H), 6.74 (d, $J = 2.7$ Hz, 1H), 6.56 (dd, $J = 8.7, 2.7$ Hz, 1H), 3.74 (s, 6H), 3.64–3.56 (m, 4H), 3.02–2.94 (m, 4H); ^{13}C NMR (100 MHz, acetone- d_6): δ 157.11, 154.69, 151.52, 150.52, 147.86, 147.27, 142.91, 142.83, 134.62, 133.65, 133.56, 131.03, 130.89, 125.41, 125.35, 122.45, 119.32, 116.74, 113.48, 112.21, 106.24, 56.51, 56.24, 46.51, 44.63; ESI-MS: m/z 647.15 $[M + Na]^+$; ESI-HRMS calcd for $C_{29}H_{28}O_8N_4NaS_2 [M + Na]^+$, 647.1254.

N-(4-Nitrophenyl)-4-((3-(2-(3,4-dimethoxyphenoxy)-5-nitrophenyl)thiophen-2-yl)sulfonyl)piperazine-1-carboxamide (FWJ-E6). Overall yield: 73.9%, purity: 95.4%. 1H NMR (400 MHz, acetone- d_6): δ 8.69 (s, 1H), 8.38 (d, $J = 2.8$ Hz, 1H), 8.25 (dd, $J = 9.2, 2.9$ Hz, 1H), 8.14 (d, $J = 9.3$ Hz, 2H), 8.01 (d, $J = 5.1$ Hz, 1H), 7.73 (d, $J = 9.3$ Hz, 2H), 7.45 (d, $J = 5.1$ Hz, 1H), 6.93 (dd, $J = 8.9, 5.1$ Hz, 2H), 6.87 (d, $J = 2.7$ Hz, 1H), 6.71 (dd, $J = 8.7, 2.7$ Hz, 1H), 3.78 (s, 3H), 3.78 (s, 3H), 3.69–3.62 (m, 4H), 3.08–3.01 (m, 4H); ^{13}C NMR (100 MHz, acetone- d_6): δ 162.62, 154.54, 151.64, 148.64, 148.21, 147.70, 142.73, 142.26, 140.46, 134.98, 133.07, 131.82, 128.88, 126.56, 125.29, 119.19, 115.65, 113.32, 112.97, 106.50, 56.33, 56.22, 46.51, 44.49; ESI-MS: m/z 667.95 $[M - H]^-$; ESI-HRMS calcd for $C_{29}H_{26}O_{10}N_5S_2 [M - H]^-$, 668.1128.

N-(3-Nitrophenyl)-4-((3-(2-(3,4-dihydroxyphenoxy)phenyl)thiophen-2-yl)sulfonyl)piperazine-1-carboxamide (FWJ-E7). Overall yield: 31.1%, purity: 98.5%. 1H NMR (400 MHz, acetone- d_6): δ 8.47 (s, 1H), 7.91–7.80 (m, 3H), 7.54–7.45 (m, 2H), 7.38–7.31 (m, 1H), 7.28 (d, $J = 5.1$ Hz, 1H), 7.10 (t, $J = 7.5$ Hz, 1H), 6.76 (dd, $J = 15.0, 8.4$ Hz, 2H), 6.56 (d, $J = 2.7$ Hz, 1H), 6.43 (dd, $J = 8.5, 2.7$ Hz, 1H), 3.64–3.55 (m, 4H), 3.01–2.93 (m, 4H); ^{13}C NMR (100 MHz, $CDCl_3$): δ 156.6, 154.4, 148.5, 147.2, 144.7, 142.0, 142.0, 138.8, 133.7, 133.5, 132.4, 130.3, 129.8, 129.7, 126.9, 122.6, 121.3, 119.0, 115.9, 115.4, 114.2, 113.2, 107.6, 45.7, 43.7; ESI-MS: m/z 595.05 $[M - H]^-$; ESI-HRMS calcd for $C_{27}H_{23}O_8N_4S_2 [M - H]^-$, 595.0960.

N-(3-Nitrophenyl)-4-((3-(2-(3,4-dimethoxyphenoxy)phenyl)thiophen-2-yl)sulfonyl)piperazine-1-carboxamide (FWJ-E8). Overall yield: 31.1%, purity: 97.1%. 1H NMR (400 MHz, acetone- d_6): δ 8.52 (dd, $J = 9.2, 7.1$ Hz, 2H), 7.86 (ddd, $J = 19.9, 8.6, 1.7$ Hz, 3H), 7.56–7.47 (m, 2H), 7.35 (dd, $J = 12.3, 5.0$ Hz, 1H), 7.30 (d, $J = 5.1$ Hz, 1H), 7.12 (t, $J = 7.5$ Hz, 1H), 6.80 (dd, $J = 12.2, 8.5$ Hz, 2H), 6.74 (d, $J = 2.7$ Hz, 1H), 6.57 (dd, $J = 8.7, 2.7$ Hz, 1H), 3.73 (s, 6H), 3.64–3.55 (m, 4H), 3.02–2.92 (m, 4H); ^{13}C NMR (100 MHz, $CDCl_3$): δ 155.5, 154.1, 149.9, 149.8, 148.3, 145.6, 142.1, 140.3, 133.0, 132.6, 132.5, 130.1, 129.8, 129.5, 125.6, 124.3, 122.1, 117.6, 116.8, 114.4, 111.7, 110.8, 104.4, 56.2, 56.0, 45.3, 43.6; ESI-MS: m/z 647.15 $[M + Na]^+$; ESI-HRMS calcd for $C_{29}H_{28}O_8N_4NaS_2 [M + Na]^+$, 647.1245.

N-(3,5-Bis(trifluoromethyl)phenyl)-4-((3-(2-(3,4-dihydroxyphenoxy)phenyl)thiophen-2-yl)sulfonyl)piperazine-1-carboxamide (FWJ-E9). Overall yield: 30.2%, purity: 95.0%. 1H NMR (400 MHz, acetone- d_6): δ 8.08 (s, 2H), 7.90 (d, $J = 5.1$ Hz, 1H), 7.72 (s, 1H), 7.48 (dd, $J = 7.6, 1.6$ Hz, 1H), 7.39–7.31 (m, 1H), 7.28 (d, $J = 5.1$ Hz, 1H), 7.10 (t, $J = 7.5$ Hz, 1H), 6.78 (dd, $J = 14.9, 8.4$ Hz, 2H), 6.61 (d, $J = 2.8$ Hz, 1H), 6.44 (dd, $J = 8.6, 2.8$ Hz, 1H), 4.14–4.00 (m, 4H), 3.14–3.02 (m, 4H); ESI-MS: m/z 702.00 $[M - H]^-$; ESI-HRMS calcd for $C_{29}H_{22}O_3N_3F_6S_3 [M - H]^-$, 702.0619.

N-(3,5-Bis(trifluoromethyl)phenyl)-4-((3-(2-(3,4-dihydroxyphenoxy)-5-nitrophenyl)thiophen-2-yl)sulfonyl)piperazine-1-carboxamide (FWJ-E10). Overall yield: 75.4%, purity: 95.8%. 1H NMR (400 MHz, acetone- d_6): δ 9.26 (s, 1H), 8.37 (d, $J = 2.8$ Hz, 1H), 8.26 (dd, $J = 9.2, 2.8$ Hz, 1H), 8.18 (s, 1H), 8.04 (dd, $J = 9.7, 5.1$ Hz, 4H), 7.72 (s, 1H), 7.44 (d, $J = 5.1$ Hz, 1H), 6.93 (d, $J = 9.2$ Hz, 1H), 6.83 (d, $J = 8.5$ Hz, 1H), 6.74 (d, $J = 2.7$ Hz, 1H), 6.56 (dd, $J = 8.5, 2.7$ Hz, 1H), 4.19–4.10 (m, 4H), 3.18–3.12 (m, 4H); ^{13}C NMR (100 MHz, DMSO- d_6): δ 180.9, 161.7, 146.6, 145.7, 143.4, 142.9, 140.6, 139.7, 132.3, 129.9, 129.6, 127.6, 126.2, 124.5, 123.7, 121.9, 115.9, 114.6, 111.2, 108.7, 47.4, 45.20; ESI-MS: m/z 746.90 $[M - H]^-$; ESI-HRMS calcd for $C_{29}H_{21}O_7N_4F_6S_3 [M - H]^-$, 747.0483.

N-(3,5-Bis(trifluoromethyl)phenyl)-4-((3-(2-(3,4-dimethoxyphenoxy)phenyl)thiophen-2-yl)sulfonyl)piperazine-1-carboxamide (FWJ-E11). Overall yield: 30.8%, purity: 96.6%. 1H NMR (400 MHz, acetone- d_6): δ 9.20 (s, 1H), 8.08 (s, 2H), 7.90 (d, $J = 5.1$ Hz, 1H), 7.73 (s, 1H), 7.49 (dd, $J = 7.6, 1.6$ Hz, 1H), 7.39–7.33 (m, 1H), 7.31 (d, $J = 5.1$ Hz, 1H), 7.12 (t, $J = 7.5$ Hz, 1H), 6.87–6.75 (m, 3H), 6.60 (dd, $J = 8.6, 2.7$ Hz, 1H), 4.12–4.06 (m, 4H), 3.75 (s, 3H), 3.72 (s, 3H), 3.12–3.05 (m, 4H); ^{13}C NMR (100 MHz, acetone- d_6): δ 183.07, 157.22, 151.71, 150.87, 147.42, 144.06, 143.29, 134.53, 133.82, 133.72, 131.93, 131.60, 131.33, 131.08, 125.57, 125.45, 122.66, 117.15, 113.70, 112.33, 106.41, 56.67, 56.46, 48.82, 46.41; ESI-MS: m/z 754.05 $[M + Na]^+$; ESI-HRMS calcd for $C_{31}H_{27}O_5N_3F_6NaS_3 [M + Na]^+$, 754.0915.

N-(3,5-Bis(trifluoromethyl)phenyl)-4-((3-(2-(3,4-dihydroxyphenoxy)phenyl)thiophen-2-yl)sulfonyl)piperazine-1-carboxamide (FWJ-E12). Overall yield: 29.3%, purity: 96.0%. 1H NMR (400 MHz, acetone- d_6): δ 8.65 (s, 1H), 8.18 (s, 2H), 8.06 (s, 1H), 7.87 (d, $J = 5.1$ Hz, 1H), 7.77 (s, 1H), 7.58 (s, 1H), 7.48 (dd, $J = 7.6, 1.6$ Hz, 1H), 7.39–7.31 (m, 1H), 7.27 (d, $J = 5.1$ Hz, 1H), 7.10 (t, $J = 7.5$ Hz, 1H), 6.79 (d, $J = 8.3$ Hz, 1H), 6.74 (d, $J = 8.5$ Hz, 1H), 6.57 (d, $J = 2.8$ Hz, 1H), 6.42 (dd, $J = 8.6, 2.8$ Hz, 1H), 3.66–3.54 (m, 4H), 3.03–2.94 (m, 4H); ^{13}C NMR (100 MHz, acetone- d_6): δ 157.44, 155.06, 149.70, 146.94, 143.44, 143.15, 142.86, 134.73, 133.73, 133.61, 132.49, 132.17, 131.11, 130.96, 126.01, 125.37, 123.31, 122.36, 119.98, 116.81, 116.51, 112.26, 108.92, 46.59, 44.61; ESI-MS: m/z 686.00 $[M - H]^-$; ESI-HRMS calcd for $C_{29}H_{22}O_6N_3F_6S_2 [M - H]^-$, 686.0869.

N-(3,5-Bis(trifluoromethyl)phenyl)-4-((3-(2-(3,4-dimethoxyphenoxy)phenyl)thiophen-2-yl)sulfonyl)piperazine-1-carboxamide (FWJ-E13). Overall yield: 31.8%, purity: 95.7%. 1H NMR (400 MHz, acetone- d_6): δ 8.63 (s, 1H), 8.20 (s, 2H), 7.87 (d, $J = 5.1$ Hz, 1H), 7.58 (s, 1H), 7.49 (dd, $J = 7.6, 1.6$ Hz, 1H), 7.39–7.31 (m, 1H), 7.30 (d, $J = 5.1$ Hz, 1H), 7.12 (t, $J = 7.5, 1.0$ Hz, 1H), 6.80 (dd, $J = 8.5, 4.6$ Hz, 2H), 6.74 (d, $J = 2.7$ Hz, 1H), 6.57 (dd, $J = 8.7, 2.7$ Hz, 1H), 3.73 (s, 6H), 3.64–3.57 (m, 4H), 3.03–2.96 (m, 4H); ^{13}C NMR (100 MHz, acetone- d_6): δ 157.26, 154.95, 151.69, 150.72, 147.42, 143.63, 143.07, 137.74, 133.79, 133.70, 132.53, 132.21, 131.17, 131.04, 125.54, 122.60, 119.87, 116.95, 113.58, 112.32, 106.35, 56.61, 56.32, 46.63, 44.60; ESI-MS: m/z 738.00 $[M + Na]^+$; ESI-HRMS calcd for $C_{31}H_{28}O_6N_3F_6S_2 [M + Na]^+$, 716.1323.

N-(4-Chlorophenyl)-4-((3-(2-(3,4-dihydroxyphenoxy)phenyl)thiophen-2-yl)sulfonyl)piperazine-1-carboxamide (FWJ-E14). Overall yield: 25.9%, purity: 97.2%. 1H NMR (400 MHz, acetone- d_6): δ 7.88 (d, $J = 5.1$ Hz, 1H), 7.48 (dd, $J = 10.9, 5.0$ Hz, 2H), 7.41 (d, $J = 8.8$ Hz, 1H), 7.38–7.26 (m, 6H), 7.09 (t, $J = 7.5$ Hz, 1H), 6.79 (dd, $J = 8.4, 4.0$ Hz, 2H), 6.64 (d, $J = 2.7$ Hz, 1H), 6.47 (dd, $J = 8.5, 2.7$ Hz, 1H), 4.06–3.95 (m, 4H), 3.07–2.96 (m, 4H); ^{13}C NMR (100 MHz, acetone- d_6): δ 183.23, 157.22, 146.63, 142.83, 140.37, 133.53, 133.33, 130.89, 130.71, 130.64, 128.73, 128.09, 127.24, 121.94, 116.33, 116.15, 112.18, 108.84, 48.46, 46.09; ESI-MS: m/z 624.05 $[M + Na]^+$; ESI-HRMS calcd for $C_{27}H_{24}O_3N_3ClNaS_3 [M + Na]^+$, 624.0461.

N-(4-Chlorophenyl)-4-((3-(2-(3,4-dimethoxyphenoxy)phenyl)thiophen-2-yl)sulfonyl)piperazine-1-carboxamide (FWJ-E15). Overall yield: 25.9%, purity: 95.6%. 1H NMR (400 MHz, acetone- d_6): δ 8.83 (s, 1H), 7.89 (d, $J = 5.1$ Hz, 1H), 7.49 (dd, $J = 7.6, 1.6$ Hz, 1H), 7.38–7.25 (m, 6H), 7.11 (t, $J = 7.5$ Hz, 1H), 6.86 (d, $J = 8.7$ Hz, 1H), 6.80 (dd, $J = 11.1, 5.5$ Hz, 2H), 6.60 (dd, $J = 8.7, 2.7$ Hz, 1H), 4.07–3.96 (m, 4H), 3.76 (s, 3H), 3.74 (s, 3H), 3.08–2.97 (m, 4H); ^{13}C NMR (100 MHz, acetone- d_6): δ 183.42, 156.97, 150.46, 147.08, 142.88, 133.53, 133.45, 130.98, 130.78, 128.76, 127.11, 122.29, 116.71, 113.37, 112.09, 106.13, 56.36, 56.19, 48.46, 46.13; ESI-MS: m/z 652.05 $[M + Na]^+$; ESI-HRMS calcd for $C_{29}H_{28}O_5N_3ClNaS_3 [M + Na]^+$, 652.0773.

N-(4-Chlorophenyl)-4-((3-(2-(3,4-dimethoxyphenoxy)-5-nitrophenyl)thiophen-2-yl)sulfonyl)piperazine-1-carboxamide (FWJ-E16). Overall yield: 73.2%, purity: 95.2%. 1H NMR (400 MHz, acetone- d_6): δ 8.87 (s, 1H), 8.40 (d, $J = 2.8$ Hz, 1H), 8.25 (dd, $J = 9.2, 2.8$ Hz, 1H), 8.03 (d, $J = 5.1$ Hz, 1H), 7.47 (d, $J = 5.1$ Hz, 1H), 7.31 (dd, $J = 21.3, 8.9$ Hz, 4H), 6.98–6.89 (m, 3H), 6.75 (dd, $J = 8.7, 2.7$ Hz, 1H), 4.11–4.03 (m, 4H), 3.80 (s, 3H), 3.78 (s, 3H), 3.13–3.05 (m, 4H); ^{13}C NMR (100 MHz, DMSO- d_6): δ 181.5, 161.4, 150.0, 147.2, 146.6, 140.8, 139.7, 139.5, 132.7, 132.4, 132.2, 128.4, 127.8, 126.6, 126.20,

123.8, 114.9, 112.3, 112.1, 105.6, 55.7, 47.3, 45.2; ESI-MS: m/z 672.95 $[M - H]^-$; ESI-HRMS calcd for $C_{29}H_{27}O_7N_4ClNaS_3$ $[M + Na]^+$, 697.0621.

N-(4-Fluorophenyl)-4-((3-(2-(3,4-dihydroxyphenoxy)-phenyl)-thiophen-2-yl)sulfonyl)piperazine-1-carboxamide (FWJ-E17). Overall yield: 29.2%, purity: 98.4%. 1H NMR (400 MHz, acetone- d_6): δ 8.10 (s, 1H), 7.87 (d, $J = 5.1$ Hz, 1H), 7.49 (dd, $J = 7.6, 1.6$ Hz, 1H), 7.46–7.40 (m, 2H), 7.36–7.28 (m, 2H), 7.08 (dd, $J = 7.4, 6.6$ Hz, 1H), 6.99 (t, $J = 8.8$ Hz, 2H), 6.76 (dd, $J = 8.0, 6.3$ Hz, 2H), 6.54 (d, $J = 2.7$ Hz, 1H), 6.46 (dd, $J = 8.5, 2.8$ Hz, 1H), 3.58–3.50 (m, 4H), 2.94–2.86 (m, 4H); ^{13}C NMR (100 MHz, acetone- d_6): δ 157.3, 148.8, 142.7, 133.5, 133.4, 130.7, 130.6, 124.5, 122.6, 122.5, 122.4, 121.7, 116.3, 116.2, 115.7, 115.5, 115.3, 112.3, 108.7, 108.6, 46.4, 44.2; ESI-MS: m/z 568.10 $[M - H]^-$; ESI-HRMS calcd for $C_{27}H_{23}O_6N_3FS_2$ $[M - H]^-$, 568.1023.

N-(4-Fluorophenyl)-4-((3-(2-(3,4-dimethoxyphenoxy)-phenyl)-thiophen-2-yl)sulfonyl)piperazine-1-carboxamide (FWJ-E18). Overall yield: 31.9%, purity: 97.3%. 1H NMR (400 MHz, acetone- d_6): δ 8.06 (s, 1H), 7.85 (d, $J = 5.1$ Hz, 1H), 7.49 (td, $J = 7.2, 3.4$ Hz, 3H), 7.38–7.27 (m, 2H), 7.11 (t, $J = 7.2$ Hz, 1H), 6.99 (t, $J = 8.8$ Hz, 2H), 6.84–6.72 (m, 3H), 6.56 (dd, $J = 8.7, 2.7$ Hz, 1H), 3.73 (s, 3H), 3.72 (s, 3H), 3.59–3.46 (m, 4H), 2.99–2.90 (m, 4H); ^{13}C NMR (100 MHz, acetone- d_6): δ 160.01, 157.64, 156.92, 155.24, 151.19, 150.15, 146.96, 142.56, 137.27, 137.25, 134.35, 133.41, 133.33, 130.72, 130.63, 125.00, 122.12, 121.94, 121.86, 116.34, 115.47, 115.25, 113.14, 112.01, 105.95, 56.20, 55.94, 46.27, 44.23; ESI-MS: m/z 596.00 $[M - H]^-$; ESI-HRMS calcd for $C_{29}H_{29}O_6N_3FS_2$ $[M + H]^+$, 598.1480.

All NMR spectra were recorded at room temperature on a Bruker AV-400 400 MHz spectrometer. They were calibrated by using residual $CHCl_3$ ($\delta H = 7.26$ ppm) and $CDCl_3$ ($\delta C = 77.16$ ppm), CH_3OH ($\delta H = 3.31$ ppm) and CD_3OD ($\delta C = 49.00$ ppm), acetone ($\delta H = 2.05$ ppm) and acetone- d_6 ($\delta C = 29.84, 206.26$ ppm), or DMSO ($\delta H = 2.50$ ppm) and DMSO- d_6 ($\delta C = 39.52$ ppm) as internal references. The following abbreviations are used to designate multiplicities: s: singlet; d: doublet; t: triplet; q: quartet; m: multiplet; quint: quintet; br: broad. High-resolution mass spectrometry (HRMS) was performed on a Bruker APEXIII 7.0 T ESI-FT mass spectrometer at an emitter voltage of 4000 V. Purity of each final compound was determined by analytical HPLC. An Agilent 1260 series HPLC (G7114A 1260 VWD detector) with an Agilent Zorbax Eclipse Plus-C18 (4.6×150 mm, $5 \mu M$) reversed-phase column was used to perform all analytical HPLC analyses. The elution buffer was a gradient of H_2O/CH_3OH . HPLC traces for all final compounds (i.e., TJ-A, TJ-B, TJ-C, FWJ-D, and FWJ-E compounds) and four lead compounds (i.e., YCW-E5, YCW-E10, YCW-E11, and YCW-E16) are given in the Supporting Information (Part III). The purity of all described compounds was $\geq 95\%$ except for three compounds (i.e., FWJ-D16: 93.6%; FWJ-D19: 91.8%; FWJ-E4: 94.5%).

The overall yields of all TJ-A, TJ-B, TJ-C, and FWJ-D compounds and most FWJ-E compounds were calculated from the starting materials (e.g., 1 and 2 in Scheme 1) as the product of the following steps. The yields of intermediate 9 (Scheme 1) and 13 (Scheme 2) were close to 100% (i.e., 98% and 99%, respectively), so they were not included in the yield calculation. For compounds FWJ-E3, FWJ-E6, FWJ-E10, and FWJ-E16, shown in Scheme 3, their yields were calculated from 16, which was purchased directly. Consequently, their yields were significantly higher than those of the other compounds.

Expression and Purification of Bcl-2, Bcl- x_L , and Mcl-1. *Bcl-2*. The Bcl-2 protein used in our study has the same construction as the one (Bcl-2/Bcl- x_L , isoform 2) in Fesik et al.'s work,⁴² which is composed of amino acid residues 1–34 of human Bcl-2, amino acid residues 29–44 of human Bcl- x_L , and amino acid residues 92–207 of human Bcl-2. Such a construction has a good solubility in water and reserves the biological function of human Bcl-2. It was cloned into the pSJ2 vector at the EcoRI and XhoI sites using the following oligonucleotides: 5'-TTTTGAATTCATGGCGCACGAGGTCG-3' and 5'-TTTTCTCGAGTCAACGCATGGACG-GGC-3'. Bcl-2 protein with a N-terminal 8 \times His tag was produced in *Escherichia coli* BL21 (DE3) cells. Cells were grown at 37 °C in the LB medium containing 100 $\mu g/mL$ ampicillin to an OD_{600} of 0.6. Protein expression

was induced by 0.4 mM isopropyl-b-d-thiogalactopyranoside (IPTG) at 37 °C for 4 h. Cells were lysed in 25 mM Tris-HCl, pH 8.0 buffer containing 300 mM NaCl, 5 mM β ME, 1% (v/v) Triton X-100, 1 \times protease inhibitor cocktail, and 0.1 mg/mL phenylmethanesulfonyl fluoride (PMSF). His-TEV-Bcl-2 protein was purified from the soluble fraction using the Ni-NTA resin (QIAGEN) following the manufacturer's instructions. The His-TEV-Bcl-2 protein was further cleaved by TEV protease (0.5 mg/mL, 4 °C, 15 h) to produce Bcl-2 protein.

Bcl- x_L . The Bcl- x_L protein used in our study is a special truncated construction of the full-length protein, with deletion of residues 45–84 on a large loop region and residues 210–233 at the C-terminal hydrophobic region. It was cloned into the pSJ2 vector (a modified pET28a vector) at the EcoRI and XhoI sites using the following oligonucleotides: 5'-TCTCGAATTCATGTCTCAGAGCAACCGGGA-3' and 5'-GGTCCCTCGAGT-CAGCGTTCCTGGCCCTTCG-3'. The Bcl- x_L protein with a N-terminal 8 \times His tag was expressed in *E. coli* BL21 (DE3) cells. Cells were grown at 37 °C in the LB medium containing 100 $\mu g/mL$ ampicillin to an OD_{600} of 0.6. Protein expression was induced by 0.4 mM IPTG at 20 °C for 16 h. Cells were lysed in 25 mM Tris-HCl, pH 8.0 buffer containing 300 mM NaCl, 5 mM β ME, 1% (v/v) Triton X-100, 1 \times protease inhibitor cocktail, and 0.1 mg/mL PMSF. His-TEV-Bcl- x_L protein was purified from the soluble fraction using the Ni-NTA resin (QIAGEN) following the manufacturer's instructions. The His-TEV-Bcl- x_L protein was further cleaved by TEV protease (0.5 mg/mL, 4 °C, 15 h) to produce Bcl- x_L protein.

Mcl-1. The Mcl-1 protein used in our study has the same construction as the one (hMcl-1BLR) in Colman et al.'s work,⁴³ which is composed of amino acid residues 152–189 of mouse Mcl-1 and 41 amino acid residues 209–327 of human Mcl-1. Such a construction has a good solubility in water and reserves the biological function of human Mcl-1. It was cloned into the pSJ2 vector (a modified pET28a vector) at the HindIII and BamHI sites using the following oligonucleotides: 5'-CCCCAAGCTTTTAAACCACCTTC-CAGGCTTCAAC-3' and 5'-TTCCGGATCCATGGAAG-ATGATCTGTACCGTCAGTC-3'. The Mcl-1 protein with a N-terminal 8 \times His tag was expressed in *E. coli* BL21 (DE3) cells. Cells were grown at 37 °C in the LB medium containing 100 $\mu g/mL$ ampicillin to an OD_{600} of 0.6. Protein expression was induced by 0.4 mM IPTG at 20 °C for 16 h. Cells were lysed in 25 mM Tris-HCl, pH 8.0 buffer containing 300 mM NaCl, 5 mM β ME, 1% (v/v) Triton X-100, 1 \times protease inhibitor cocktail, and 0.1 mg/mL PMSF. His-TEV-Mcl-1 protein was purified from the soluble fraction using the Ni-NTA resin (QIAGEN) following the manufacturer's instructions. The His-TEV-Mcl-1 protein was further cleaved by TEV protease (0.5 mg/mL, 4 °C, 15 h) to produce Mcl-1 protein.

In Vitro Binding Assay. In our binding assay, a 26-residue peptide derived from the BH3 domain on the Bid protein with 5 carboxy-fluorescein (5-FAM) on the N-terminus, that is, 5-FAM-QEDIIR-NIARHLAQVGDMSD-RSIPPG, was used as the fluorescence tracer. This peptide was ordered from the HD Biosciences Cooperation Company. The desired sequences were verified by amino acid component analysis and the MS spectrum. The purity of this peptide was over 95% as verified by HPLC results. Our dose-dependent saturation experiments determined that this Bid-BH3 peptide bound to Bcl- x_L with $K_d = 215$ nM, to Bcl-2 with $K_d = 215$ nM, and to Mcl-1 with $K_d = 160$ nM.

In competitive binding experiments, each protein (Bcl- x_L , Bcl-2, or Mcl-1) and the tested compound (in 1% DMSO- d_6 solution) were pre-incubated in the assay buffer (PBS, pH 7.3, 140 mM NaCl, 2.7 mM KCl, 10 mM Na_2HPO_4 , 1.8 mM KH_2PO_4) at 37 °C for 30 min. 20 μL of a solution in PBS of the FAM-Bid peptide was then added to the solution to produce a final volume of 200 μL and incubated at 37 °C for another 20 min. The total concentration of the Bid-BH3 peptide used in the assay was 10 nM, while the total concentration of protein was set to 5 times the K_d value of the fluorescence tracer, that is, 205 nM in the case of Bcl- x_L , 445 nM in the case of Bcl-2, and 145 nM in the case of Mcl-1. At last, the solutions were transferred into Corning 384-well, black, flat-bottom plates (Corning Incorporated) with 60 μL per well and 3 wells

per sample. The polarization values in millipolarization units (mP) were measured at an excitation wavelength at 485 nm and an emission wavelength at 535 nm using the Tecan Genios Pro Injector Reader (Tecan Group Ltd.). For each experiment, a positive control containing the protein (Bcl-x_L, Bcl-2, or Mcl-1), the Bid-BH3 peptide, and 1% (v/v) [d₆]DMSO and a negative control containing only Bid-BH3 peptide were included on each assay plate.

Each compound was tested against all three target proteins (Bcl-x_L, Bcl-2, and Mcl-1) at seven different concentrations, that is, 1 nM, 10 nM, 100 nM, 1 μM, 10 μM, 50 μM, and 100 μM. At each concentration, the average mP value of three parallel measurements was used to perform nonlinear fitting to obtain the final binding curve. The nonlinear fitting job was conducted by using the GraphPad Prism software (version 5, <http://www.graphpad.com>). The concentration of the given compound where 50% of the bound peptide was displaced (IC₅₀) was derived from the binding curve. The competitive inhibition constant (K_i) of each tested compound was then calculated with the following equation developed by Wang et al.⁴⁴ assuming that it forms a binary complex with the target protein

$$K_i = \frac{[I]_{50}}{\left(\frac{[L]_{50}}{K_d} + \frac{[P]_0}{K_d} + 1\right)}$$

In this equation, [I]₅₀ and [L]₅₀ denote the concentrations of the free small-molecule inhibitor (I) and the free fluorescence-labeled peptide ligand (L) at 50% inhibition, respectively, and [P]₀ is the concentration of the free protein (P) before the inhibitor is added, that is, 0% inhibition. In order to solve this equation, one needs to supply the total concentration of the protein used in the assay ([P]_T), the total concentration of the fluorescence-labeled ligand used in the assay ([L]_T), the dissociation constant (K_d) between these two species, and the IC₅₀ value of the tested compound as inputs.

¹⁵N-Heteronuclear Single-Quantum Coherence Spectroscopy. The human Mcl-1 protein (172–327aa) was used in this experiment. The pET28a-His-hMcl-1 vector donated by Zhang's Group (Dalian University of Technology) was expressed in *E. coli* BL21(DE3) cells. Cells were grown at 37 °C in the M9 medium containing ¹⁵N-ammonium chloride and Kana. Protein expression was induced by addition of 0.4 mM IPTG at 37 °C for 4 h. Cells were lysed in 25 mM tris(hydroxymethyl)aminomethane (Tris)-HCl buffer at pH 7.0 containing 100 mM NaCl and 0.1 mg mL⁻¹ PMSF. ¹⁵N-labeled His-hMcl-1 protein was purified from the soluble fraction by using the Ni-NTA resin (Qiagen). The ¹⁵N-labeled His-hMcl-1 protein was further purified on Superdex75 (GE Healthcare) in phosphate-buffered saline (PBS) solution.

¹⁵N-heteronuclear single-quantum coherence (HSQC) NMR spectra were recorded on the Agilent 800 MHz NMR spectrometer at 25 °C. The ¹⁵N-labeled His-hMcl-1 protein was dissolved in 20 mM sodium phosphate buffer at pH 6.5, with 1 mM DTT, 1% DMSO-d₆, and 10% D₂O. The final concentration of the protein was 0.15 mM. Then, HSQC NMR spectra of the protein at its free state were recorded. After that, the tested compounds dissolved in DMSO-d₆ (final concentration: 0.3 mM) were added into the above solution, which was incubated at 4 °C for 1 h and then centrifuged. HSQC NMR spectra of the protein-compound complex were recorded. The resulting NMR spectra were processed and analyzed by using the Sparky software (<http://nmrfam.wisc.edu/nmrfam-sparky-distribution/>). The HSQC spectrum of free Mcl-1, which is publicly available from the Biological Magnetic Resonance Data Bank (<http://www.bmrb.wisc.edu/>; access number: 19654), was used as the reference for the assignment of chemical shifts. The Ω-value computed as the following equation was used to quantify the chemical shift of each residue on the two-dimensional HSQC spectra.

$$\Omega = \sqrt{(0.2\Delta\delta^{15N})^2 + (\Delta\delta^1H)^2}$$

Molecular Modeling. Binding modes to Mcl-1 for compounds YCW-E10 and FWJ-D4 were predicted by molecular modeling. As the first step, a rough binding mode was generated by using the molecular docking program GOLD (version 2018, Cambridge Crystallographic

Data Centre, United Kingdom).⁴⁵ The receptor used for docking was extracted from the complex structure formed between human Mcl-1 and a small-molecule inhibitor (PDB entry: 4WMR).⁴⁶ Both ligand molecules were sketched with the “Builder” module in the MOE software (version 2018, Chemical Computing Group, Canada) and then minimized with the MMFF94x force field. The binding site on Mcl-1 was defined as all amino acid residues within 10 Å around the bound ligand. The GOLD program employs a genetic algorithm (GA) to control the docking process. The main GA parameters used in our docking job were set as follows: the whole population was placed on 5 separate islands with 100 individuals on each. The total number of GA operations was 100,000. The probabilities for crossover, mutation, and migration operations were 0.95, 0.95, and 0.10, respectively. The ChemPLP scoring function was employed to compute binding scores during docking.⁴⁷ A total of 30 binding poses were finally generated for each ligand molecule, which were clustered with a root-mean-square deviation (rmsd) cutoff of 2.0 Å. The most reasonable binding pose was selected among the best-scored ones in each cluster through visual inspection.

The selected docking poses of YCW-E10 and FWJ-D4 were then refined through MD simulation by using the AMBER program (version 14, University of California San Francisco).⁴⁸ Each ligand molecule was assigned GAFF parameters by using the “Antechamber” module in the AMBER program. Atomic partial charges on the ligand molecule were calculated with the BCC method. Mcl-1 protein atoms were assigned the PARM14 template charges implemented in the AMBER program. All ionizable residues were set at their default protonation states under a neutral pH value. The complex structure was soaked in a box of TIP3P water molecules with a margin of 10 Å along each dimension. The whole system was neutralized by adding an appropriate number of counterions. The whole system was then subjected to a multi-step minimization process: (i) the complex structure was relaxed by 100 cycles of steepest descent minimization and then 4900 cycles of conjugated gradient minimization, where all heavy atoms on the protein and the ligand were constrained with a constant of 10.0 kcal mol⁻¹ Å⁻². (ii) The whole complex went through the same minimization process as the previous step, but no constraint was applied. Then, the system was gradually heated up from 0 to 300 K in 150 ps, followed by 100 ns MD simulation at a constant temperature of 300 K and a constant pressure of 1 atm. During the simulation, electrostatic interactions were calculated with the PME algorithm, and the distance cutoff of nonbonded interactions was set as 10 Å. The SHAKE algorithm was applied to fix the lengths of all chemical bonds connecting hydrogen atoms. A total of 5000 snapshots were retrieved at a 10 ps interval from the last 50 ns MD trajectory. These snapshots were grouped into clusters based on mass-weighted rmsd values calculated on the residues in the binding site, with a cutoff value of 1.5 Å by using the MMTSB tool (http://blue11.bch.msu.edu/mmtsb/Main_Page). The snapshot closest to the cluster center in the largest cluster was selected as the representative model of the given complex. The final binding modes of YCW-E10 and FWJ-D4 to Mcl-1 are shown in Figure 2b.

The representative conformation of the Mcl-1 protein was used as the initial structure for hydration site prediction by WATsite.⁴¹ Side-chain conformations of Asn, Gln, and His residues and tautomers and protonation states of His residues were adjusted by using Reduce.⁴⁹ Hydrogen atoms were added to the structures by using GROMACS (v4.6.1).⁵⁰ The protein was solvated in an octahedron water box using the SPC water model with a water layer of a minimum of 10 Å between any protein atom and the edge of the box. MD simulation was performed by using GROMACS with the AMBER03 force field.⁴⁸ The system was equilibrated first for 250 ps with harmonic restraints applied to all protein atoms (force constant = 1000 kJ mol⁻¹ nm⁻²). Then, a total of 2 ns MD simulation was performed at a constant temperature of 300 K and a constant pressure of 1 atm. The last 1 ns of the trajectory generated 1000 snapshots for identifying the water molecule locations by using a quality threshold (QT) clustering algorithm. All the above jobs were executed on a DELL T7810 desktop workstation (dual Intel Xeon E5-2620 v3 processors, 16 GB memory, and Intel C602 motherboard) running RedHat Linux.

Cytotoxicity Assay. The cytotoxicity activities of our compounds were tested by a refined MTT assay, that is, the CCK8 cell viability assay, on four cell lines. These four cell lines included human cervical tumor cell HeLa, two leukemia tumor cells, HL-60 and RS4;11, and human renal epithelial HEK293T cells as a control. All cell lines were originally obtained from the American Type Culture Collection (ATCC, Manassas, VA) and were cultured in Dulbecco's modified Eagle's medium (HEK293T) and the RPMI-1640 medium (HeLa, HL-60, RS4;11) with 10% fetal bovine serum (FBS) and supplemented with 1% penicillin–streptomycin (P/S). Cell Counting Kit-8 was bought from MesGen (Cat. MG6432, MesGen, China) for the cytotoxicity assay. In each test, 100 μ L of a suspension of 8000 HeLa/HEK293T cells and 50 mL of a suspension of 16,000 HL-60/RS4;11 cells were seeded in each well on 96-well plates. They were treated with the tested compounds of five concentrations (2.5, 5, 10, 20, and 40 μ M) and incubated in a CO₂ incubator for 48 h at 37 °C. After that, the CCK-8 solution (10 μ L) was added to each well. Plates were incubated for an additional 2 h at 37 °C. The supernatant was carefully removed, and DMSO (100 mL) was added to dissolve the formazan crystals. The absorbance at 450 nm was then recorded by using a SpectraMax-190 microplate reader (Molecular Devices, USA). The absorbance at the same wavelength for the well with only the medium or the well with the medium and cells was defined as the blank value or control value, respectively. The cell viability was calculated as the following equation:

$$\text{cell viability (\%)} = \frac{(\text{absorbance (compound)} - \text{absorbance(blank)})}{(\text{absorbance (control)} - \text{absorbance(blank)})} \times 100\%$$

If necessary, the concentration at 50% inhibition (IC₅₀) of each tested compound was derived through nonlinear fitting of the average inhibition rates read from three independent wells by using the Graphpad Prism software (version 5, www.graphpad.com).

Apoptotic Mechanism Studies. Cell Culture and Treatment of Compounds. RS4;11 cells were cultured in the RPMI-1640 medium supplemented with 10% (v/v) FBS, 100 g mL⁻¹ streptomycin, and 100 IU mL⁻¹ penicillin. Cells were incubated under a 5% CO₂ humidified atmosphere at 37 °C. Cells were seeded into a 75 cm² Corning cell culture flask (for mitochondria isolation) or 6- or 12-well cell culture plates (for drug stimulation) and maintained by addition of a new medium every day. Cells were plated at a density of 5 × 10⁵ mL 24 h before compound treatment. Before mitochondria isolation or drug induction of normal cells, cell viability was confirmed to be >95% by using the trypan blue exclusion assay. **ABT-199** and other tested compounds were dissolved in DMSO to a final concentration lower than 0.1%. The control cells were treated with the same volume of the vehicle. The medium was cultured in the presence of multiple doses of **ABT-199** (0.125, 0.25, 0.5, 1.0, and 2.0 μ M) or tested compounds (2.5, 5.0, 10, 20, and 40 μ M) for 24 h. Three parallel experiments were conducted for each compound under the same conditions.

Flow Cytometry Analysis (Mitodamage Staining). RS4;11 cells were incubated with tested compounds for 24–48 h. They were measured by flow cytometry with a MitoDamage Kit (FCCH100106, Merck Millipore). Cell pellets were suspended in 1× assay buffer with MitoSense Red Dye 1:50 and Annexin V stock solution 1:20 at a concentration of 1 × 10⁵ cells/200 μ L for 15 min in a 37 °C CO₂ incubator. Washing was done two more times with 200 μ L of 1× assay buffer, and cells were resuspended in each well with 200 μ L of 1× assay buffer. 5 μ L of the 7-AAD reagent was added to each well. A total of 10,000 events were obtained by using the green channel for Annexin V-FITC, the RED2 channel for MitoSense, and the red channel for 7-AAD. Data presented in this work were representative of those obtained from at least three independent experiments done in triplicate.

West Blot Detection of Caspase-9 and Caspase-3 Activation. RS4;11 cells were lysed in the lysis buffer [1% Triton X-100, 50 mM Tris (pH 7.4), and 150 mM NaCl, containing protease inhibitors (Complete, Roche)] maintained on ice and vortexed gently every 10 min. The sample was centrifuged for 15 min at 12,000g and 4 °C to get rid of cell debris. The protein concentration was assayed by using bicinchoninic acid (Pierce). The cytosolic protein (40 mg) was then

subjected to electrophoresis on 10% sodium dodecylsulfate polyacrylamide gels by using a Bio-Rad mini-gel apparatus and blotted to polyvinylidene difluoride membranes (Millipore, MA, USA) through electrotransfer. Membranes were blocked for 1 h with 5% nonfat dry milk in Tris-buffered saline containing 0.1% Tween-20 (TBST) and then incubated with antibodies (mouse monoclonal anti-caspase-9 antibodies at a 1:1000 dilution, rabbit monoclonal anti-caspase-3 antibodies at a 1:1000 dilution, rabbit monoclonal anti-PARP antibodies at a 1:1000 dilution, and mouse monoclonal anti-Actin antibodies at a 1:2000 dilution) overnight at 4 °C. Primary antibodies were labeled with goat anti-mouse immunoglobulin G (IgG) at a 1:5000 dilution or goat anti-rabbit IgG at a 1:5000 dilution conjugated with horseradish peroxidase (Pierce) and shocked on a shaking table for 1 h at room temperature. Immunoreactive bands were detected by incubation of the membranes with enhanced chemiluminescence (ECL) reagents.

Co-Immunoprecipitation. MCF-7 cells were incubated at 37 °C for 24 h with **ABT-199** (1 μ M), **A-1210477** (3 μ M), **FWJ-D4** (10 μ M), **FWJ-D5** (10 μ M), or **YCW-E16** (10 μ M). Cells were harvested and then lysed on ice in IP buffer (10 mM HEPES, pH 7.4, 50 mM NaCl, 5 mM MgCl₂, 1 mM EGTA, 5% glycerol, 0.5% Triton X-100) supplemented with 1% protease/phosphatase inhibitor for 30 min. After centrifugation (15 min, 12,000g, 4 °C), supernatants were collected and normalized to the protein content. 2 μ g of the anti-Bim antibody was added to an input volume of 200 μ L with 5–10 mg/mL protein. After shaking overnight at 4 °C, 20 μ L of protein G sepharose beads (GE Healthcare, Madison, WI, USA) was added and the samples incubated for 2 h at 4 °C with constant rotation. Immunocomplexes were washed three times with IP buffer. Immunoprecipitated proteins were analyzed by western blot using the anti-Mcl-1 antibody or anti-Bcl-2 antibody. Proteins were detected with an ECL kit.

Anti-tumor Effect on the Xenograft Mouse Model. All procedures for this animal experiment were approved by the Institutional Animal Care and Use Committee of SMOC (Shanghai Model Organisms Center, Inc.) with IACUC no. 2018-0004. To develop xenograft tumors, 5 × 10⁶ RS4;11 cells with 50% Matrigel (BD Biosciences, United States) were injected subcutaneously in the right abdomen of 6-week-old, male NOD/SCID mice (*N* = 37), which were obtained from the Shanghai Model Organisms Center, Inc. (Shanghai, China). The width and length of the tumors were measured 2–3 times each week using an electronic caliper. Tumor volume was calculated as volume = (length × width²)/2. When tumors reached approximately 250 mm³, mice were size-matched into different dosing groups and control groups, where each dosing group consisted of eight individuals and each control group consisted of five individuals. Compounds **ABT-199** and **FWJ-D5** were formulated in 60% polyethylene glycol 400 (Sangon Biotech, China) and administrated at the doses and schedules shown in [Figure 9](#) (i.e., **ABT-199** at a dose of 12.5 mg/kg; **FWJ-D5** at doses of 12.5, 25, and 50 mg/kg). Weights of the mice were measured weekly. Tumor tissues were placed in liquid nitrogen for cryo-sectioning. Then, sections were analyzed by immunohistochemical staining. Proliferation was detected using the Ki-67 antibody (ABcam, USA). Images were captured with a Leica SP8 microscope (Leica, Germany).

■ ASSOCIATED CONTENT

Supporting Information

The Supporting Information is available free of charge at <https://pubs.acs.org/doi/10.1021/acs.jmedchem.1c00690>.

Information of the predicted hydration sites in the Mcl-1 binding pocket, flow cytometric analysis of three selected compounds, and HPLC traces for the reported compounds ([PDF](#))

Molecular formula strings of all reported compounds ([CSV](#))

Structural files of the predicted binding modes of YCW-E10 and FWJ-D4 with Mcl-1 ([ZIP](#))

Statement on the ethnicity of all animal experiments performed in this work (PDF)

AUTHOR INFORMATION

Corresponding Authors

Zhichao Zhang – State Key Laboratory of Fine Chemicals, Zhang Dayu School of Chemistry, Dalian University of Technology, Dalian, Liaoning 116024, People's Republic of China; orcid.org/0000-0002-2774-2384; Email: zczhang@dlut.edu.cn

Ran Hong – CAS Key Laboratory of Synthetic Chemistry of Natural Substances, Chinese Academy of Sciences, Shanghai 200032, People's Republic of China; orcid.org/0000-0002-7602-539X; Email: rhong@sioc.ac.cn

Renxiao Wang – Department of Medicinal Chemistry, School of Pharmacy, Fudan University, Shanghai 201203, People's Republic of China; State Key Laboratory of Bioorganic and Natural Products Chemistry, Center for Excellence in Molecular Synthesis, Shanghai Institute of Organic Chemistry, Chinese Academy of Sciences, Shanghai 200032, People's Republic of China; Shanxi Key Laboratory of Innovative Drugs for the Treatment of Serious Diseases Basing on Chronic Inflammation, College of Traditional Chinese Medicines, Shanxi University of Chinese Medicine, Taiyuan, Shanxi 030619, People's Republic of China; orcid.org/0000-0003-0485-0259; Email: wangrx@fudan.edu.cn

Authors

Yan Li – Department of Medicinal Chemistry, School of Pharmacy, Fudan University, Shanghai 201203, People's Republic of China; State Key Laboratory of Bioorganic and Natural Products Chemistry, Center for Excellence in Molecular Synthesis, Shanghai Institute of Organic Chemistry, Chinese Academy of Sciences, Shanghai 200032, People's Republic of China; orcid.org/0000-0002-8259-2470

Wenjie Fan – State Key Laboratory of Bioorganic and Natural Products Chemistry, Center for Excellence in Molecular Synthesis, Shanghai Institute of Organic Chemistry, Chinese Academy of Sciences, Shanghai 200032, People's Republic of China

Qineng Gong – Department of Medicinal Chemistry, School of Pharmacy, Fudan University, Shanghai 201203, People's Republic of China

Jie Tian – State Key Laboratory of Bioorganic and Natural Products Chemistry, Center for Excellence in Molecular Synthesis, Shanghai Institute of Organic Chemistry, Chinese Academy of Sciences, Shanghai 200032, People's Republic of China

Mi Zhou – Department of Medicinal Chemistry, School of Pharmacy, Fudan University, Shanghai 201203, People's Republic of China

Qing Li – State Key Laboratory of Bioorganic and Natural Products Chemistry, Center for Excellence in Molecular Synthesis, Shanghai Institute of Organic Chemistry, Chinese Academy of Sciences, Shanghai 200032, People's Republic of China

Laura B. Uwituze – State Key Laboratory of Fine Chemicals, Zhang Dayu School of Chemistry, Dalian University of Technology, Dalian, Liaoning 116024, People's Republic of China

Complete contact information is available at:

<https://pubs.acs.org/10.1021/acs.jmedchem.1c00690>

Author Contributions

[†]Y.L., W.F., and Q.G. equal contributions to this work.

Notes

The authors declare no competing financial interest.

ACKNOWLEDGMENTS

This study was financially supported by the National Natural Science Foundation of China (grant nos. 81725022, 81430083, 21472227, 21661162003, 21673276, and 21472226), the Ministry of Science and Technology of China (National Key Research Program, grant no. 2016YFA0502302), and the Chinese Academy of Sciences (Strategic Priority Research Program, grant no. XDB20000000).

REFERENCES

- (1) Kerr, J. F. R.; Wyllie, A. H.; Currie, A. R. Apoptosis: a basic biological phenomenon with wide-ranging implications in tissue kinetics. *Br. J. Cancer* **1972**, *26*, 239–257.
- (2) Anderson, M. H.; Becker, J. C.; Straten, P. Regulators of apoptosis: suitable targets for immune therapy of cancer. *Nat. Rev. Drug Discovery* **2005**, *4*, 399–409.
- (3) Cotter, T. G. Apoptosis and cancer: the genesis of a research field. *Nat. Rev. Cancer* **2009**, *9*, 501–507.
- (4) Hanahan, D.; Weinberg, R. A. Hallmarks of cancer: the next generation. *Cell* **2011**, *144*, 646–674.
- (5) Czabotar, P. E.; Lessene, G.; Strasser, A.; Adams, J. M. Control of apoptosis by the BCL-2 protein family: implications for physiology and therapy. *Nat. Rev. Mol. Cell Biol.* **2014**, *15*, 49–63.
- (6) Petros, A. M.; Nettesheim, D. G.; Wang, Y.; Olejniczak, E. T.; Meadows, R. P.; Mack, J.; Swift, K.; Matayoshi, E. D.; Zhang, H.; Thompson, C. B.; Fesik, S. W. Rationale for Bcl-xL/Bad peptide complex formation from structure, mutagenesis, and biophysical studies. *Protein Sci.* **2000**, *9*, 2528–2534.
- (7) Cory, S.; Huang, D. C. S.; Adams, J. M. The Bcl-2 family: roles in cell survival and oncogenesis. *Oncogene* **2003**, *22*, 8590–8607.
- (8) Konopleva, M.; Zhao, S.; Hu, W.; Jiang, S.; Snell, V.; Weidner, D.; Jackson, C. E.; Zhang, X.; Champlin, R.; Estey, E.; Reed, J. C.; Andreeff, M. The anti-apoptotic genes Bcl-X(L) and Bcl-2 are over-expressed and contribute to chemoresistance of non-proliferating leukaemic CD34⁺ cells. *Br. J. Haematol.* **2002**, *118*, 521–534.
- (9) Palve, V.; Mallick, S.; Ghaisas, G.; Kannan, S.; Teni, T. Overexpression of Mcl-1L splice variant is associated with poor prognosis and chemoresistance in oral cancers. *PLoS One* **2014**, *9*, No. e111927.
- (10) Lessene, G.; Czabotar, P. E.; Colman, P. M. BCL-2 family antagonists for cancer therapy. *Nat. Rev. Drug Discovery* **2008**, *7*, 989–1000.
- (11) Delbridge, A. R. D.; Grabow, S.; Strasser, A.; Vaux, D. L. Thirty years of BCL-2: translating cell death discoveries into novel cancer therapies. *Nat. Rev. Cancer* **2016**, *16*, 99–109.
- (12) Garner, T. P.; Lopez, A.; Reyna, D. E.; Spitz, A. Z.; Gavathiotis, E. Progress in targeting the BCL-2 family of proteins. *Curr. Opin. Chem. Biol.* **2017**, *39*, 133–142.
- (13) Souers, A. J.; Levenson, J. D.; Boghaert, E. R.; Ackler, S. L.; Catron, N. D.; Chen, J.; Dayton, B. D.; Ding, H.; Enschede, S. H.; Fairbrother, W. J.; Huang, D. C. S.; Hymowitz, S. G.; Jin, S.; Khaw, S. L.; Kovar, P. J.; Lam, L. T.; Lee, J.; Maecker, H. L.; Marsh, K. C.; Mason, K. D.; Mitten, M. J.; Nimmer, P. M.; Oleksijew, A.; Park, C. H.; Park, C.-M.; Phillips, D. C.; Roberts, A. W.; Sampath, D.; Seymour, J. F.; Smith, M. L.; Sullivan, G. M.; Tahir, S. K.; Tse, C.; Wendt, M. D.; Xiao, Y.; Xue, J. C.; Zhang, H.; Humerickhouse, R. A.; Rosenberg, S. H.; Elmore, S. W. ABT-199, a potent and selective BCL-2 inhibitor, achieves antitumor activity while sparing platelets. *Nat. Med.* **2013**, *19*, 202–208.
- (14) Nguyen, M.; Marcellus, R. C.; Roulston, A.; Watson, M.; Serfass, L.; Murthy Madiraju, S. R.; Goulet, D.; Viallet, J.; Belec, L.; Billot, X.; Acoca, S.; Purisima, E.; Wiegman, A.; Cluse, L.; Johnstone, R. W.; Beuparlant, P.; Shore, G. C. Small molecule obatoclax (GX15-070)

antagonists MCL-1 and overcomes MCL-1-mediated resistance to apoptosis. *Proc. Natl. Acad. Sci. U.S.A.* **2007**, *104*, 19512–19517.

(15) Tse, C.; Shoemaker, A. R.; Adickes, J.; Anderson, M. G.; Chen, J.; Jin, S.; Johnson, E. F.; Marsh, K. C.; Mitten, M. J.; Nimmer, P.; Roberts, L.; Tahir, S. K.; Xiao, Y.; Yang, X.; Zhang, H.; Fesik, S.; Rosenberg, S. H.; Elmore, S. W. ABT-263: a potent and orally bioavailable Bcl-2 family inhibitor. *Cancer Res.* **2008**, *68*, 3421–3428.

(16) Oltersdorf, T.; Elmore, S. W.; Shoemaker, A. R.; Armstrong, R. C.; Augeri, D. J.; Belli, B. A.; Bruncko, M.; Deckwerth, T. L.; Dinges, J.; Hajduk, P. J.; Joseph, M. K.; Kitada, S.; Korsmeyer, S. J.; Kunzer, A. R.; Letai, A.; Li, C.; Mitten, M. J.; Nettesheim, D. G.; Ng, S.; Nimmer, P. M.; O'Connor, J. M.; Oleksijew, A.; Petros, A. M.; Reed, J. C.; Shen, W.; Tahir, S. K.; Thompson, C. B.; Tomaselli, K. J.; Wang, B.; Wendt, M. D.; Zhang, H.; Fesik, S. W.; Rosenberg, S. H. An inhibitor of Bcl-2 family proteins induces regression of solid tumors. *Nature* **2005**, *435*, 677–681.

(17) Oliver, C. L.; Miranda, M. B.; Shangary, S.; Land, S.; Wang, S.; Johnson, D. E. (-)-Gossypol acts directly on the mitochondria to overcome Bcl-2- and Bcl-X(L)-mediated apoptosis resistance. *Mol. Cancer Ther.* **2005**, *4*, 23–31.

(18) Porter, J.; Payne, A.; de Candole, B.; Ford, D.; Hutchinson, B.; Trevitt, G.; Turner, J.; Edwards, C.; Watkins, C.; Whitcombe, I.; Davis, J.; Stubberfield, C. Tetrahydroisoquinoline amide substituted phenyl pyrazoles as selective Bcl-2 inhibitors. *Bioorg. Med. Chem. Lett.* **2009**, *19*, 230–233.

(19) Wu, Y.; Lakhani, N. J.; Boyer, M.; Zhou, Q.; Rasco, D. W.; Huang, Y.; Men, L.; Li, Y.; Xia, Z.; Wang, H.; Ji, J.; Lu, B.; He, Z.; Dong, Q.; Yang, D.; Zhai, Y. A phase I study of novel Bcl-2/Bcl-xL inhibitor APG-1252 in patients with advanced SCLC or other solid tumor. *J. Thorac. Oncol.* **2018**, *13*, S1048–S1049.

(20) Caenepeel, S. R.; Belmontes, B.; Sun, J.; Coxon, A.; Moody, G.; Hughes, P. E. Abstract 2027: preclinical evaluation of AMG176, a novel, potent and selective Mcl-1 inhibitor with robust anti-tumor activity in Mcl-1 dependent cancer models. *Cancer Res.* **2017**, *77*, 2027.

(21) Konopleva, M.; Contractor, R.; Tsao, T.; Samudio, I.; Ruvolo, P. P.; Kitada, S.; Deng, X.; Zhai, D.; Shi, Y.-X.; Sneed, T.; Verhaegen, M.; Soengas, M.; Ruvolo, V. R.; McQueen, T.; Schober, W. D.; Watt, J. C.; Jiffar, T.; Ling, X.; Marini, F. C.; Harris, D.; Dietrich, M.; Estrov, Z.; McCubrey, J.; May, W. S.; Reed, J. C.; Andreeff, M. Mechanisms of apoptosis sensitivity and resistance to the BH3 mimetic ABT-737 in acute myeloid leukemia. *Cancer Cell* **2006**, *10*, 375–388.

(22) van Delft, M. F.; Wei, A. H.; Mason, K. D.; Vandenberg, C. J.; Chen, L.; Czabotar, P. E.; Willis, S. N.; Scott, C. L.; Day, C. L.; Cory, S.; Adams, J. M.; Roberts, A. W.; Huang, D. C. S. The BH3 mimetic ABT-737 targets selective Bcl-2 proteins and efficiently induces apoptosis via Bak/Bax if Mcl-1 is neutralized. *Cancer Cell* **2006**, *10*, 389–399.

(23) Ashkenazi, A.; Fairbrother, W. J.; Levenson, J. D.; Souers, A. J. From basic apoptosis discoveries to advanced selective BCL-2 family inhibitors. *Nat. Rev. Drug Discovery* **2017**, *16*, 273–284.

(24) Krajewski, S.; Bodrug, S.; Krajewska, M.; Shabaik, A.; Gascoyne, R.; Berean, K.; Reed, J. C. Immunohistochemical analysis of Mcl-1 protein in human tissues: Differential regulation of Mcl-1 and Bcl-2 protein production suggests a unique role for Mcl-1 in control of programmed cell death in vivo. *Am. J. Pathol.* **1995**, *146*, 1309–1319.

(25) Brunelle, J. K.; Ryan, J.; Yecies, D.; Opferman, J. T.; Letai, A. Mcl-1-dependent leukemia cells are more sensitive to chemotherapy than BCL-2-dependent counterparts. *J. Cell Biol.* **2009**, *187*, 429–442.

(26) Han, L.; Wang, R. Rise of the selective inhibitors of anti-apoptotic Bcl-2 family proteins. *ChemMedChem* **2013**, *8*, 1437–1440.

(27) Beekman, A. M.; Howell, L. A. Small-molecule and peptide inhibitors of the pro-survival protein Mcl-1. *ChemMedChem* **2016**, *11*, 802–813.

(28) Negi, A.; Murphy, P. V. Development of Mcl-1 inhibitors for cancer therapy. *Eur. J. Med. Chem.* **2021**, *210*, 113038.

(29) Kotschy, A.; Szlavik, Z.; Murray, J.; Davidson, J.; Maragno, A. L.; Le Toumelin-Braizat, G.; Chanrion, M.; Kelly, G. L.; Gong, J.-N.; Moujalled, D. M.; Bruno, A.; Csekei, M.; Paczal, A.; Szabo, Z. B.; Sipos, S.; Radics, G.; Prosenyak, A.; Balint, B.; Ondi, L.; Blasko, G.; Robertson, A.; Surgenor, A.; Dokurno, P.; Chen, I.; Matassova, N.;

Smith, J.; Pedder, C.; Graham, C.; Studeny, A.; Lysiak-Auvity, G.; Girard, A.-M.; Gravé, F.; Segal, D.; Riffkin, C. D.; Pomilio, G.; Galbraith, L. C. A.; Aubrey, B. J.; Brennan, M. S.; Herold, M. J.; Chang, C.; Guasconi, G.; Cauquil, N.; Melchiorre, F.; Guigal-Stephan, N.; Lockhart, B.; Colland, F.; Hickman, J. A.; Roberts, A. W.; Huang, D. C. S.; Wei, A. H.; Strasser, A.; Lessene, G.; Geneste, O. The MCL1 inhibitor S63845 is tolerable and effective in diverse cancer models. *Nature* **2016**, *538*, 477–482.

(30) Lee, T.; Bian, Z.; Zhao, B.; Hogdal, L. J.; Sensintaffar, J. L.; Goodwin, C. M.; Belmar, J.; Shaw, S.; Tarr, J. C.; Veerasamy, N.; Matulis, S. M.; Koss, B.; Fischer, M. A.; Arnold, A. L.; Camper, D. V.; Browning, C. F.; Rossanese, O. W.; Budhraja, A.; Opferman, J.; Boise, L. H.; Savona, M. R.; Letai, A.; Olejniczak, E. T.; Fesik, S. W. Discovery and biological characterization of potent myeloid cell leukemia-1 inhibitors. *FEBS Lett.* **2017**, *591*, 240–251.

(31) Bruncko, M.; Wang, L.; Sheppard, G. S.; Phillips, D. C.; Tahir, S. K.; Xue, J.; Erickson, S.; Fidanze, S.; Fry, E.; Hasvold, L.; Jenkins, G. J.; Jin, S.; Judge, R. A.; Kovar, P. J.; Madar, D.; Nimmer, P.; Park, C.; Petros, A. M.; Rosenberg, S. H.; Smith, M. L.; Song, X.; Sun, C.; Tao, Z.-F.; Wang, X.; Xiao, Y.; Zhang, H.; Tse, C.; Levenson, J. D.; Elmore, S. W.; Souers, A. J. Structure-guided design of a series of MCL-1 inhibitors with high affinity and selectivity. *J. Med. Chem.* **2015**, *58*, 2180–2194.

(32) Abulwerdi, F.; Liao, C.; Liu, M.; Azmi, A. S.; Aboukameel, A.; Mady, A. S. A.; Gulappa, T.; Cierpicki, T.; Owens, S.; Zhang, T.; Sun, D.; Stuckey, J. A.; Mohammad, R. M.; Nikolovska-Coleska, Z. A novel small-molecule inhibitor of Mcl-1 blocks pancreatic cancer growth in vitro and in vivo. *Mol. Cancer Ther.* **2014**, *13*, 565–575.

(33) Doi, K.; Li, R.; Sung, S.-S.; Wu, H.; Liu, Y.; Manieri, W.; Krishnegowda, G.; Awwad, A.; Dewey, A.; Liu, X.; Amin, S.; Cheng, C.; Qin, Y.; Schonbrunn, E.; Daughdrill, G.; Loughran, T. P.; Sebt, S.; Wang, H.-G. Discovery of marinopyrrole A (Maritoclax) as a selective Mcl-1 antagonist that overcomes ABT-737 resistance by binding to and targeting Mcl-1 for proteasomal degradation. *J. Biol. Chem.* **2012**, *287*, 10224–10235.

(34) Richard, D. J.; Lena, R.; Bannister, T.; Blake, N.; Pierceall, W. E.; Carlson, N. E.; Keller, C. E.; Koenig, M.; He, Y.; Minond, D.; Mishra, J.; Cameron, M.; Spicer, T.; Hodder, P.; Cardone, M. H. Hydroxyquinoline-derived compounds and analoguing of selective Mcl-1 inhibitors using a functional biomarker. *Bioorg. Med. Chem.* **2013**, *21*, 6642–6649.

(35) Bernardo, P. H.; Sivaraman, T.; Wan, K.-F.; Xu, J.; Krishnamoorthy, J.; Song, C. M.; Tian, L.; Chin, J. S. F.; Lim, D. S. W.; Mok, H. Y. K.; Yu, V. C.; Tong, J. C.; Chai, C. L. L. Structural insights into the design of small molecule inhibitors that selectively antagonize Mcl-1. *J. Med. Chem.* **2010**, *53*, 2314–2318.

(36) Ding, X.; Li, Y.; Lv, L.; Zhou, M.; Han, L.; Zhang, Z.; Ba, Q.; Li, J.; Wang, H.; Liu, H.; Wang, R. De novo design, synthesis and evaluation of benzylpiperazine derivatives as highly selective binders of Mcl-1. *ChemMedChem* **2013**, *8*, 1986–2014.

(37) Tron, A. E.; Belmonte, M. A.; Adam, A.; Aquila, B. M.; Boise, L. H.; Chiarparin, E.; Cidado, J.; Embrey, K. J.; Gangl, E.; Gibbons, F. D.; Gregory, G. P.; Hargreaves, D.; Hendricks, J. A.; Johannes, J. W.; Johnstone, R. W.; Kazmirski, S. L.; Kettle, J. G.; Lamb, M. L.; Matulis, S. M.; Nooka, A. K.; Packer, M. J.; Peng, B.; Rawlins, P. B.; Robbins, D. W.; Schuller, A. G.; Su, N.; Yang, W.; Ye, Q.; Zheng, X.; Secrist, J. P.; Clark, E. A.; Wilson, D. M.; Fawell, S. E.; Hird, A. W. Discovery of Mcl-1-specific inhibitor AZD5991 and preclinical activity in multiple myeloma and acute myeloid leukemia. *Nat. Commun.* **2018**, *9*, 5341.

(38) Yang, C.; Chen, S.; Zhou, M.; Li, Y.; Li, Y.; Zhang, Z.; Liu, Z.; Ba, Q.; Li, J.; Wang, H.; Yan, X.; Ma, D.; Wang, R. Development of 3-phenyl-N-(2-(3-phenylureido)ethyl)-thiophene-2-sulfonamide compounds as inhibitors of antiapoptotic Bcl-2 family proteins. *ChemMedChem* **2014**, *9*, 1436–1452.

(39) Zhou, B.; Li, X.; Li, Y.; Xu, Y.; Zhang, Z.; Zhou, M.; Zhang, X.; Liu, Z.; Zhou, J.; Cao, C.; Yu, B.; Wang, R. Discovery and development of thiazolo[3,2-a]pyrimidinone derivatives as general inhibitors of Bcl-2 family proteins. *ChemMedChem* **2011**, *6*, 904–921.

(40) Xu, Y.; Zhou, M.; Li, Y.; Li, C.; Zhang, Z.; Yu, B.; Wang, R. Characterization of the stereochemical structures of 2H-thiazolo[3,2-

a]pyrimidine compounds and their binding affinities for anti-apoptotic Bcl-2 family proteins. *ChemMedChem* **2013**, *8*, 1345–1352.

(41) Masters, M. R.; Mahmoud, A. H.; Yang, Y.; Lill, M. A. Efficient and accurate hydration site profiling for enclosed binding sites. *J. Chem. Inf. Model.* **2018**, *58*, 2183–2188.

(42) Petros, A. M.; Medek, A.; Nettlesheim, D. G.; Kim, D. H.; Yoon, H. S.; Swift, K.; Matayoshi, E. D.; Oltersdorf, T.; Fesik, S. W. Solution structure of the antiapoptotic protein bcl-2. *Proc. Natl. Acad. Sci. U.S.A.* **2001**, *98*, 3012–3017.

(43) Czabotar, P. E.; Lee, E. F.; van Delft, M. F.; Day, C. L.; Smith, B. J.; Huang, D. C. S.; Fairlie, W. D.; Hinds, M. G.; Colman, P. M. Structural insights into the degradation of Mcl-1 induced by BH3 domains. *Proc. Natl. Acad. Sci. U.S.A.* **2007**, *104*, 6217–6222.

(44) Nikolovska-Coleska, Z.; Wang, R.; Fang, X.; Pan, H.; Tomita, Y.; Li, P.; Roller, P. P.; Krajewski, K.; Saito, N. G.; Stuckey, J. A.; Wang, S. Development and optimization of a binding assay for the XIAP BIR3 domain using fluorescence polarization. *Anal. Biochem.* **2004**, *332*, 261–273.

(45) Jones, G.; Willett, P.; Glen, R. C. Molecular recognition of receptor sites using a genetic algorithm with a description of desolvation. *J. Mol. Biol.* **1995**, *245*, 43–53.

(46) Clifton, M. C.; Dranow, D. M.; Leed, A.; Fulroth, B.; Fairman, J. W.; Abendroth, J.; Atkins, K. A.; Wallace, E.; Fan, D.; Xu, G.; Ni, Z. J.; Daniels, D.; Van Drie, J.; Wei, G.; Burgin, A. B.; Golub, T. R.; Hubbard, B. K.; Serrano-Wu, M. H. A maltose-binding protein fusion construct yields a robust crystallography platform for MCL1. *PLoS One* **2015**, *10*, No. e0125010.

(47) Korb, O.; Stütze, T.; Exner, T. E. Empirical scoring functions for advanced protein-ligand docking with PLANTS. *J. Chem. Inf. Model.* **2009**, *49*, 84–96.

(48) Case, D. A.; Babin, V.; Berryman, J. T.; Betz, R. M.; Cai, Q.; Cerutti, D. S.; Cheatham, T. E.; Darden, T. A.; Duke, R. E.; Gohlke, H.; Goetz, A. W.; Gusarov, S.; Homeyer, N.; Janowski, P.; Kaus, J.; Kolossvary, I.; Kovalenko, A.; Lee, T. S.; LeGrand, S.; Luchko, T.; Luo, R.; Madej, B.; Merz, K. M.; Paesani, F.; Roe, D. R.; Roitberg, A.; Sagui, C.; Salomon-Ferrer, R.; Seabra, G.; Simmerling, C. L.; Smith, W.; Swails, J.; Walker, R. C.; Wang, J.; Wolf, R. M.; Wu, X.; Kollman, P. A. *AMBER 14*; University of California: San Francisco, 2014.

(49) Word, J. M.; Lovell, S. C.; Richardson, J. S.; Richardson, D. C. Asparagine and glutamine: using hydrogen atom contacts in the choice of side-chain amide orientation. *J. Mol. Biol.* **1999**, *285*, 1735–1747.

(50) Hess, B.; Kutzner, C.; van der Spoel, D.; Lindahl, E. GROMACS 4: algorithms for highly efficient, load-balanced, and scalable molecular simulation. *J. Chem. Theory Comput.* **2008**, *4*, 435–447.